State of Oregon
Department of Geology and Mineral Industries
Vicki S. McConnell, State Geologist

Open-File Report

OFR O-04-20

EVALUATION OF COASTAL EROSION HAZARD ZONES FROM SISTERS ROCKS TO NORTH GOLD BEACH, CURRY COUNTY, OREGON:

TECHNICAL REPORT TO CURRY COUNTY

By

George R. Priest[1], Ron Sonnevil[2], and Jonathan C. Allan[1]

2004

[1]Oregon Department of Geology and Mineral Industries, Coastal Field Office, 313 SW 2nd St., Suite D, Newport, OR 97365
[2]Terra Firma Geologic Services, 27766 Hunter Creek Rd., Gold Beach, OR 97444

Photo is from Oregon Department of Geology archives and was taken at Nesika Beach April 29, 2002. It illustrates how coastal bluff erosion is threatening many houses in the area.

NOTICE

The Oregon Department of Geology and Mineral Industries is publishing this paper because the information furthers the mission of the Department. To facilitate timely distribution of the information, this report is published as received from the authors and has not been edited to our usual standards.

Oregon Department of Geology and Mineral Industries Open-File Report
Published in conformance with ORS 516.030

For copies of this publication or other information about Oregon's geology and natural resources, contact:
Nature of the Northwest Information Center
800 NE Oregon Street #5
Portland, Oregon 97232
(503) 872-2750
http://www.naturenw.org

TABLE OF CONTENTS

1.0 EXECUTIVE SUMMARY 1
2.0 INTRODUCTION 5
3.0 METHODS 7
3.1 Active Erosion Hazard Zone 7
3.2 Dune-backed Shorelines 8
3.2.1 The Geometric Model 8
3.2.1.1 Wave Runup 10
3.2.1.2 Tides 11
3.2.1.3 Relative Sea Level Rise 12
3.2.1.4 Beach Morphology 13
3.2.2 Senarios of Coastal Change 14
3.3 Bluff-Backed Shorelines 16
3.3.1 Introduction 16
3.3.2 The Bluff Retreat Model 16
3.3.3 Data Used for Drawing Bluff Erosion Hazard Zones 19
3.3.3.1 Angle of Repose 19
3.3.3.2 Erosion Rate Data 25
3.3.3.2.1 Bluff Top Retreat 25
3.3.3.2.2 Bluff Toe Retreat 25
3.3.3.2.3 Gradual Subaerial Erosion 32
3.3.3.3 Block Failure Data 32
3.4 Landslide Mapping (Mass Movements) 33
3.4.1 Introduction 33
3.4.2 Prehistoric Mass Movements (PHls, PHb, PHf) 34
3.4.3 Potentially Active Mass Movements (PAls, PAb, PAf) 34
3.4.4 Active Mass Movements (Als, Ab, Af) 34
3.4.5 Extent and Quality of Landslide Mapping 34
3.5 Explanation of Geologic Data 34
3.6 Shoreline Protection Structures 36
3.7 Mapping Technique for Bluff Erosion Hazard Zones 36
3.7.1 Description of the zones 36
3.7.2 Uncertainty in Spatial Location of the Zones 37
3.7.3 General Procedure for Drawing Bluff Hazard Zones 37
4.0 RESULTS AND DISCUSSION 39
4.1 Landslide Hazards 39
4.2 Active Hazard Zone 39
4.3 Beach-dune Erosion Hazard Zones 40
4.4 Bluff Erosion Risk Zones 44
5.0 SUMMARY AND CONCLUSIONS 46
6.0 RECOMMEDATIONS 50
7.0 ACKNOWLEDGMENTS 52
8.0 REFERENCES CITED 53

APPENDIX A – EROSION HAZARD ZONES 56
EROSION HAZARD RISK ZONES – SISTERS ROCKS AREA........ 57
EROSION HAZARD RISK ZONES – DEVILS BACKBONE AREA 58
EROSION HAZARD RISK ZONES – EUCHRE CREEK-OPHIR-AREA 59
EROSION HAZARD RISK ZONES – SOUTH EUCHRE CREEK TO WELSH DRIVE 60
EROSION HAZARD RISK ZONES – GREGGS CREEK TO MILLER ROAD 61
EROSION HAZARD RISK ZONES – NORTH NESIKA BEACH 62
EROSION HAZARD RISK ZONES – CENTRAL NESIKA BEACH (ANDY-GRANGE ROAD) 63
EROSION HAZARD RISK ZONES – SOUTH NESIKA BEACH (ANDY-GUN CLUB ROAD) 64
EROSION HAZARD RISK ZONES – WAKEMAN BEACH TO HUBBARD MOUND 65
EROSION HAZARD RISK ZONES – SOUTH HUBBARD MOUND TO OTTER POINT........ 66
EROSION HAZARD RISK ZONES – BAILEY BEACH 67
EROSION HAZARD RISK ZONES – SANDY – COBBLESTONE ROAD AREA 68
EROSION HAZARD RISK ZONES – NORTH JETTY OF ROGUE RIVER 69

APPENDIX B – LANDSLIDE AND GEOLOGY MAPS 70
LANDSLIDE AND GEOLOGY MAP – SISTERS ROCKS AREA........ 73
LANDSLIDE AND GEOLOGY MAP – DEVILS BACKBONE AREA 74
LANDSLIDE AND GEOLOGY MAP – EUCHRE CREEK-OPHIR-AREA 75
LANDSLIDE AND GEOLOGY MAP – SOUTH EUCHRE CREEK TO WELSH DRIVE........ 76
LANDSLIDE AND GEOLOGY MAP – GREGGS CREEK TO MILLER ROAD 77
LANDSLIDE AND GEOLOGY MAP – NORTH NESIKA BEACH 78
LANDSLIDE AND GEOLOGY MAP – CENTRAL NESIKA BEACH (ANDY-GRANGE ROAD) 79
LANDSLIDE AND GEOLOGY MAP – SOUTH NESIKA BEACH (ANDY-GUN CLUB ROAD) 80
LANDSLIDE AND GEOLOGY MAP – WAKEMAN BEACH TO HUBBARD MOUND 81
LANDSLIDE AND GEOLOGY MAP – SOUTH HUBBARD MOUND TO OTTER POINT........ 82
LANDSLIDE AND GEOLOGY MAP – BAILEY BEACH 83
LANDSLIDE AND GEOLOGY MAP – SANDY – COBBLESTONE ROAD AREA 84
LANDSLIDE AND GEOLOGY MAP – NORTH JETTY OF ROGUE RIVER........ 85

APPENDIX C: DIGITAL FILES 86

FIGURES

1 Map showing location of the study area. Heavy line shows extent of project area covered by digital geographic information files containing data on geology, landslides, and erosion hazards. Erosion information covers only open coastal (versus estuarine or river) areas and is mapped only in areas with base map coverage from 2003 color orthophotos........ 5

2 Schematic diagram showing possible dune erosion hazard zones. 7

3 The foredune erosion model (Komar and others, 1999). NAVD'88 = National Vertical Datum of 1988........ 9

4 The geometric model used to assess the maximum potential beach erosion in response to an extreme storm (After Komar and others, 1999). 9

5 Uplift rate along the Oregon coast, measured by geodetic surveys (solid black line) relative to uplift measured from tide gauges (points with error bars) and long term uplift inferred from elevation of Pleistocene marine terraces (dashed black line). Blue dashed lines show uplift rate of the study area (42.423 and 42.563 N Latitude), which is essentially equal to global sea level rise (red dashed line). Large dotted black line is an approximate cross section from the map of estimated North American post-glacial rebound by Peltier (1986). The elevation changes are relative to the geodetic mean sea level, with positive values representing a rise in the land, while negative values represent the progressive subsidence. Stippled regions are inferred to represent elastic strain accumulation; note that some areas will go up (coarse stippling) and others will go down (fine stippling), when this strain is released during an earthquake. The study area is an area of current tectonic uplift and significant coseismic subsidence. Graph is modified slightly from Mitchell and others (1994). 13

6 Schematic illustration of block failure on a bluff, angle of repose, and erosion rate in relation to possible hazard zones. These factors can be combined in a variety of different ways to produce hazard zones. 17

7 Gradual versus episodic bluff erosion. Note how the landslide toe position remains stable as the headwall retreats; hence erosion rate for bluffs with large landslides is more accurately measured at the headwall. Also note that the dangerous part of the bluff is much wider for the landslide-prone bluff, since another maximum block failure could occur at any point in the erosion cycle. 19

8 Vegetated bluff 1 mile south of Otter Point is completely protected from wave erosion by vegetated dunes (upper left). Bluff is composed of Pleistocene marine terrace deposits overlying Jurassic sedimentary rocks. Bluff face is mantled by talus lying at a 1.5:1 (horizontal:vertical) slope. Bluff is locally near vertical in upper ten feet where it is not mantled by significant talus. In these areas it probably erodes back by a combination of wind erosion, slope wash, and cantilevered block fall processes. Blue lines are topographic contours at intervals of two feet. Red lines are index contours at intervals of ten feet. 20

9 Close-up of scar of a cantilevered block in Pleistocene marine terrace sand at Nye Beach, Lincoln County, Oregon. The lower slope is vegetated talus at the angle of repose. Future retreat of the uppermost

escarpment will add to the talus until the entire slope is at the angle of repose and the block falls stop. 21

10 Nesika Beach near vertical sea cliff of Pleistocene marine terrace deposits (horizontally bedded sand in the uppermost part of bluff) overlying sheared Jurassic sedimentary rocks (Figure 11). Cliff erosion is chiefly from undercutting by waves, groundwater-induced sloughing or slumping of the terrace deposits, and cantilevered block falls in terrace deposits. Wave attack is vigorous enough to remove talus except for very recent sloughing events (e.g., left foreground). 22

11 Sheared Jurassic mudstone and sandstone typical of the lower part of many bluffs in the study area. This material has little resistance to wave erosion or slope failure when it is as highly sheared as in this example. Shears are in so many different directions that bluffs are highly vulnerable to slope failure from rotational and translational landslides or block falls. 22

12 Slump block about 30 feet wide in Pleistocene paleosol, laminated carbonaceous clayey silt and sand deposits at Nye Beach. Note that cantilevered block falls are keeping the upper part of the bluff near vertical. Note also that this slump and the cantilevered block falls occurred on a well-vegetated slope. While the vegetation does not prove that wave undercutting did not trigger this slump, the vegetation is suggestive that waves were probably not the main factor for either type of failure. Groundwater saturation probably played a more significant role in this particular case. 23

13 Sisters Rocks area illustrating steep lower sea cliffs where waves have access at all times. 23

14 Partially sheltered north side of Sisters Rocks has talus slopes of broken hard metamorphic rock that average about 1:1, horizontal to vertical. Individual blocks up to 20 feet wide have toppled onto this talus slope from the steeper rock slope above. Orange and yellow lines are topographic contours at intervals of 2 feet derived from a 2002 LIDAR survey of this area by USGS. 24

15 Projection of angle of repose for landslides. 24

16 Bluff toe versus bluff top retreat at Nesika Beach between 1967 and 2003; determined from rubbersheeting 1967 air photo to 2003 orthophoto of the area. Note how irregular bluff top retreat is relative to bluff toe retreat over this time interval. The bluff toe retreat occurs by fairly constant wearing away by waves, whereas bluff top retreat

is more episodic, proceeding more by gravitational failures from slope undercutting and groundwater processes. It is apparent from the illustration that bluff top retreat is approximately equal to toe retreat, but only over a long time interval. The 36-year interval in this example was inadequate to see mean bluff top retreat but adequate for gradual bluff toe erosion. The large changes in bluff top position in several places are probably from local landslide failures. These can happen at anytime and must be taken into account when estimating risk. 26

17 Location map of segments of shoreline with coherent erosion characteristics (black numbers with boundary lines). Headlands like Otter Point, Hubbard Mound and Sisters Rocks are considered a sixth type of bluff segment. Orange areas are outcrops of Quaternary marine terrace deposits; green in upper part of figure are high bluffs of Mesozoic metamorphic and sedimentary rocks; reddish diamond and line patterns in upper part of figure are large landslides in the high bluffs. 28

18 Vegetation on Quaternary marine terrace sand bluff south of Otter Point shows that waves rarely erode the bluff. Mean high water lines from 1928 to 2002 illustrate that the shoreline has fluctuated up to 180 feet in this area. Seaward location of the later shorelines is suggestive that beach sand accretion has occurred during the last 74 years. The star is the location of the erosion measurement listed in Table 6 for this area. Blue lines are topographic contours at intervals of 2 feet. 29

19 Geologic mapping for the study area covers the full extent of 2003 orthophoto coverage plus a small additional area on the north end of the area. Coverage is generally within about 2000 feet of the coastline, except at the north end where it was expanded to cover the large landslides there. Reddish colored dotted and lined areas at the north end of the study are examples of mapped areas of active landside. Similar but smaller landslides occur to the south. Green area north of Euchre Creek is a high bluff of Mesozoic metamorphic and sedimentary rocks. Orange area areas to the south are much lower bluffs capped by Quaternary marine terrace deposits. See Appendix B for detailed views of the mapping plus a complete map legend explaining geologic map units. 30

20 Historic shorelines in the Euchre Creek area. Red line is the 2002 mean higher high water shoreline defined from LIDAR data; dashed line is the same shoreline taken from a 1928 topographic map; blue shoreline is from the 1980-1982 USGS topographic base map. Note that there is overall accretion of the beach from 1928 but little change

between 1982 and 2003. Also note the complex changes in position of the Euchre Creek channel. 42

21 Historic shoreline change at northern Nesika Beach (Ophir Wayside). See Figure 20 for explanation of symbols. 42

22 Beach accretion caused by construction of jetties at Gold Beach. The effect is most pronounced on the north side of the North Jetty where the pre-jetty shoreline of 1928 (dashed line) is hundreds of feet east of the 2002 shoreline (red) defined by LIDAR. The effect decreases north. The base map is a 1980/1982 USGS DRG (digital raster graphic quadrangle). Note the eastward translation of the shoreline from 1980-1982 to 2002 probably resulting from the extreme storms that occurred during the 1997-98 El Niño and 1998-99 La Niña winters. 43

TABLES

1 Peak storm wave statistics for the Newport wave buoy for the major 1997-98 El Niño and 1998-99 La Niña winters and for the period 1999 to 2003. 11

2 Average extreme-wave projections based on data from four NDBC wave buoys located offshore the Pacific Northwest coast. 11

3 Extreme annual tides (Shih and others, 1994). Note all elevations are relative to the NGVD'29 datum. 12

4 Summary of bluff erosion data that can be used to calculate bluff hazard zones. Only maximum observed (empirical) block failure width is listed (versus most probable or average width), because this is generally the only empirical data that can be easily obtained in most areas. Quantitative slope modeling or regional empirical analyses would be required to establish a mean or most probable block failure width. Angle of repose refers to the ideal slope angle for unconsolidated talus of the bluff material. 17

5 Slopes of repose by material type. 25

6 Bluff toe erosion data based on comparison of 2003 and 1994 digital orthophotos to 1939 and 1967 air photos and derived from east-west change of the bluff toe. Erosion Rate for point data is the mean of measurements; for the continuous segment rubber sheeted at segment 2 at Nesika Beach (Figure 16), it is the mean of 33 segments of similar retreat weighted for the shoreline length represented by each. Std. Dev = Standard deviation from the mean of measurements; for the rubber sheeted segment at Nesika Beach, standard deviation is the mean of deviations

from the mean of measurements weighted by the shoreline length represented by each measurement. Measurement error is the inherent uncertainty in locations because of photo scale and resolution; RMS = root mean square error (square root of sum of squares of measurement error and standard deviation). 27

7 Summary of the high and low erosion rates that will be used here for mapping erosion hazard zones on the coastal bluffs. See discussion in text for derivation of the low and high (conservative) rates. 30

8 Recommended maximum block failure widths for coastal bluffs of the study area. All data are from empirical observations of local landslides. 33

9 Landslide map units; “Present?” refers to presence in the study area. 35

10 Maximum potential erosion distances determined for the Euchre Creek area. Mean is calculated from the total area of the erosion east of the beach-dune toe junction divided by the shoreline length. 41

11 Maximum potential erosion distances determined for northern Nesika Beach (Ophir Wayside). 41

12 Maximum potential erosion distances determined for the beach north of the North Jetty at Gold Beach. 43

13 Minimum, mean, and maximum lateral distances of bluff top retreat should erosion continue for 60-100 years. These distances define the landward boundaries of the high-, moderate-, and low-risk hazard zones, respectively, when added to the lateral distance of the projected angle of repose for talus of each bluff. Table illustrates the uncertainty of predicting future bluff retreat from erosion rate and maximum block failure width. Values in parentheses are actual mapped widths, taking into account the limitations of the digital base maps, topographic data, and drawing accuracy. “Fine-grained interbeds” in the table refers to interbeds of siltstone, mudstone, or silty fine-grained sandstone with low resistance to shearing forces and consequent slope failure. 44

A 1 Digital vector files used to produce map views in Appendices A and B. 86

A 2 GIS data files of erosion hazard map guidelines, erosion data, and slide block width measurements. All GIS files have as their first attribute a data field labeled ID, which gives a number to each row of attribute data. This ID field is not listed in the table. 87

1.0 EXECUTIVE SUMMARY

This report describes and documents a range of coastal geologic hazard zones distinguished for the Curry County coastline. In particular, the report focuses on identifying minimum and maximum potential erosion distances (MPED) for bluffs and for dune backed shorelines using two quite different but complementary approaches. In both types of shorelines four zones were defined, an *active hazard zone* characterized by existing, active erosion processes, and three zones of potential future erosion, *high-, moderate-, and low-risk zones* that respectively depict decreasing risks of becoming active in the future. Of most interest to planners are the landward boundaries of the high- and low-risk zones. The landward boundary of the high-risk zone defines a conservative but reasonable limit of expansion of the active hazard zone in the next 60-100 years. The landward boundary of the low-risk zone defines the outermost limit of expansion of the active hazard zone in a worst-case scenario. This scenario could be a catastrophic event such as a great earthquake on the Cascadia subduction zone, coupled with severe storms. For example, a Cascadia earthquake would directly cause widespread landsides on steep slopes, while remobilizing existing landslides. Near instantaneous subsidence of the coast in the Gold Beach area by up to ~6.2 feet (1.9 m) during a Cascadia event would probably lead to extensive retreat of dune and bluff backed beaches.

The erosion hazard risk zones were defined by detailed analysis of coastal erosion processes affecting the area. The most important conclusions reached from this analysis are:

1) Analyses of historical shoreline changes in the coastline indicate that the dune-backed shorelines respond episodically to such processes as the El Niño/La Niña Southern Oscillation, and as a result of rip current embayments that cause "hotspot erosion" of the coast. The response is particularly dynamic (fast) on reflective beaches like the ones in the study area, because such beaches do not dissipate wave energy. Previous work in both Lincoln and in Tillamook County suggests that such processes can cause up to 125 ft of beach erosion in one or a few large storm cycles. Thus, the coastline undergoes periods of both localized and widespread erosion, with subsequent intervening periods in which the beaches and dunes rebuild. Nevertheless, because the record of such occurrences is relatively short, limited to 30 years at best, the effects of extremely large storms, or storms-in-series remain largely unknown, except for qualitative observations (e.g., sawed logs in dunes).

2) Coastal change at the mouth of the Rogue River is strongly affected by construction of jetties. The north jetty has caused hundreds of feet of beach accretion (increase in width) in the beach to the north. As a result, bluffs within about one mile north of the jetty are guarded from erosion by a wide beach and dune system. A narrower but still significant dune system greatly decreases wave erosion for an additional 1.4 miles north of the north jetty. The shoreline near the North Jetty has experienced about 250 feet of erosion since the 1980s, probably in response to extreme storms that occurred during the 1997-98 El Niño and 1998-99 La Niña winters; so the dune system is vulnerable to further erosion episodes.

3) An extensive dune system at the mouth of Euchre Creek limits bluff erosion north and south of the creek. Specification of dune and bluff erosion hazard risk zones at Euchre Creek was complicated by complex interaction between wave and fluvial erosion processes. Lack of geographic points

that could be used to estimate erosion rate from historical photos created further uncertainties for prediction of erosion risk in the Euchre Creek area.

4) Hazard zones on dune-backed beaches were determined from a geometric model, whereby erosion occurs when the total water level produced by the combined effect of extreme wave runup (R) plus the tidal elevation (ET), exceeds some critical elevation of the fronting beach, typically the elevation of the beach-dune junction (EJ). Three scenarios were used to model erosion hazard zones on dune-backed beaches:

   - *Scenario 1* **(HIGH risk)**. This scenario is based on a large storm wave event (wave heights ~41.3 ft high) occurring over the cycle of an above average high tide, coincident with a 3.3 ft storm surge. Under this scenario maximum potential erosion distances (MPED) ranged on average from **141 to 343 ft**, depending on beach slope of the particular dune-backed beach, lower slopes giving wider zones. These values approximately equal maximum shoreline variability observed between shorelines mapped in 1928, 1980-1982, and 2003.

The following two scenarios (MODERATE and LOW-risk events) are one of two "worst case" events identified for the study area. Both scenarios have low probabilities of occurrence.

   - *Scenario 2* **(MODERATE-risk)**. This scenario is based on an extremely severe storm event (waves ~43.3 ft high) coupled with a 5.6 ft storm surge on the same tide as Scenario 1. Under this scenario average MPED ranged from 239 to 587 ft.

   - Scenario 3 (LOW-risk) is the second "worst case" scenario, and is the same as scenario 2, but incorporating a 6.2 feet (1.9 m) subsidence from a Cascadia subduction zone earthquake. MPED estimated for scenario 3 ranged on average from 350 to 1036 ft.

5) Hazard zones on bluff-backed shorelines were mapped based on an understanding of several geological parameters including bluff erosion rates, potential for block failures, and empirically determined angles of repose for the bluff materials. Three risk zones were mapped:

   - Scenario 1 (HIGH-risk) portrays the zone of bluff retreat that would occur if only gradual erosion at a relatively low mean rate were to occur after the slope reaches and maintains its ideal angle of repose (for talus of the bluff material). The time interval of erosion was assumed to be 60 years. The width of the high-risk hazard zone generally ranged from 20 to 78 ft wide, depending on the type of geology. In one small area at the south end of Nesika Beach local erosion data supported a width of 114 ft. Where slopes were steeper than the angle of repose for talus of the bluff material, the zone width was increased by the lateral distance necessary to accommodate retreat to the angle of repose.

   - Scenario 2 (MODERATE risk) portrays an average amount of bluff retreat that would occur from the combined processes of block failures, retreat to an angle of repose, and erosion for ~60-100 years. The moderate-risk hazard zone boundary was placed halfway between the high- and low-risk boundaries, and resulted in bluff retreat that generally ranged from 40 to 735 ft, depending on the type of geology.

- o Scenario 3 (LOW risk) illustrates a "worst case" for bluff retreat in ~60-100 years. This zone accommodates a maximum bluff slope failure, subsequent erosion back to its ideal angle of repose, and gradual bluff retreat for ~100 years. For bluffs composed of Pleistocene marine terrace deposits and paleosols, an additional retreat of the bluff top in response to subaerial erosion is achieved by making sure that the projected bluff top retreat corresponds to at least a 50 percent factor safety for the ideal slope of repose of 1.5 horizontal to 1 vertical (i.e., a 2:1 slope). Low-risk hazard zone widths ranged from 60 to 1450 ft wide, depending on the type of geology. The largest zone width occurred in an area of unusually large slide blocks in the highlands east of Sisters Rocks.

6) In all cases, the minimum risk zone width that could be mapped at the scale of the base maps is 20 feet, so even hard rock bluffs (generally headlands) or dune-guarded bluffs with negligible (subaerial) erosion rates on the order of –0.1 ft/yr were assigned zones with this minimum width. Risk zones in these areas have high-, moderate-, and low-risk zones of 20 feet each mapped east of the Active Hazard Zone (total of 60 feet).

7) An analysis of maximum single slide block failure width revealed that maximum width increases with bluff height but at different rates in bluffs of different composition. The two main types of bluff are high bluffs of Mesozoic metamorphic and sedimentary rock in the Sisters Rocks area and much lower bluffs to the south. The bluffs to the south are composed of similar but less erosion resistant rocks that were beveled off by Pleistocene marine transgressions. These lower bluffs are capped by poorly consolidated Pleistocene marine terrace deposits prone to slope failure from both wave undercutting and groundwater effects. Linear regression equations for all bluff types were developed from empirical data to estimate maximum block failure width from bluff height.

8) Large landslides with single block failures hundreds of feet wide are limited to the high bluffs of Mesozoic rocks in the Sisters Rocks area. Lower bluffs at Nesika Beach composed of highly fractured Mesozoic rocks overlain by poorly consolidated Quaternary sedimentary deposits did not form large landslides but failed in small slumps up to ~35 feet wide. Landslides with single block failures intermediate in size between these two extremes characterized bluffs at pocket beaches between Nesika Beach and Otter Point where bluffs are somewhat higher than at Nesika Beach.

9) Low bluffs capped by poorly consolidated Pleistocene marine and colluvial deposits at Nesika Beach have wave erosion rates that are some of the highest yet documented for Oregon coastal bluffs. Rates of -1.6 to -1.9 ft/yr are typical of this area; hence building close to the edge of the bluff there is particularly hazardous.

10) The bluffed coastline between Nesika Beach and Otter Point is characterized by erosion rates on the order of -0.5 ft/yr, which is similar to rates measured on sand-starved pocket beaches in Lincoln County. While these bluffs are similar in overall geology to the bluffs at Nesika Beach, there is clearly more hard rock in the geologic section, which consequently lowers the rate of coastal retreat.

11) Local field observations indicate that a large but undefined proportion of the bluff retreat measured by comparison of 1967, 1939 and 2003 historic photos between Nesika Beach and Otter Point probably occurred over the last 20 years owing to episodic wave and storm events. This 20-year erosion rate is not known, but if it is considerably higher than rates documented from historical photography and characterizes future rates, then the width of mapped erosion risk zones could be too low.

12) The report (and geographic information system files) identifies active and potentially active landslides. All of the mapped landslides should be considered unsuitable for development without extensive remediation, unless a site-specific investigation can demonstrate that proposed development sites are not within an active portion of the landslide feature and have a low risk of being impacted.

13) The erosion risk zones probably overestimate actual erosion risk to areas east of Highway 101 embankments, because any erosion to the highway will probably be repaired.

2.0 INTRODUCTION

The Oregon Department of Geology and Mineral Industries (DOGAMI) has been commissioned by Curry County to carry out an assessment of existing and potential coastal erosion and landslide hazards along the shoreline from the North Jetty at Gold Beach 12.6 miles north to the north side of Sisters Rocks (Figure 1). It should be stressed that this is a regional investigation and is not intended for use as a site-specific analysis tool. However, the investigation can be used to identify areas in need of more detailed site-specific geotechnical studies.

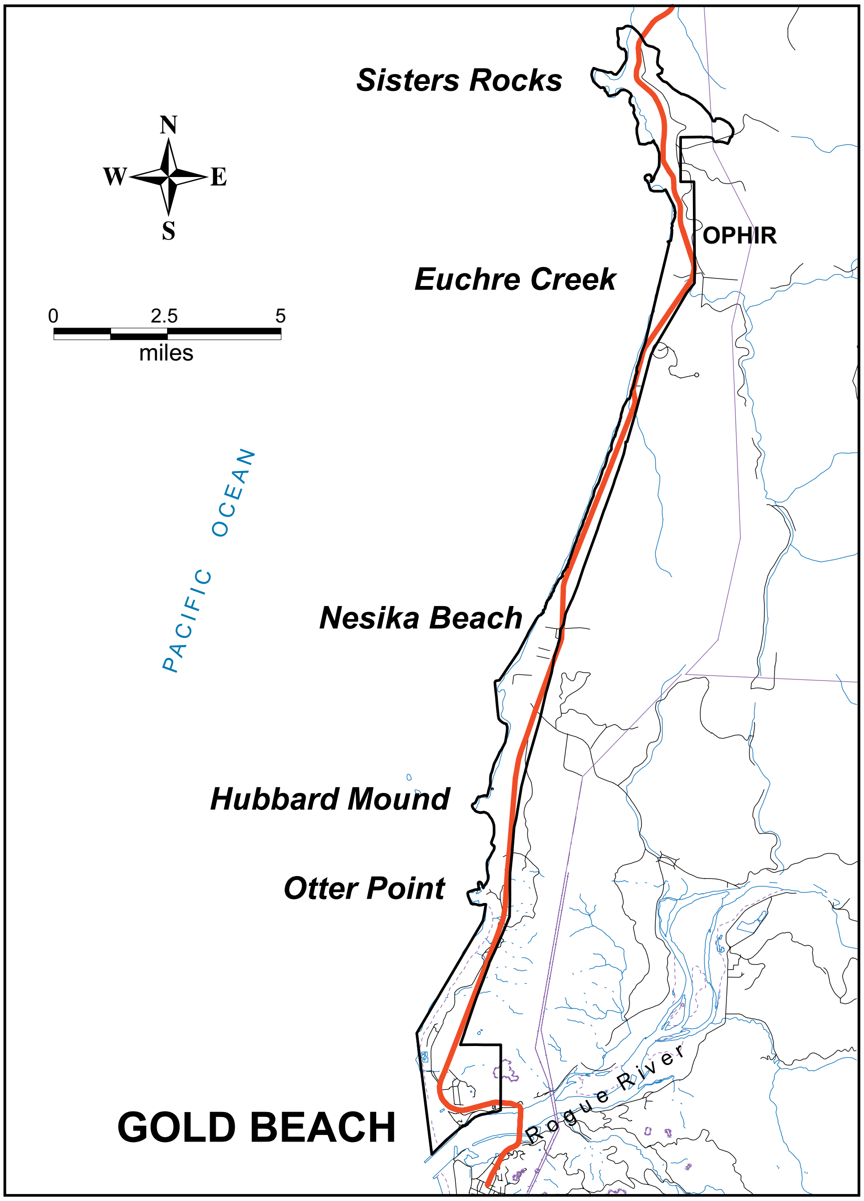

The response of coastal shorelines in the form of erosion or accretion is exceedingly sensitive to a multitude of complex factors that include the beach sediment budget, wave energy, water-level fluctuation, near-shore morphology, shoreline orientation, and the geology. Because many shorelines are composed of unconsolidated sediments, including significant stretches of the Oregon coast, they are able to respond rapidly and are among the most dynamic and changeable of all landforms. It is this dynamism at the coast that makes beaches such integral and important landforms as they moderate the effects of wave energy. Beaches and dunes, therefore, provide an essential buffering mechanism, protecting properties and infrastructure from wave attack. Notwithstanding this, because bluffs are also characteristic of much of the Oregon coast, erosion of these features is often accelerated by large storms during the winter months due to removal of beach sediment from the base of the bluffs. This process enables waves to directly attack the bluff toe, causing it to be undercut. Eventually, the bluff begins to retreat, either gradually

Figure 1. Map showing location of the study area. Heavy line shows extent of project area covered by digital geographic information files containing data on geology, landslides, and erosion hazards. Erosion information covers only open coastal (versus estuarine or river) areas and is mapped only in areas with base map coverage from 2003 color orthophotos.

or in the form of major landslides that can cause catastrophic loss of property. These problems may be exacerbated by earthquakes, extreme rainfall events and associated high groundwater levels that can trigger landslides, regardless of wave erosion.

Increasingly, the natural response of coastal shorelines to erode has come into conflict with the "built" environment due to the rapid growth in population and increased urbanization of coastal margins. Such development is characteristic of much of the Oregon coast, including significant sections of the Curry County shoreline (e.g., Nesika Beach and Gold Beach), and is the product of escalating property values and the desire to establish infrastructure as close as possible to the ocean's edge (Schlicker and others, 1973; Komar, 1997; Priest, 1999). Once the properties are established, the expectation is that the coast will remain where it is. Clearly, for sensible shoreline management to occur, sufficient technically sound information on the likelihood and magnitude of shoreline change must be provided to decision makers so they can make informed choices regarding shoreline management practices. That is the objective of this investigation.

3.0 METHODS

The erosion hazard mapping methods used here are substantially the same as those used by Allan and Priest (2001) for Tillamook County and Priest and Allan (2004) for northern Lincoln County. A variety of approaches have been used to define coastal erosion hazard zones in the project area. In particular, significant time was spent during the summer of 2003 examining the area in the field, mapping shoreline geology and determining the degree of activity of coastal landslides. All map data have subsequently been incorporated into MAPINFO, Geographic Information System (GIS) software. Digital files of all vector and point data were also translated into ArcView (shape file) format in two map projections, Oregon State Plane Southern Zone, 1983 feet and Oregon Lambert Conformal, 1997 feet (see Appendix C for summary of digital data files included on this disk). The following sections present in more detail the approaches that have been used to establish erosion hazard zones on dune- and bluff-backed shorelines.

3.1 Active Erosion Hazard Zone

An active erosion hazard zone (AHZ) (Figure 2) was mapped for dune- and bluff-backed shorelines throughout the study area based on a combination of purely geomorphic observations, and from an analysis of historical shoreline positions. The AHZ is the least speculative of the designated coastal hazard zones since it depends on easily identifiable coastal features that may be seen on modern aerial photos supplemented with current field and topographic data. On

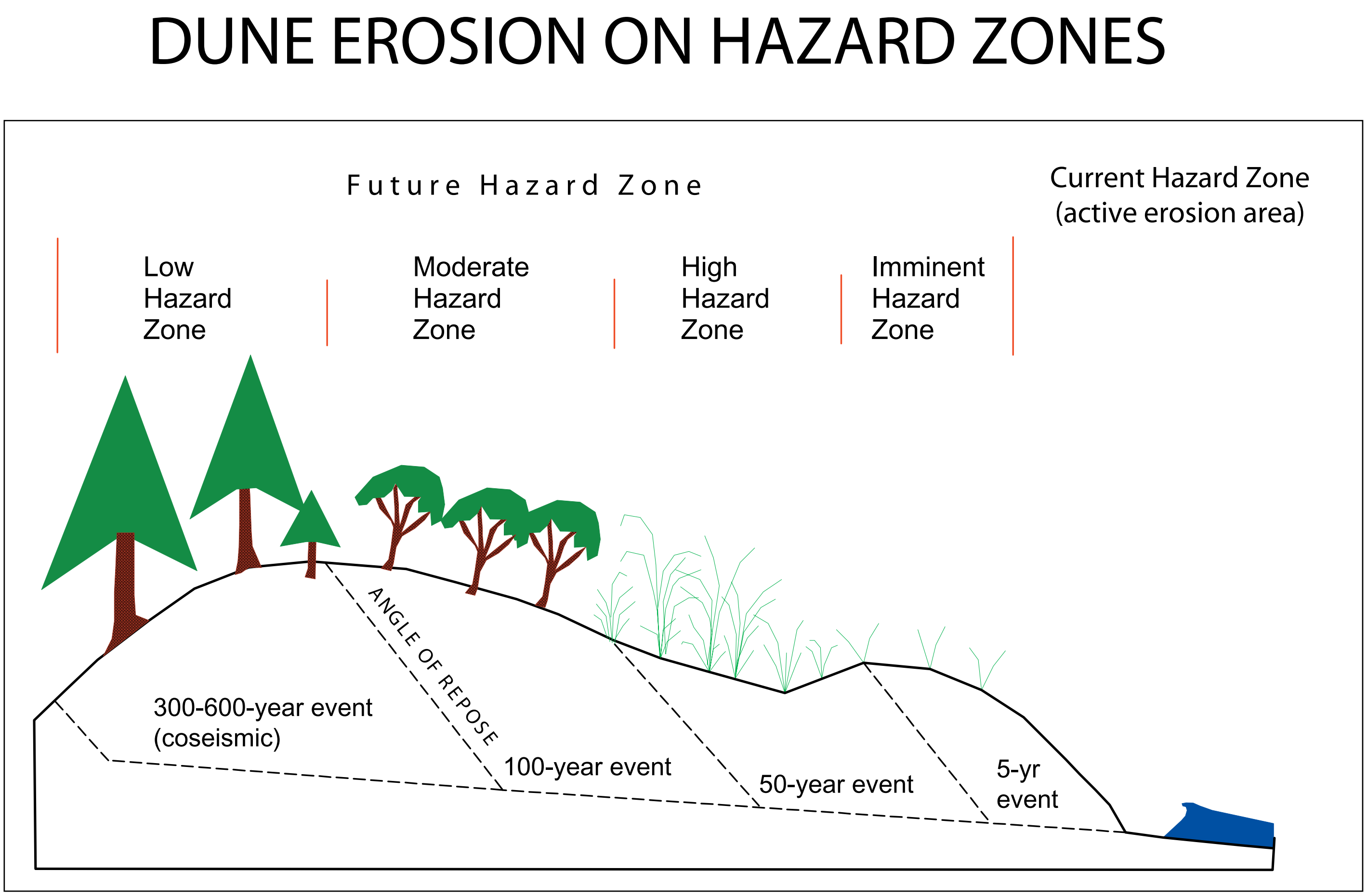

Figure 2. Schematic diagram showing possible dune erosion hazard zones.

dune-backed beaches, the AHZ distinguishes the zone of beach variability, a region in which beaches undergo considerable change (e.g., changes in the position of the shoreline (height and width) relative to some known datum point). Thus, it represents the portion of beach that is known to have changed in recent times due to large wave events and changes in sediment supply. It is, therefore, the zone that can be expected to change in the immediate future. As a result, there can be no doubt that building within the active hazard zone represents considerable risk. The landward boundary of the AHZ was drawn on the 2003 orthophotos at the top of the first continuously vegetated foredune.

It is important to note that the AHZ as defined here should not be confused with the "active dune" or "active foredune" used by State regulators (e.g., OCZMA, 1979; DLCD, 1995). For example, OCZMA (1979) defines the Active Foredune as those dunes that possess insufficient vegetative cover to retard wind erosion, while Goal 18 (Beaches and Dunes) of Oregon's Statewide Planning Goals and Guidelines prohibits the residential and commercial development of beaches and active foredunes (DLCD, 1995).

On bluff-backed beaches the AHZ was mapped from the shoreline to the top edge of bluffs, sea cliffs, and the headwall of active, or potentially active shoreline landslides. Consistent with the view held for dune-backed shorelines, building within the active hazard zone along bluff-backed shorelines also reflects considerable risk from direct wave attack at the bluff toe or from slope instability.

The seaward boundary of the AHZ was established as the mean high water level (MHWL) derived from an analysis of the NOS T-sheet shoreline positions and from LIDAR data. This approach is discussed further below. These data were also used to identify the AHZ around the mouths of the estuaries.

Supplementary mapping of the AHZ was carried out through field reconnaissance. All map data were then transferred by inspection using MapInfo software to standard color digital orthophotos produced for the project in 2003. Some interpretation was needed when mapping the AHZ around the mouths of rivers and creeks with abundant sediment supply to the beach. In particular, where considerable accretion has occurred, we drew the landward boundary at the top of the first major foredune, even if only sparsely vegetated.

The maximum extent of shoreline variability on dune-backed beaches can also be estimated from oceanographic factors using empirical modeling techniques rather than direct geomorphic observations. The advantage of these techniques is that they can depict erosion events that may be difficult or impossible to define by geomorphic field observations of the effects of past erosion events. An example is sea level rise, which to some extent makes all past storm events and even coseismic subsidence events, somewhat less erosive than equivalent events in the future. The geometric model of Komar and others (1999) will be used in this investigation.

3.2 Dune-Backed Shorelines

3.2.1 The Geometric Model

For property erosion to occur on sandy beaches, the total water level produced by the combined effect of wave runup (*R*) plus the tidal elevation (E_T), must exceed some critical elevation of the fronting beach, typically the elevation of the beach-dune junction (E_J). This basic concept is depicted in Figure 3, and in an expanded form as the geometric model in Figure 4. Clearly, the more extreme the total water level elevation, the greater the resulting erosion that occurs along both dunes and bluffs (Komar and others, 1999).

As can be seen from Figure 4, estimating the maximum amount of dune erosion (DE_{MAX}) is dependant on identifying the total water level elevation, T_{WL}, which includes the combined effects of extreme high tides plus storm surge plus wave runup, relative to the elevation of the beach-dune junction (E_J). Therefore, when the $T_{WL} > E_J$ the beach retreats landward by some distance, until a new beach-dune junction is established, whose elevation approximately equals

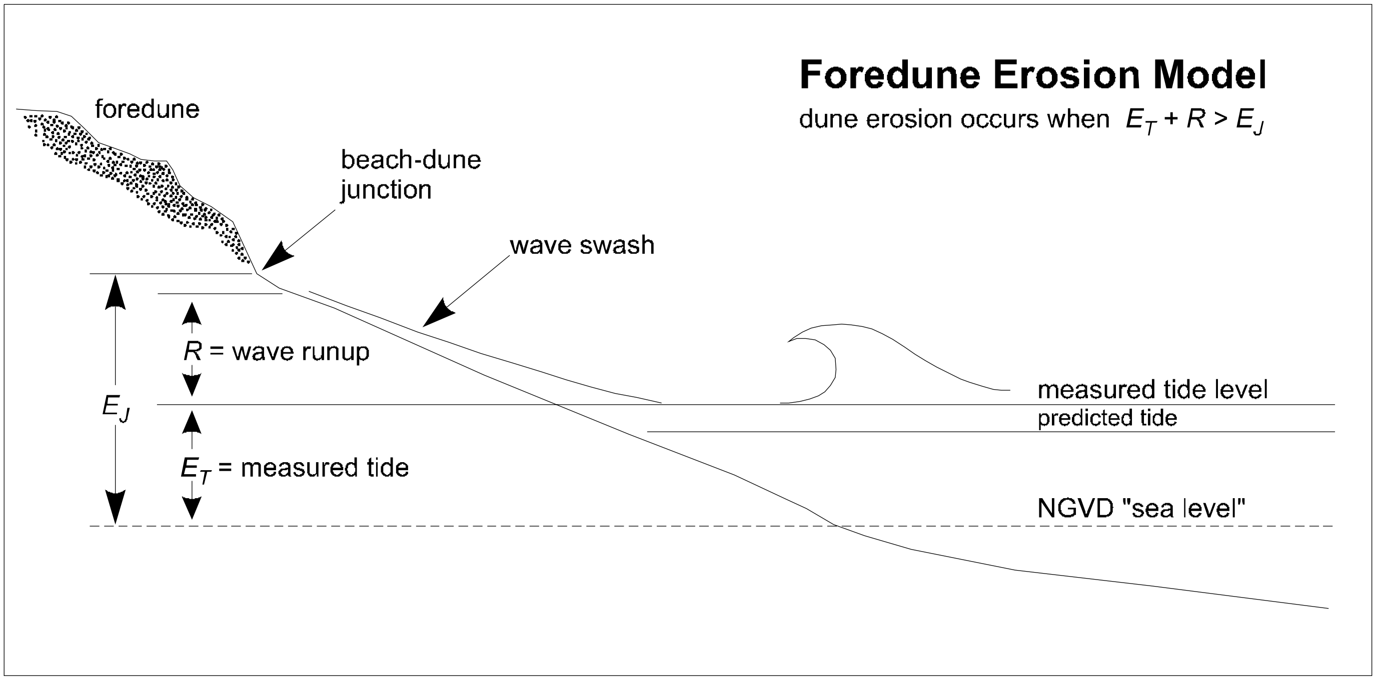

Figure 3. The foredune erosion model (Komar and others, 1999). NGVD '88 = national geodetic vertical datum of 1988.

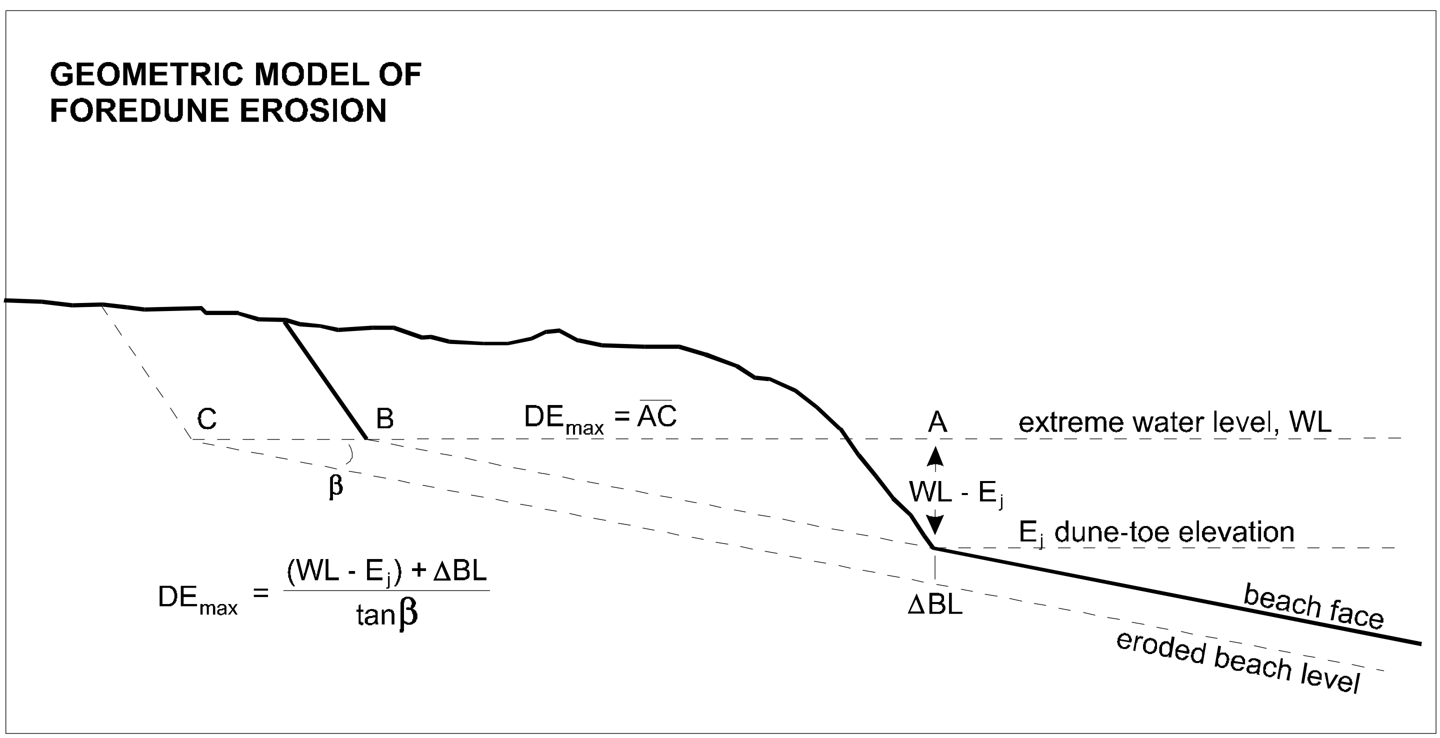

Figure 4. The geometric model used to assess the maximum potential beach erosion in response to an extreme storm (After Komar and others, 1999).

the extreme water level. Since beaches along the high-energy Oregon coast are typically wide and have a nearly uniform slope (*tan ß*), the model assumes that this slope angle is maintained, and the dunes are eroded landward until the dune face reaches point B in Figure 4. As a result, the model is geometric in that it assumes an upward and landward shift of a triangle, one side of which corresponds to the elevated water levels, and then the upward and landward translation of that triangle and beach profile to account for the total possible retreat of the dune (Komar and others, 1999). An additional feature of the geometric model is its ability to accommodate further lowering of the beach face due to the presence of a rip current. This feature of the model is represented by the beach-level change ΔBL shown in Figure 4, which causes the dune to retreat some additional distance landward until it reaches point C. As can be seen from Figure 4, the distance from point A to point C depicts the total retreat, DE_{max}, expected during a particularly severe event that includes the localized effect of a rip current. Critical then in applying the model to evaluate the susceptibility of coastal properties to erosion, is an evaluation of the occurrence of extreme tides (E_T), the runup of waves (R), and the joint probabilities of these processes along the coast (Ruggiero and others, 2001).

3.2.1.1 Wave Runup

Detailed studies of wave runup along the Oregon Coast, under a range of wave conditions and beach slopes (Ruggiero and others, 1996; 2001), have yielded the following relationship

$$R_{2\%} = 0.27(SH_{SO}L_O)^{½} \quad (1)$$

for estimating the 2% exceedence runup (R) elevation, where S is the beach slope (*tan ß*), H_{SO} is the deep-water significant wave height, L_O is the deep-water wave length given by $L_o=(g/2\pi)T^2$ where T is the wave period, and g is acceleration due to gravity (9.81 $m.s^2$). Therefore, estimates of the wave runup elevation depend on knowledge of the wave heights and periods. Since a major objective of this investigation is to estimate the maximum potential erosion (DEmax) that may occur in response to sustained periods of wave attack during extreme storm events (Figure 4), it is important to examine the probabilities of extreme wave occurrence offshore from the Pacific Northwest (PNW) coast.

Wave data (wave heights and periods) have been measured in the North Pacific using wave buoys and sensor arrays for almost 30 years. These data have been collected by NOAA, which operates the National Data Buoy Center (NDBC), and by the Coastal Data Information Program (CDIP) of Scripps Institution of Oceanography. Previous analyses of these data through 1996 by Ruggiero and others (1996; 2001) indicated that the projected 100-year extreme storm would generate a deep-water significant wave height on the order of 33 ft. However, during the 1997-98 El Niño that height was exceeded by one storm, and by four 100-year storms during the 1998-99 La Niña winter, with the March 2-3, 1999 storm having generated deepwater significant wave heights of 46 ft (Table 1). Since the major winters of 1997-98 and 1998-99, the Oregon coast has been subjected to an additional four 100-year storms.

For the purposes of this study, additional analyses have been undertaken of the extreme wave statistics at the Eel River NDBC wave buoy (#46022), located 30 miles west-southwest of Eureka, California and 100 miles south-southwest of Nesika Beach, Oregon. This particular buoy has been in operation since 1982 and thus has a relatively long record for analyses of extreme wave heights. In contrast, although the NDBC does have a buoy (#46015) located offshore from Port Orford (i.e., only 32 miles northwest of Nesika Beach), this particular buoy has only been operating for 2 years, which precludes it from analyzing the extreme wave statistics for this part of the coast. The decision to use the Eel River buoy over other buoys to the north is largely due to its proximity to Nesika Beach, its relatively long temporal record and because the wave climate offshore from southern Oregon/northern California lies in a transition zone with predominantly smaller waves to the south compared with waves measured in the north (Allan and Komar, 2000b).

Analyses of the extreme wave statistics was undertaken using the Coastal Engineering & Design Analysis System software using procedures described in Komar and Allan (2000). The results of the extreme wave analyses are presented in Table 2 and have been used in Equation 1 for the calculation of the maximum potential erosion distance for dune backed shorelines. For the 50-year event, the estimated extreme wave height shown in Table 1 represents about a 13 percent reduction in the extreme waves used in similar calculations along the central to northern Oregon coast (Allan and Priest, 2001; Priest and Allan, 2004), while the 100-year event reflects an 18 percent decrease in the estimated extreme wave. These changes are unlikely to result in significant changes to the calculated erosion hazard zones since Equation 1 shows a greater dependency on the peak spectral wave period (i.e., period squared) than on the significant wave heights.

Analyses have also been undertaken of the range of wave periods that are experienced in the eastern North Pacific (Komar and Allan, 2000). These data have been examined using joint-frequency graphs of the significant wave heights versus the spectral-peak periods, the latter being the region where most of the wave energy occurs. The analyses have revealed that the largest wave heights tend to correspond to spectral-peak periods that range from 15 to 17 seconds, with some storm events producing periods up to 20 seconds. Since Equation 1 is particularly sensitive to the magnitude of the wave period, we have focused on the longer period wave events in our modeling of wave runup elevations.

Table 1. Peak storm wave statistics for the Newport wave buoy for the major 1997-98 El Niño and 1998-99 La Niña winters and for the period 1999 to 2003.

Buoy #46050	*Date*	*Significant wave height (feet)*	*Wave Period (s)*	*Wave Breaker height (feet)*
El Niño (1997-98)	19-20 Nov.	34.5	14.3	38.4
La Niña (1998-99)	25-26 Nov.	35.4	12.5	37.1
	6-7 Feb.	33.1	12.5	35.4
	16-17 Feb.	32.8	20.0	42.3
	2-3 Mar.	46.3	16.7	51.8
La Niña (1999-00)	16-17 Jan.	39.7	14.2	43.0
2001/02	21-22 Nov.	33.8	16.7	40.0
	28-29 Nov.	35.1	14.3	38.7
2002/03	14 Dec	36.4	12.5	-

Table 2. Average extreme-wave projections based on data from four NDBC wave buoys located offshore the Pacific Northwest coast.

Projection (years)	*Extreme wave heights (feet)*
10	35.7
25	39.0
50	41.2
75	42.3
100	43.2

3.2.1.2 Tides

The elevation of the sea, in part controlled by the astronomical tide, is extremely important for the occurrence of beach and property erosion along the Oregon coast (Komar, 1986). This process is particularly enhanced when large waves are superimposed on top of elevated water levels, so that wave processes are able to reach much higher elevations on the shore. It is the combined effect of these processes that invariably leads to toe erosion on coastal dunes and bluffs, and eventually shoreline recession.

The actual level of the measured tide can be considerably higher than the predicted level provided in most standard tide tables, and is a function of a variety of atmospheric and oceanographic forces, which ultimately combine to raise the mean elevation of the sea. These latter processes also vary over a wide range of time-scales, and may have quite different effects on the coastal environment. For example, strong onshore winds coupled with the extreme low atmospheric pressures associated with a major storm, can cause the water surface to be raised along the shore as a storm surge. Along the PNW coast, the role of storm surges in coastal hazard applications has for the most part been ignored, largely because the storm surge elevations were thought to be quite small. For example, analyses of daily mean water levels up through 1996 at Newport, Oregon, revealed that the surges are typically of the order of 0.3 to 0.5 ft (Ruggiero and others, 1996). However, recent analyses of storm surges that occurred during the 1997-98 El Niño and 1998-99 La Niña winters revealed surges that were on the order of 1.3 to 2.0 ft, which suggest that much larger storm surge heights can be experienced along the PNW coast (Allan and Komar, 2002). As a result, any analysis of future coastal change should include a storm surge component.

Much longer-term processes that depend on offshore water temperatures and ocean currents can also influence the monthly-averaged water levels observed along the coast (Komar and Allan, 2000). In particular, analyses of the South Beach, Yaquina Bay tide gauge located in Newport, reveal a seasonal increase in mean water levels along the Oregon coast that occurs between summer and winter. This seasonal rise in mean water levels is on the order of 0.7 to 1.3 ft, and is a function of changes in the water temperature and effects from ocean currents (Komar and others, 2000). As noted earlier, major climate events such as El Niños can also have a dramatic impact on water level elevations along the U.S. West Coast. For example, during the 1982-83 El Niño, water levels along the Oregon coast were raised by about 1.6 ft, and remained elevated for several months (Huyer and others, 1983). These findings were reinforced in a subsequent investigation of water levels during the 1997-98 El Niño by Komar and others (2000).

To accommodate the huge variability in tidal elevations experienced along the Oregon coast, an extreme value analysis (similar to that used to estimate the probabilities of the extreme wave heights) has been used to analyze the tidal elevations for the South Beach, Yaquina Bay tide gauge (Shih and others, 1994; Ruggiero and others, 1996; 2001). Table 3 presents the 5- through 100-year expected extreme tide levels (ET) determined for the South Beach, Yaquina Bay tide gauge. These data are referenced to the National Geodetic Vertical Datum of 1929 (NGVD'29) datum. As can be seen from Table 3, the expected 50- and 100-year tide is on the order of 8.2 ft, and likely includes the effects of an El Niño. Furthermore, it is apparent from Table 3 that there is in effect little difference in the extreme tidal elevations estimated for the 5- through 100-year expected tides, with the difference amounting to only about 1.0 ft.

Table 3. Extreme annual tides (Shih and others, 1994). Note all elevations are relative to the NGVD'29 datum.

Projection (years)	*Mean water elevation (feet)*
5	7.2
10	7.5
25	7.9
50	8.2
100	8.2

3.2.1.3 Relative Sea Level Rise

Long-term trends in the level of the sea can also be identified along the Oregon coast, which relate to the global (eustatic) rise in mean sea level that has been occurring over the past several thousand years. However, these changes in mean sea level are complicated due to on-going changes in the level of the land that are also occurring along the Oregon coast. For example, Vincent (1989) and Mitchell and others (1994) demonstrated that the southern Oregon coast is rising at a faster rate than the global rise in mean sea level, whereas the northern Oregon coast is being slowly submerged by the rise in mean sea level (Figure 5).

There is no local tide gauge data at Gold Beach that could be used to estimate long term sea level rise. Cabanes and others (2001) measured a global sea level rise rate of 3.2 ± 0.2 mm/yr from 1993 to 1998 using satellite altimetry data. Tectonic uplift in the Nesika Beach area is ~3.35 mm/yr based on geodetic leveling data of Mitchell and others (1994, p. 12,273, Figure 5). Relative sea level rise should therefore be ~-0.15 mm/yr (sea level falls), or –0.03-0.05 feet in 60-100 years. Given the relatively large errors in the Mitchell and others (1994) geodetic data, relative sea level rise is effectively zero and will be ignored as a factor.

An earthquake will eventually release the elastic strain component of the tectonic uplift, resulting in sudden sea level rise. A subduction zone earthquake of about moment magnitude 9 could cause 6.2 feet (1.9 m) of subsidence according to a fault dislocation model of Priest and others (2003; digital file def_1A_II.bp.txt). Such subsidence will persist for a number of years and will accelerate coastal erosion, especially on dune-backed shorelines.

3.2.1.4 Beach Morphology

Having described the various process elements that are required as input into the geometric model, it remains for the morphological variables of the beach to be determined. These last variables include determinations of the beach slope (tan ß) and the beach-dune toe elevation (EJ).

A remote sensing technology, LIDAR, was used to assess the morphology of beaches in the fall of 2002. These data were obtained from the United States Geological Survey (USGS). The LIDAR data consists of x, y, and z values of land topography that are derived using a laser ranging system mounted on board a De Havilland Twin Otter aircraft. To measure the coastal

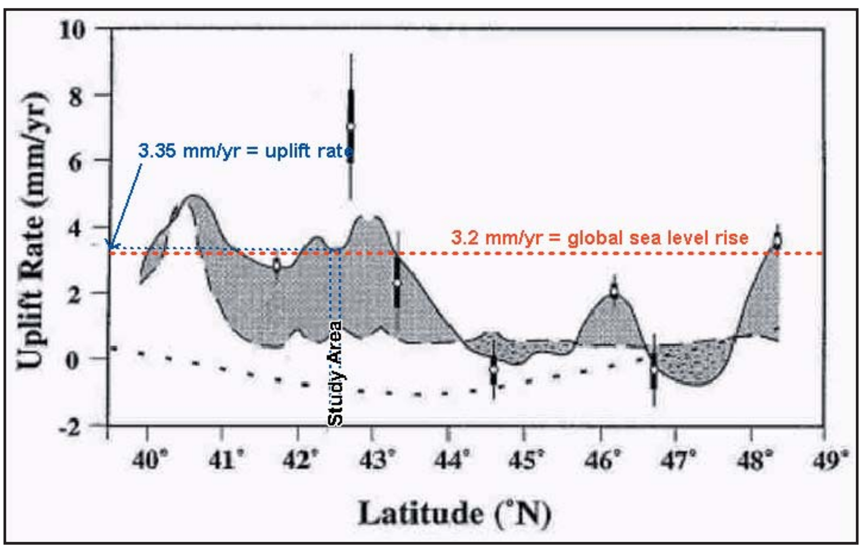

Figure 5. Uplift rate along the Oregon coast, measured by geodetic surveys (solid black line) relative to uplift measured from tide gauges (points with error bars) and long term uplift inferred from elevation of Pleistocene marine terraces (dashed black line). Blue dashed lines show uplift rate of the study area (42.423 and 42.563 N Latitude), which is essentially equal to global sea level rise (red dashed line). Large dotted black line is an approximate cross section from the map of estimated North American post-glacial rebound by Peltier (1986). The elevation changes are relative to the geodetic mean sea level, with positive values representing a rise in the land, while negative values represent the progressive subsidence. Stippled regions are inferred to represent elastic strain accumulation; note that some areas will go up (coarse stippling) and others will go down (fine stippling), when this strain is released during an earthquake. The study area is an area of current tectonic uplift and significant coseismic subsidence. Graph is modified slightly from Mitchell and others (1994).

topography, the aircraft flies at an altitude of approximately 700 meters at a rate of about 60 $m.s^{-1}$, and surveys a several hundred meter wide swath of the shoreline, acquiring a value of the surface elevation every few square meters (USGS, 2000). Subsequent analyses of the LIDAR data by NOAA staff have revealed that the data have a vertical accuracy within ±0.5 ft, while the horizontal accuracy of these measurements are within ± 2.6 ft. As noted by the USGS, use of LIDAR enables hundreds of kilometers of coastline to be mapped in a single day, with data densities that are unsurpassed using traditional survey technologies. Furthermore, subsequent survey runs using the same system can provide unprecedented data, which may be used to investigate the magnitude, spatial variability, and causes of coastal changes that occur during severe storms. All LIDAR data were in the 1983 Oregon State Plane Coordinate system, while the elevations were relative to the North American Vertical Datum of 1988 (NAVD' 88).

3.2.2 Scenarios of Coastal Change

The previous sections have described the ranges of variables required for input into the geometric model. This section discusses the three scenarios used for modeling maximum potential erosion distances (MPED) on dune-backed beaches in the study area.

Figures 4 and 5 reveal that the measured tides (E_T) and the wave runup levels (R) calculated from Equation 1 are combined to yield a total water level (T_{WL}) elevation, which is then input into the geometric model. When T_{WL} exceeds the elevation of the beach-dune toe, erosion occurs and the dune retreats landward until a new beach-dune toe is established, which approximately equals the total water elevation caused by the storm. However, the addition of the measured tides and wave runup components together, e.g., the 50-year runup level combined with the 50-year tide, is not as straightforward as it seems, due to the fact that these processes have been found to operate independently from each other (Komar and others, 1999; Ruggiero and others, 2001). In other words, the occurrence of an extreme storm does not necessarily mean that it will occur concurrently with an extreme tide. As a result, because both variables are occurring independently, it is necessary to consider their joint probabilities of occurrence, which is the product of the two individual probabilities. Thus, a 50-year runup level combined with a 50-year tide would yield a joint return period of about 2,500 years (50 x 50 = 2500 years). To some degree, one can get around this problem by applying various combinations of the extreme tides plus the wave runup elevations. For example, a 50-year storm runup event may be combined with a 2-year extreme tide to yield a 100-year total water level. A better approach might be to evaluate the total water levels associated with particular storms, the combined mean-water level (tides + surge + El Niño effects) and the wave runup, and then analyze the probabilities of these levels (Komar and others, 1999). Analyses of this type however, have yielded values that closely approximate those derived using the approach that sums the individual values, suggesting that either technique is useful. Finally, it should be noted that the analyses of extreme water levels undertaken previously (Shih and others, 1994; Ruggiero and others, 1996; 2001), excludes the most recent high water levels generated during the 1997-98 El Niño and 1998-99 La Niña winter. As a result, future efforts are planned to better establish the total water levels that may be experienced along the Oregon coast.

The LIDAR data were analyzed using a triangulation approach to generate a grid data set. This process was accomplished using VERTICAL MAPPER (contour modeling and display software), which operates seamlessly within MAPINFO's GIS software. Having generated the grid data, detailed contour maps and cross-sections of the beach morphology could then be constructed. Identification of the beach-dune junction (EJ) was accomplished by inspection of the topographic maps contoured at intervals of two feet. Features used to distinguish the beach-dune junction included erosion scarps, major breaks in slope, or some combination. Average beach slopes west of the EJ were determined from representative cross sections across the detailed contour maps. Segments of shoreline with similar slope were identified and a these slopes were used in calculations of erosion from the geometric model.

In developing the three scenarios below, we have attempted to steer clear of such terminology as the 100-year extreme event, which can often be misconstrued. Instead, we have defined our scenarios according to high-, moderate-, and low-risk hazard zones, which respectively indicate decreasing probability levels of occurrence, with the high-risk scenario having the greatest chance of occurrence during the next 60 - 100 years. These time intervals are typical planning horizons of interest to coastal planners. Because of the difficulties of identifying the most appropriate combination of extreme high waves and tides, the following scenarios assume that a major storm occurs over the course of an above average high tide. This is consistent with the approach taken by Komar and Allan (2000) in developing their scenarios of high waves and water levels. Along the southern Oregon coast, the Mean Higher High Tide averages about 7.29 ft (2.22 m) relative to Mean Lower Low Water and is based on the Port Orford tide gauge. When converted to the NAVD'88 datum, this amounts to an elevation of 6.79 ft (2.07 m). Thus, when other variables are added to this, all of the elevations will be relative to the NAVD'88 datum.

<u>Scenario 1</u> describes a HIGH-risk hazard zone. The variables included in this scenario are:

- 41.3 ft (12.6 m) significant wave height,
- 17 second peak spectral wave period,
- 6.79 ft (2.07 m) Mean Higher High Tide,
- 1.31 ft (0.4 m) monthly mean water level,
- 3.28 ft (1.0 m) storm surge.

This particular scenario is similar to the 2-3 March 1999 La Niña storm, which caused widespread damage along the Oregon coast. The scenario assumes that a major storm occurs over the course of an above average high tide. To accommodate the monthly rise in mean water levels between summer and winter, an additional 1.31 ft has been added to the high tide. Furthermore, because the extreme storms that occurred during the 1997-98 El Niño and 1998-99 La Niña winter produced significant storm surges, we have included a 3.28 ft storm surge component as part of this scenario.

<u>Scenario 2</u> describes a MODERATE-risk hazard zone, and includes the following variables:

- 43.3 ft (13.2 m) significant wave height,
- 20 second peak wave period,
- 6.79 ft (2.07 m) Mean Higher High Tide,
- 1.31 ft (0.4 m) monthly mean water level,
- 5.58 ft (1.7 m) storm surge,
- 0.0 ft (0.0 m) sea level rise.

The MODERATE-risk hazard zone is one of two "worst case" scenarios. This particular scenario assumes that the rise in wave heights identified offshore from the PNW coast by Allan and Komar (2000a; 2000b; 2002) continues over the course of the next century. In effect, the 43.3 ft significant wave height used in this scenario is similar to the predicted 100-year storm wave shown in Table 2. The variables used to generate the water levels are the same as those shown in scenario 1, except that we have incorporated a larger storm surge component (5.58 ft). This combination of events has an extremely low probability of occurrence. However, the results are still useful in that they provide a landward limit of potential erosion (assuming no long-term trends in the coast) due to a particularly severe storm.

<u>Scenario 3</u> describes a LOW-risk hazard zone, and includes the following variables:

- 43.3 ft (13.2 m) significant wave height,
- 20 second peak wave period,
- 6.79 ft (2.07 m) Mean Higher High Tide,
- 1.31 ft (0.4 m) monthly mean water level,
- 5.58 ft (1.7 m) storm surge,
- 0.0 ft (0.0 m) sea level rise.
- 6.2 ft (1.9 m) lowering of the coast due to a Cascadia subduction zone earthquake.

The LOW-risk hazard zone is the second "worst case" scenario, and incorporates all of the variables used in scenario 2, but with the added feature of coseismic subsidence from a subduction zone earthquake. These events have been shown to occur in response to large earthquakes in the Cascadia margin, and have irregular recurrence intervals varying from 200 to 1000 years, averaging approximately 580 years (Atwater and others, 1995; Darienzo and Peterson, 1995; Atwater and Hemphill-Haley, 1997). These types of events can cause some parts of the PNW coast to be abruptly lowered by 0 – 6.6 ft (Peterson and others, 2000). As previously explained, 6.2 feet (1.9 m) of subsidence can be expected, according to the fault dislocation data of Priest and others (2003) for a ~moment magnitude 9 earthquake. Priest and others (2003) used this earthquake as a reasonable scenario event for use in tsunami hazard mapping of the Oregon coast.

3.3 Bluff-Backed Shorelines

3.3.1 Introduction

This section describes a methodology whereby four coastal erosion hazard zones can be drawn for coastal bluffs in this area. The basic techniques used here are modified from Gless and others (1998), Komar and others (1999), Allan and Priest (2001), and Priest and Allan (2004). The zones are as follows:

1) *Active hazard zone*: The zone of currently active mass movement, slope wash, and wave erosion.

2) The other three zones define high-, moderate-, and low-risk scenarios for expansion of the active hazard zone by bluff top retreat. Similar to the dune-backed shorelines, the three hazard zones depict decreasing levels of risk that they will become active in the future. These hazard zone boundaries are mapped as follows:

   a. *High-risk hazard zone*: The boundary of the high-risk hazard zone will represent a best case for erosion. It will be assumed that erosion proceeds gradually at a mean erosion rate for 60 years, maintaining a slope at the angle of repose for talus of the bluff materials.

   b. *Moderate-risk hazard zone*: The boundary of the moderate-risk hazard zone will be drawn at the mean distance between the high- and low-risk hazard zone boundaries.

   c. *Low-risk hazard zone*: The low-risk hazard zone boundary represents a "worst case" for bluff erosion. The worst case is for a bluff to erode gradually at a maximum erosion rate for 100 years, maintaining its slope at the angle of repose for talus of the bluff materials. The bluff will then be assumed to suffer a maximum slope failure (slough or landslide). For bluffs composed of poorly consolidated sand subject to direct wave attack, another worst case scenario will be mapped that assumes that the bluff face will reach a 2:1 slope as rain washes over it and sand creeps downward under the forces of gravity. For these sand bluffs, whichever method produces the most retreat will be adopted.

In order to understand how these zones are defined, it is useful to examine what variables are generally used for erosion hazard zone calculations and how they relate to the way bluffs actually erode.

3.3.2 The Bluff Retreat Model

Table 4 summarizes those variables that are generally used for calculating bluff erosion hazard zones (see Komar, 1997, Gless and others, 1998, and Komar and others, 1999 for further discussions), while Figure 6 illustrates those parameters, and one approach (of many) that may be used to map bluff hazard zones. Note that the major policy decisions used for delineating the hazard zones are:

1) Which hazard zones will be useful for planning, and;

2) What planning horizons (projected number of years in the future) should be used for erosion rate calculations.

To understand how to apply these factors, it is useful to discuss first how bluffs actually erode.
Bluff erosion generally occurs in the following steps:

1. Erosion of the bluff toe occurs in response to waves, and subaerial processes (weathering, slope wash, mass wasting, and wind erosion).

2. Slope failure occurs and blocks of various sizes may slide, fall, or topple. The final forcing event for failure may be a function of:

- The critical slope stability angle is exceeded;
- Exposure of weak rock layers in the bluff face;
- Unusually high ground water pressure (i.e. pore pressure);
- Stress-release fracturing (see Hampton, 2002, for explanation);
- Severe wave erosion event;
- Seismic shaking from an earthquake, or;

Table 4. Summary of bluff erosion data that can be used to calculate bluff hazard zones. Only maximum observed (empirical) block failure width is listed (versus most probable or average width), because this is generally the only empirical data that can be easily obtained in most areas. Quantitative slope modeling or regional empirical analyses would be required to establish a mean or most probable block failure width. Angle of repose refers to the ideal slope angle for unconsolidated talus of the bluff material.

Erosion Data	*Planning Horizon*	*Added to Account for Uncertainties*
Average Erosion Rate (ft/year)	x 60-100 years	+ error (1-2σ or some %)
Stable Slope Angle or Angle of Repose (Projected from the bluff toe to top)	Not applicable	+ error (generally 10-50%)
Maximum Block Failure Width (ft)	x number of blocks per 60-100 years	+ error (generally 10-50 %)

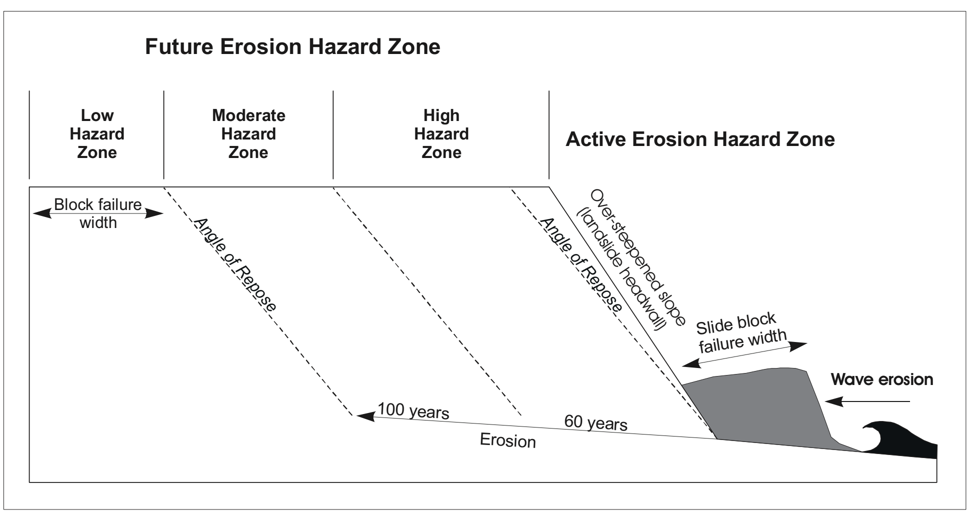

Figure 6. Schematic illustration of block failure on a bluff, angle of repose, and erosion rate in relation to possible hazard zones. These factors can be combined in a variety of different ways to produce hazard zones.

- Combination of any or all of the above factors.

3. The size of blocks that fall or slide is a function of the strength and the type of material, degree of weathering, its structure (bedding, jointing, faulting, and fracturing), and bluff height. If only small sloughs, topples, and falls of material occur, then the bluff will erode back gradually, maintaining a more or less constant slope angle until wave erosion is no longer effective in causing bluff retreat (Figure 7). Wave erosion generally keeps the slope steep enough so the forces tending to cause the bluff to suffer a slope failure are just balanced by the forces opposing failure; in other words, the ratio of these forces, or factor of safety, is equal to ~1.0. On the other hand, some bluffs subject to deep bedrock landslides retreat in a highly episodic fashion, resisting erosion for long periods and then failing in large slide blocks, once the factor safety decreases below 1.0[1].

4. Subaerial erosion (sheet wash, soil creep, etc.) becomes the main process of bluff retreat once waves cannot reach the bluff effectively, either because of slide debris or sand in front of the bluff or because the bluff has retreated so far that waves cannot reach the base. Where landslide debris continues moving seaward in front of the bluff escarpment or headwall, additional block failures at an unstable headwall can also occur. These failures may occur virtually in lock step with slide movement on highly unstable headwalls.

   If the toe of the bluff does get protected for an extended period of time and it is relatively resistant to large landslide failures, subaerial weathering, slope wash, and mass movement will erode the slope to progressively lower angles as talus accumulates in front of the bluff. This process will continue until the talus cone reaches the top of the bluff. At this point retreat of the bluff becomes extremely slow, and the slope will maintain an angle approximately equal to the angle of repose of the bluff material. Bluffs in this condition are generally vegetated from top to bottom. See the discussion below on angle of repose for examples of this process.

In drawing erosion hazard zones, we will endeavor to emulate these various modes of bluff retreat.

Predicting whether a particular part of a bluff will erode away over the life of a proposed development depends on understanding the influence of several parameters. These include:

- Bluff slope;
- Bluff height;
- Bluff material properties
- Vulnerability to stress-release fracturing;
- Groundwater level and resulting pore pressures;
- Surface water runoff;
- Wave climate;
- How much and what type of material is present at the toe of the bluff (e.g., slide debris, dune sand, logs, gravel, etc.) that can buttress the slope, dissipate wave energy, or, in some cases, act as ballistics that will erode the bluff;
- Whether any buttressing material is moving seaward (active slide blocks), and;
- Vegetative cover.

[1]The factor of safety is the ratio of forces resisting slope failure to forces promoting failure.

It is critical to understand that each bluff must be judged based on the local geology, likely future climate (rainfall and storms), and its current state of instability in the erosion cycle. Owing to limitations of this regional investigation, we will only be able to take into account parameters such as the bluff slope, height, material properties (rock or soil composition), and the historical response of broad classes of bluff to coastal erosion. **As a result, detailed, site-specific investigations are necessary to provide projections of the erosion hazard for a particular development on coastal bluffs. This report is no substitute for site-specific investigations.**

3.3.3 Data Used for Drawing Bluff Erosion Hazard Zones

3.3.3.1 Angle of Repose

Overall slope angles in the study area are ~34° ± 2º (1.5 horizontal: 1 vertical) or ~45° ± 2º (1:1). The former slope is characteristic of talus slopes in Quaternary marine terrace sediment or sheared Mesozoic sedimentary and metamorphic rocks, while the latter is for talus-laden slopes of hard rocks making up the headlands. The angle of repose for loose clean sand is 33° 41’, while 45° is the angle of repose for hard weathered rock (Merriman and Wiggin, 1947), so these values make sense for slopes composed of talus of these bluff materials.

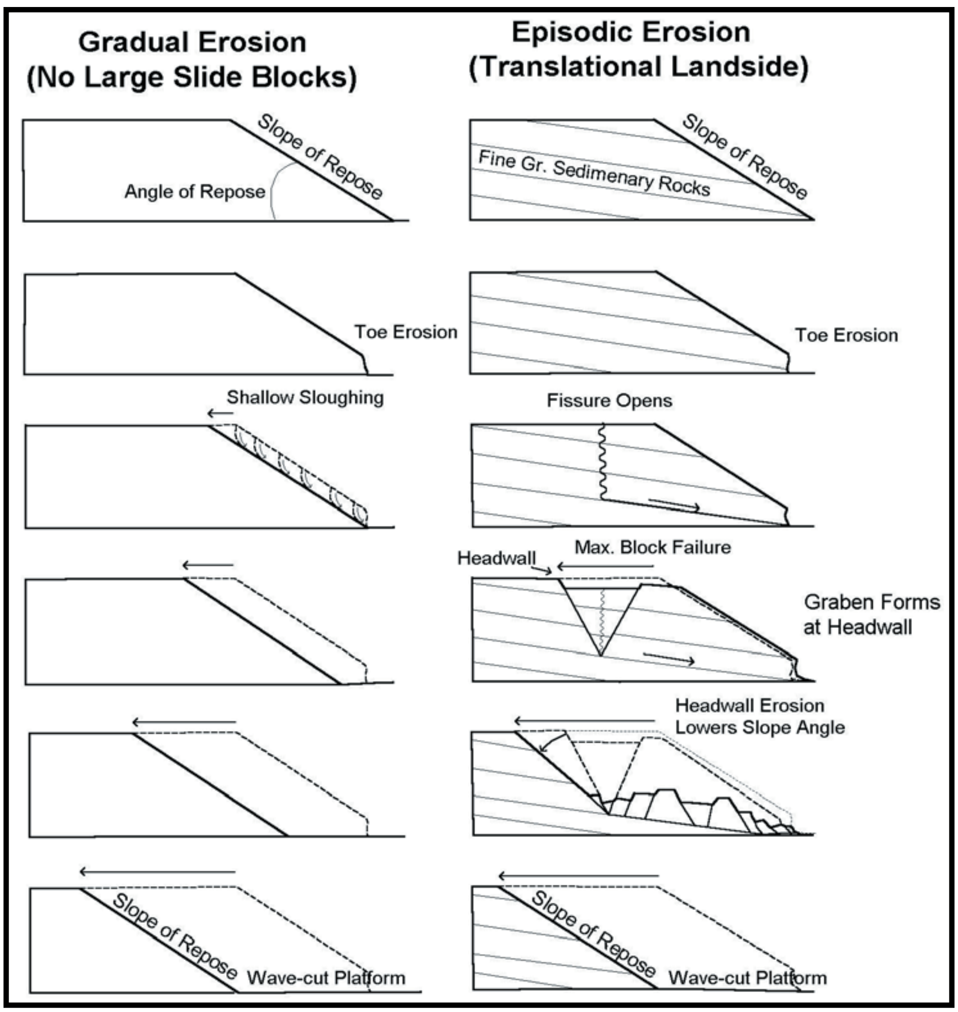

Figure 7. Gradual versus episodic bluff erosion. Note how the landslide toe position remains stable as the headwall retreats; hence erosion rate for bluffs with landslides is better measured at the headwall. Also note that the dangerous part of the bluff is much wider for the landslide-prone bluff, since another maximum block failure could occur at any point in the erosion cycle.

Vegetated, talus-laden slopes of Pleistocene marine terrace deposits overlying Otter Point Formation a mile south of Otter Point (Figure 8) are at a mean angle of 34° (1.5:1), while the same material more fully exposed to wave attack on the south side of Otter Point reaches an overall slope angle of 40-42° (Figure 9).

Near-vertical slopes in Quaternary sedimentary deposits erode in part by stress-release fracturing punctuated by periodic sloughing as groundwater seeps and wave attack undermine the slopes (Figures 9 and10). In all types of Pleistocene soil and sand deposits, there are local exposures near the top of the coastal bluff that tend to reach near-vertical slope owing to stress-release fracturing and cantilevered block falls[2] (Figures 8 and 9; see Hampton, 2002, for explanation). These failures are facilitated by reduction of cohesion from groundwater saturation (Hampton, 2002). Talus accumulation on the bluff face eventually shuts off this process; thereafter erosion is by gradual soil creep or episodic events like debris flows, undercutting by big storm wave events, or slide block failures (e.g., Figure 12). Where wave energy is sufficient to clean off talus and vegetation, the entire sea cliff can become near vertical (Figure 10). If continuously attacked by waves, such slopes will remain steep and never reach the angle of repose of the talus material.

The stress-release block fall process does not mean that larger block failures, either rotational slumps or translational slides, do not occur in these Pleistocene deposits. In fact slumps can be common in the same areas where gradual erosion by cantilevered block fall is occurring (Figure 12). That is why hazard zones

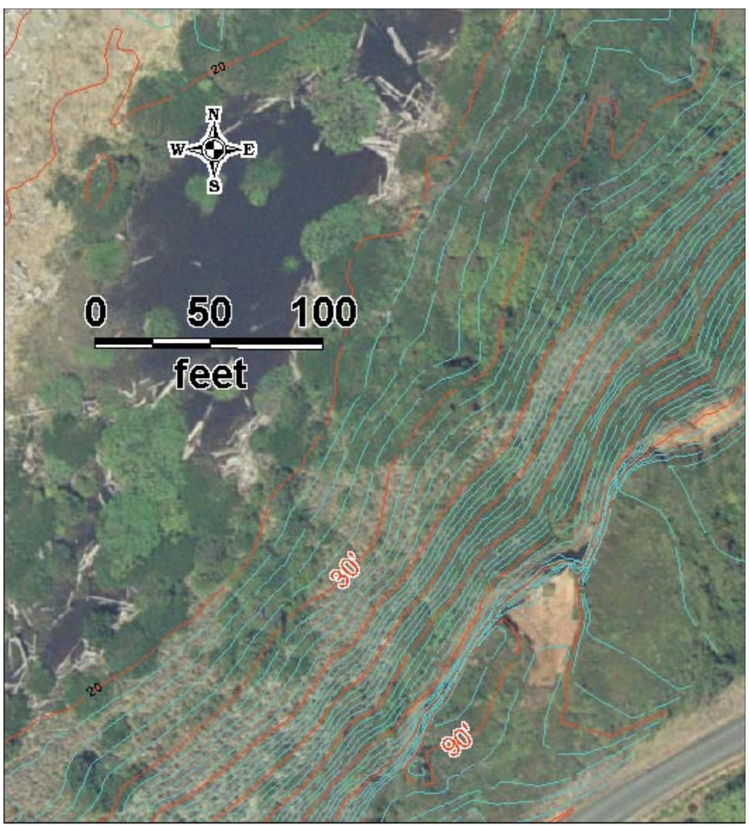

Figure 8. Vegetated bluff 1 mile south of Otter Point is completely protected from wave erosion by vegetated dunes (upper left). Bluff is composed of Pleistocene marine terrace deposits overlying Jurassic sedimentary rocks. Bluff face is mantled by talus lying at a 1.5:1 (horizontal: vertical) slope. Bluff is locally near vertical in upper ten feet where it is not mantled by significant talus. In these areas it probably erodes back by a combination of wind erosion, slope wash, and cantilevered block fall processes. Blue lines are topographic contours at intervals of two feet. Red lines are index contours at intervals of ten feet.

[2]According to Hampton (2002) cantilevered block falls are protrusions on the cliff face or thin tabular blocks that fall off and leave behind a near vertical cliff surface. The initial failures commonly leave an arch-shaped overhang. They occur in weakly lithified sea cliffs owing to release of horizontal confining stress as increasing groundwater saturation decreases sediment cohesion. Individual failures are generally less than 1 cubic meter and only the outer meter or so of sediment is removed in any one failure episode.

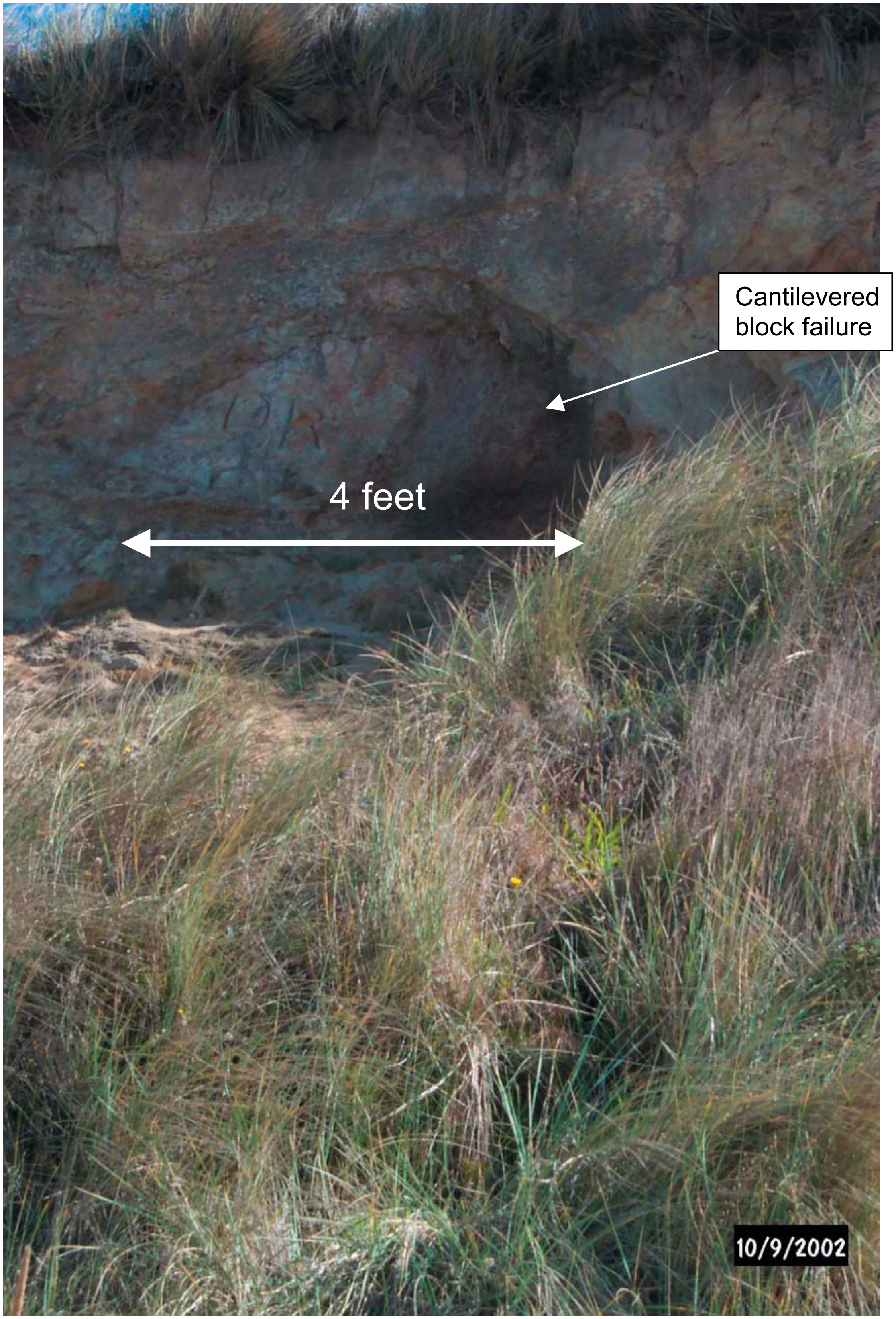

Figure 9. Close-up of scar of a cantilevered block in Pleistocene marine terrace sand at Nye Beach, Lincoln County, Oregon. The lower slope is vegetated talus at the angle of repose. Future retreat of the uppermost escarpment will add to the talus until the entire slope is at the angle of repose and the block falls stop.

Figure 10. Nesika Beach near vertical sea cliff of Pleistocene marine terrace deposits (horizontally bedded sand in the uppermost part of bluff) overlying sheared Jurassic sedimentary rocks (Figure 11). Cliff erosion is chiefly from undercutting by waves, groundwater-induced sloughing or slumping of the terrace deposits, and cantilevered block falls in terrace deposits. Wave attack is vigorous enough to remove talus except for very recent sloughing events (e.g., left foreground).

Figure 11. Sheared Jurassic mudstone and sandstone typical of the lower part of many bluffs in the study area. This material has little resistance to wave erosion or slope failure when it is as highly sheared as in this example. Shears are in so many different directions that bluffs are highly vulnerable to slope failure from rotational and translational landslides or block falls.

mapped in this investigation take into account block failures in addition to slope angle and gradual erosion rate.

Many hard rock cliffs are near-vertical and appear to have persisted in this condition with only minor erosion for many decades, even where fully exposed to wave attack at headlands (Figure 13). Clearly, these slopes are maintained by vigorous wave erosion that undercuts the bluff and removes talus. In sheltered areas, talus from hard metamorphic rocks in the study area maintains a slope of ~1:1 (Figure 14).

On bluffs with an existing landslide, the slope of repose was projected from the inferred base of the headwall landward to the bluff top using the techniques of

Figure 12. Slump block about 30 feet wide in Pleistocene paleosol, laminated carbonaceous clayey silt and sand deposits at Nye Beach. Note that cantilevered block falls are keeping the upper part of the bluff near vertical. Note also that this slump and the cantilevered block falls occurred on a well-vegetated slope. While the vegetation does not prove that wave undercutting did not trigger this slump, the vegetation is suggestive that waves were probably not the main factor for either type of failure. Groundwater saturation probably played a more significant role in this particular case.

Figure 13. Sisters Rocks area illustrating steep lower sea cliffs where waves have access at all times.

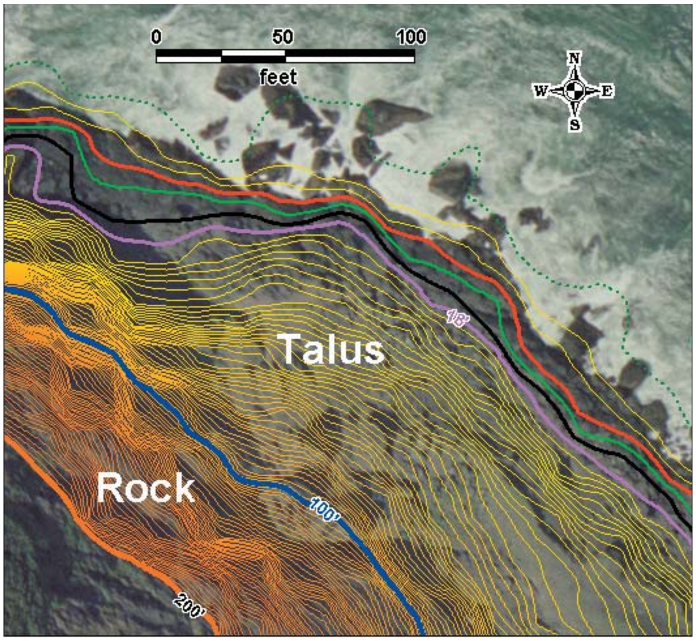

Figure 14. Partially sheltered north side of Sisters Rocks has talus slopes of broken hard metamorphic rock that average about 1:1, horizontal to vertical. Individual blocks up to 20 feet wide have toppled onto this talus slope from the steeper rock slope above. Orange and yellow lines are topographic contours at intervals of 2 feet derived from a 2002 LIDAR survey of this area by USGS.

Allan and Priest (2001, their Appendix D). The following formula or a graphical projection (Figure 15) was used for slides in the area:

$$S = R\,[D + H - (\tan\beta\,(D - L\tan\mu)/(\tan\beta - \tan\alpha))] \qquad 2$$

S = horizontal distance from the slide contact at the foot of the headwall to the projected intersection of the slope of repose behind the headwall
α = shear plane dip below the headwall = 60°
β = dip of the main slide plane beneath the slide block = 12° or 4.7:1
R = slope of repose (cotangent of angle of repose) for the headwall material = 1.5
H = Vertical height of the exposed headwall
D = (Elevation of slide top at foot of headwall) – (elevation at the slide toe)
L = Horizontal width of the slide mass from toe to its top at the foot of the headwall

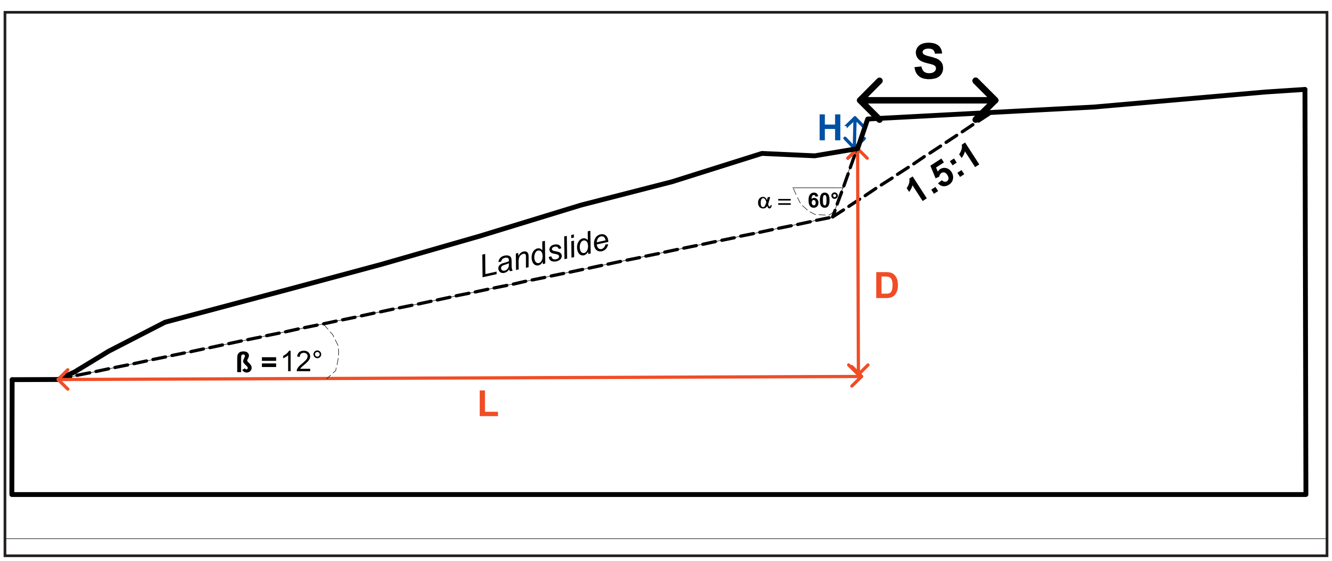

Figure 15. Projection of angle of repose for landslides.

Table 5. Slopes of repose by material type.

Bluff Material	*Slope of Repose (horizontal:vertical)*
Hard metamorphic rocks (headlands)	1:1
Highly sheared metamorphic and sedimentary rocks (pocket beaches)	1.5:1
Pleistocene marine terrace deposits, paleosols, colluvium, and alluvium	1.5:1

The 1.5:1 slope of repose is the value assumed for rocks typically found in the headwall of landslides in the area. The headwall shear plane dip of 60° and slide plane dip of 12° is based on the values given by Peterson and others (1998) for the Arizona Inn Landslide located 19 miles north of Gold Beach. This is the only well-studied landslide in the sheared Mesozoic rocks of the study area. Where geometry of local slides precluded using a 12° dip (e.g., hill slope <12° inclination), the slide dip was assumed to roughly parallel overall slope of the hillside underlain by the slide. This technique is consistent with the geometry of the Arizona Inn Landslide slip plane, which dips roughly parallel to the slide surface (see Peterson and others, 1998, p. 243).

3.3.3.2 Erosion Rate Data

3.3.3.2.1 Bluff Top Retreat

Time and funding for this project were insufficient to carry out a detailed analysis of mean rates of bluff top retreat from combinations of gradual toe erosion and episodic block failures. This type of analysis requires precise measurement of local bluff retreat on historical photos through detailed field measurements tied to geographic markers, and by rectification of historical photography. Owing to the infrequency of block failures, especially large ones, large observation times are necessary to establish an overall rate of retreat. The irregularity of bluff top retreat relative to bluff toe retreat over relatively short observation intervals is illustrated in Figure 16.

3.3.3.2.2 Bluff Toe Retreat

Methods: As illustrated in Figure 16, bluff toe retreat is a better estimate of gradual wave erosion not influenced by large block failures. In this study we treat block failure events as a separate variable, so it is important to obtain some estimate of gradual erosion of bluff toes not influenced by large (≥ ~40 feet-wide) blocks. We tried to establish some conservative estimates of these rates by rubbersheeting historical photography to modern orthophotos in areas that are fully exposed to wave action for large portions of the year, but we only found enough geographic points to do this accurately for the 1967 air photo of Nesika Beach (Figure 17). In this case a mean erosion rate for the entire shoreline segment was then calculated by weighting the east-west change in bluff toe position with the length of affected shoreline north-south (Table 6). We also estimated toe erosion at individual points along the shoreline by estimating air photo scale on 1939 and 1967 photos from local geographic data visible on 2003 orthophotos, and then measuring distances to the bluff toe from distinctive features like sea stacks. These point data were then compiled and mean values calculated. Both sets of erosion data are summarized in Table 6. Point data is also given in digital file **Cliff_Retreat_Meas_Sites.xls** (see Appendix C for summary of all digital data included with this report). For mapping erosion risk zones we will define a low and high erosion rate for geologically and geomorphically coherent bluff segments (Figure 17). No erosion data are available for bluff segments with shoreline protection or altered by emplacement of highway fill.

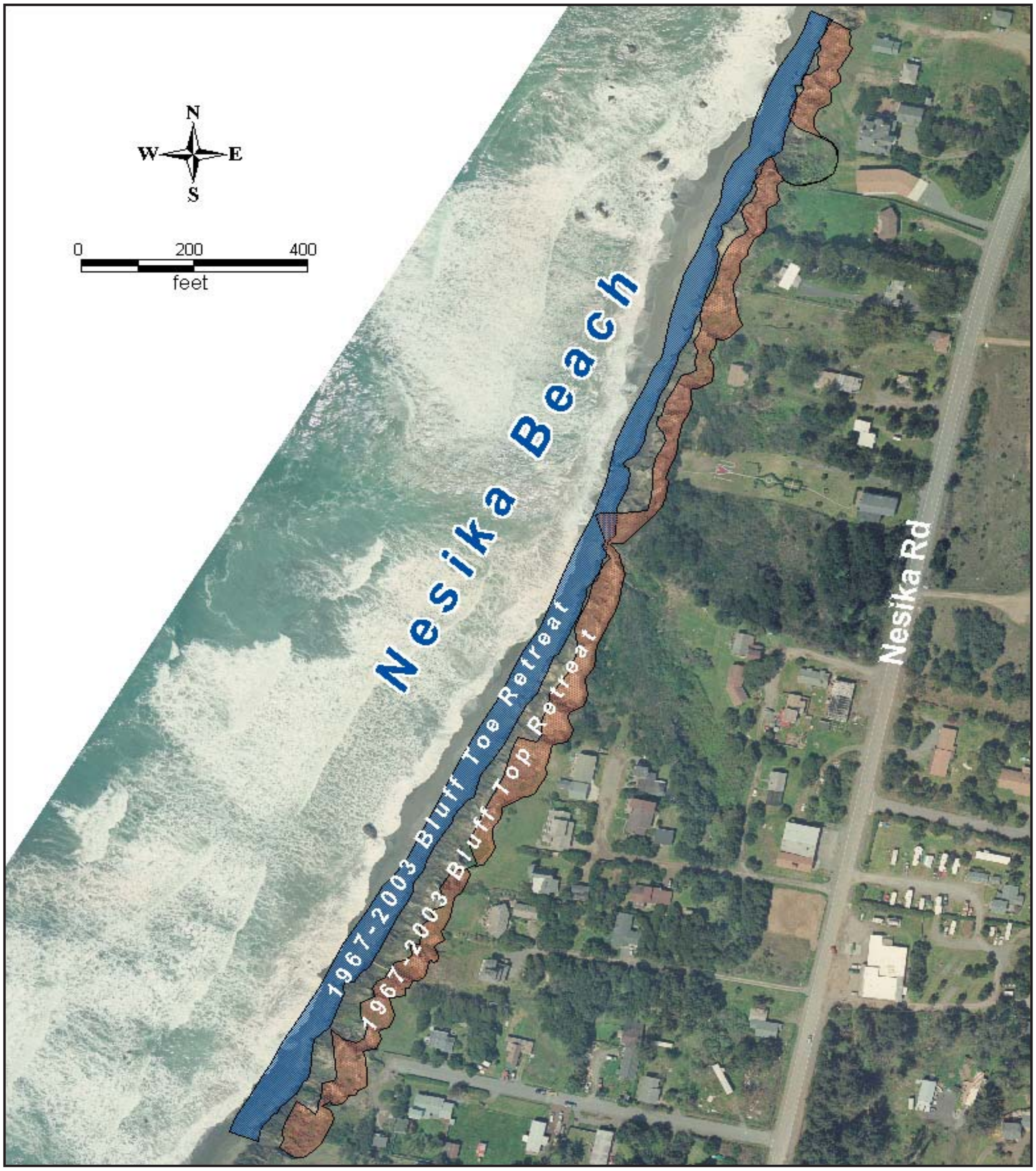

Figure 16. Bluff toe versus bluff top retreat at Nesika Beach between 1967 and 2003; determined from rubbersheeting[3] 1967 air photo to 2003 orthophoto of the area. Note how irregular bluff top retreat is relative to bluff toe retreat over this time interval. The bluff toe retreat occurs by fairly constant wearing away by waves, whereas bluff top retreat is more episodic, proceeding more by gravitational failures from slope undercutting and groundwater processes. It is apparent from the illustration that bluff top retreat is approximately equal to toe retreat, but only over a long time interval. The 36-year interval in this example was inadequate to see mean bluff top retreat but adequate for gradual bluff toe erosion. The large changes in bluff top position in several places are probably from local landslide failures. These can happen at anytime and must be taken into account when estimating risk.

[3]Rubbersheeting is a process whereby a digital scan of an aerial photo is digitally deformed to fit a base map by locating features common to both the map and the photo.

Table 6. Bluff toe erosion data based on comparison of 2003 and 1994 digital orthophotos to 1939 and 1967 air photos and derived from east-west change of the bluff toe. Erosion Rate for point data is the mean of measurements; for the continuous segment rubber sheeted at segment 2 at Nesika Beach (Figure 16), it is the mean of 33 segments of similar retreat weighted for the shoreline length represented by each. Std. Dev = Standard deviation from the mean of measurements; for the rubber sheeted segment at Nesika Beach, standard deviation is the mean of deviations from the mean of measurements weighted by the shoreline length represented by each measurement. Measurement error is the inherent uncertainty in locations because of photo scale and resolution; RMS = root mean square error (square root of sum of squares of measurement error and standard deviation).

Location	*Segment #*	*Interval*	*Beach type*	*Bluff composition*	*Erosion Rate (ft/yr)*	*Meas. Error (ft/yr)*	*Std. Dev. (ft/yr)*	*RMS (ft/yr)*	*N-S[4] length (ft)*	*Data Points*
Headlands	--	1939-2003 and 1994	Negligible Beach	Hard Mesozoic Metamorphic Rocks	-0.06	0.29	0.07	0.3	--	8
High Bluffs and Pocket Beaches south of Sisters Rocks	1	1939-2003	Reflective narrow; coarse sand	Cretaceous and Jurassic sedimentary and metamorphic rocks	-0.07	0.29	0.11	0.31	--	3
Euchre Creek to Nesika Beach	2	1967-2003	Reflective narrow; coarse sand	Marine terrace deposits over Jurassic sedimentary and metamorphic rock	-1.31	0.28	0.01	0.28	2400	33
South End of Nesika Beach	3	1967-2003	Reflective; narrow; coarse sand	Marine terrace deposits over Jurassic sedimentary and metamorphic rock	-1.94	0.28	0.04	0.28	--	6
Pocket Beaches: Nesika Beach to Otter Point	4	1967-2003	Reflective narrow; coarse sand	Marine terrace deposits over Jurassic sedimentary and metamorphic rock	0.84	0.28	0.32	0.42	--	27
Pocket Beaches: Nesika Beach to Otter Point	4	1939-2003	Reflective narrow; coarse sand	Marine terrace deposits over Jurassic sedimentary and metamorphic rock	0.51	0.29	0.21	0.36	--	21
South of Otter Point to N Jetty	5	1939-2003	Reflective; coarse sand with extensive dune protection of bluff	Marine terrace deposits over Jurassic sedimentary and metamorphic rock	-0.08	0.29	0	0.29	--	11

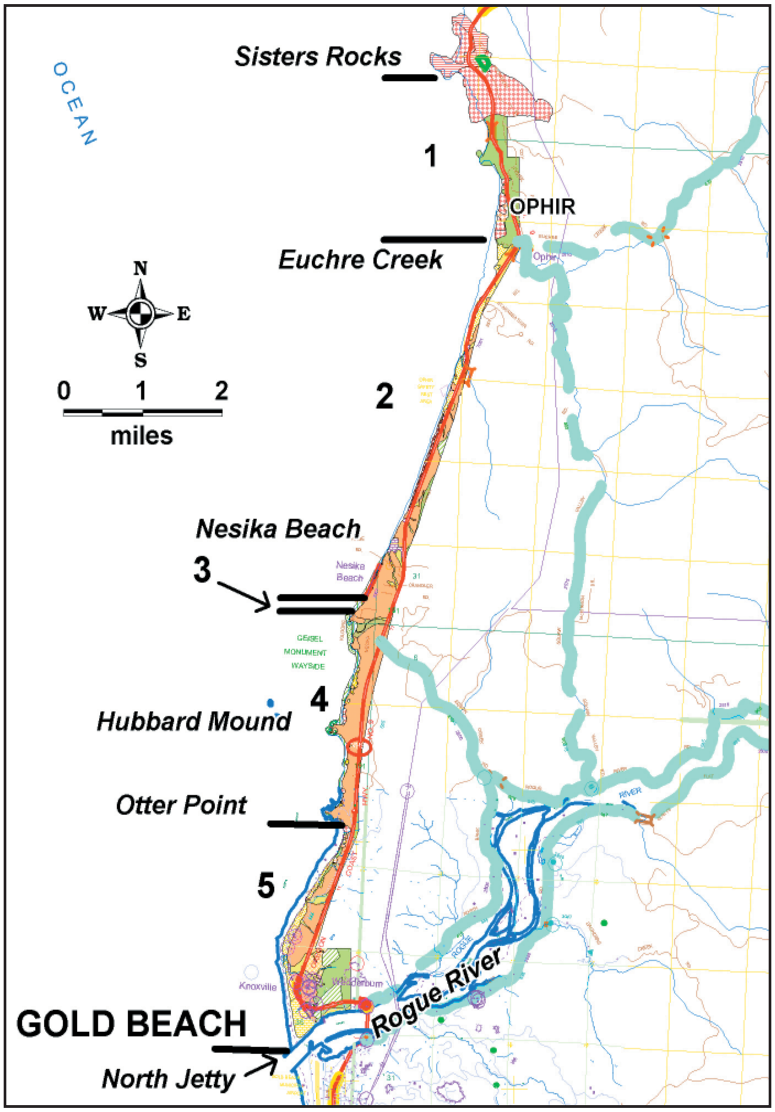

Figure 17. Location map of segments of shoreline with coherent erosion characteristics (black numbers with boundary lines). Headlands like Otter Point, Hubbard Mound and Sisters Rocks are considered a sixth type of bluff segment. Orange areas are outcrops of Quaternary marine terrace deposits; green in upper part of figure are high bluffs of Mesozoic metamorphic and sedimentary rocks; reddish diamond and line patterns in upper part of figure are large landslides in the high bluffs.

South Side of Otter Point to the North Jetty (Segment 5): Although only one data point could be measured for dune-guarded bluffs south of Otter Point, bluff retreat is probably negligible. Waves rarely strike the bluffs because of effective shielding by dunes; this leads to a backshore bluff of Quaternary marine terrace sand that is almost wholly vegetated (Figure 8). The erosion rate is essentially the default subaerial erosion rate of ~0.1 ft/yr used in erosion hazard mapping in Lincoln County (Priest and Allan, 2004). The one data point listed in Table 6 for this area is where there is a small protrusion of the bluff through the dunes (Figure 18); even at this point the rate is only -0.08 ± 0.29 ft/yr (Table 6). For this mapping exercise, we will assume a low erosion rate of 0.1 ft/yr and a high rate of this value plus the error or ~0.4 ft/yr (Table 7). These will be the rates used for all areas that are within the zone at risk for erosion of the fronting dunes. In Section 3.3.3.2.3 we will discuss what erosion rate applies to areas that are likely to experience only subaerial erosion.

Headlands: The basal rock in headlands in this area is generally a hard crystalline metamorphic rock. Bluffs composed of these rocks have negligible retreat on historical photos (Table 6). Headlands on the 1939 air photos look almost exactly like their images on the 2003 photos. For a minimum rate, we will assume the mean erosion rate of 0.06 ft/yr, rounding to 0.1 ft/yr to account for measurement error. A rate of 0.4 ft/yr will be used for a conservative (high) rate; this is the mean plus the root mean squared (RMS) error of the measurements (Table 7).

Pocket Beach South of Sisters Rocks (Segment 1): The pocket beach immediately south of Sisters Rocks has three erosion rate measurements that are not significantly different from the headland erosion rate (Table 6). We will assume the same high and low rates of 0.1 and 0.4 ft/yr for this mapping exercise (Table 7).

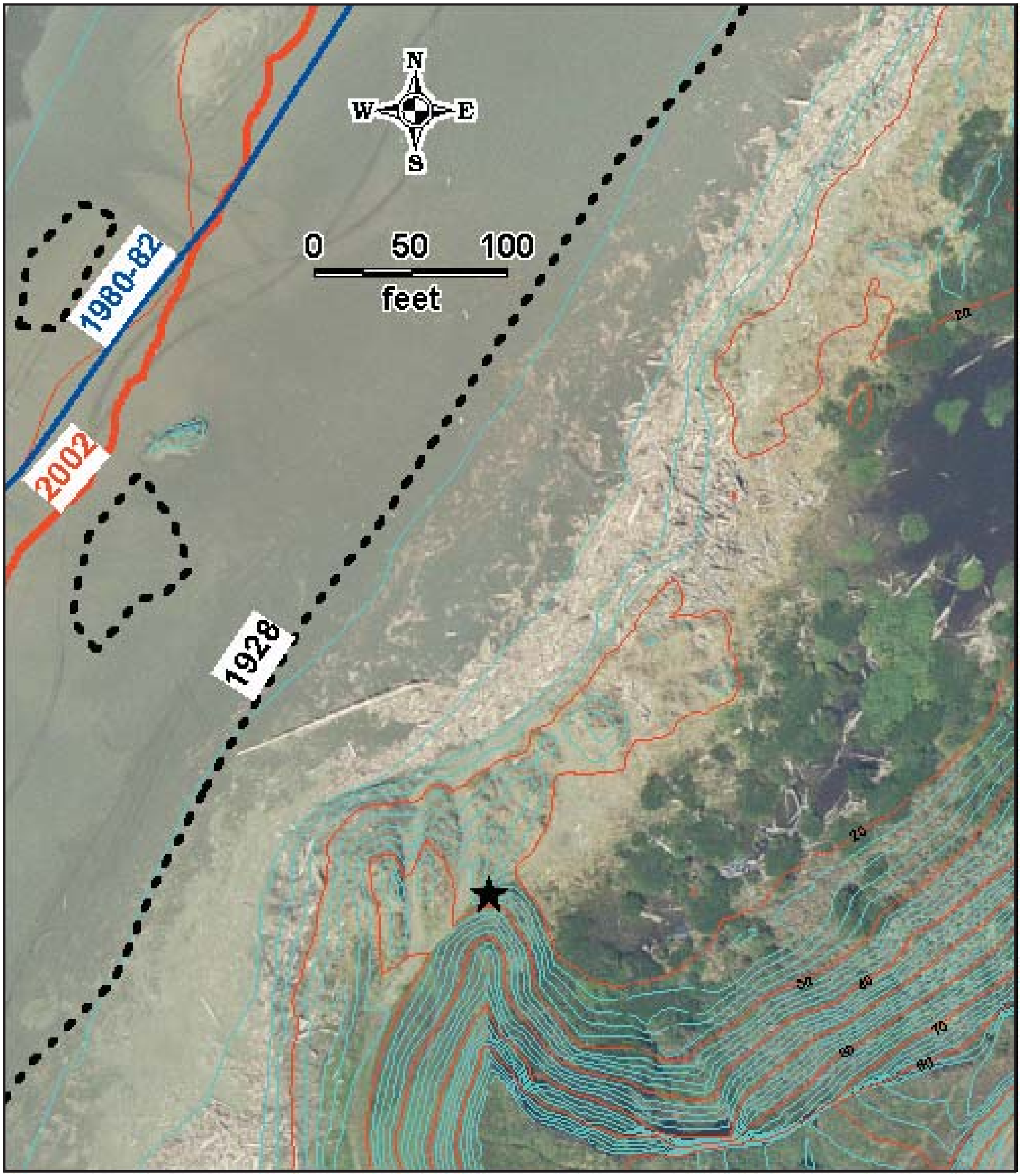

Figure 18. Vegetation on Quaternary marine terrace sand bluff south of Otter Point shows that waves rarely erode the bluff. Mean high water lines from 1928 to 2002 illustrate that the shoreline has fluctuated up to 180 feet in this area. Seaward location of the later shorelines is suggestive that beach sand accretion has occurred during the last 74 years. The star is the location of the erosion measurement listed in Table 6 for this area. Blue lines are topographic contours at intervals of 2 feet.

Table 7.. Summary of the high and low erosion rates that will be used here for mapping erosion hazard zones on the coastal bluffs. See discussion in text for derivation of the low and high (conservative) rates.

Location	Segment (Figure 17)	Low (ft/yr)	High (ft/yr)
Pocket Beach: south of Sisters Rocks	1	0.1	0.4
Pocket Beaches: Otter Point to Nesika Beach	4	0.9	1.3
Central Nesika Beach	2	1.3	1.6
South Nesika Beach	3	1.9	2.2
Headlands	--	0.1	0.4
South of Otter Point to N Jetty	5	0.1	0.4

Pocket Beaches, Otter Point to Nesika Beach (Segment 4): Pocket beaches from Otter Point to Nesika Beach are composed of sheared mudstone, sandstone, serpentine, and metavolcanic rocks overlain by Quaternary marine terrace deposits. The fronting beaches are narrow, allowing almost daily wave attack at all times of the year. Many offshore rocks and reefs, however, break up some of the wave energy. The bluffs in the pocket beaches are not as resistant to erosion as the bounding headlands, having mean erosion rates of 0.54 ft/yr for 1939 to 2003 and 0.84 ft/yr for 1967 to 2003. The higher rate in the latter interval is probably due to increased erosion from elevated water levels associated with the 1982-1983 El Niño and large storm wave events in the last several years (Allan and Komar, 2000a; Graham and Diaz, 2001). Local field observations by one of us (Ron Sonnevil) are consistent with accelerated rates of coastal retreat in these pocket beaches and at Nesika Beach in the last 20 years. It is possible that a general trend toward increasingly large storm wave events over the last 50 years (Graham and Diaz, 2001) will continue in the future, but there is no way to predict if this will really happen or quantitatively estimate how such an eventuality would affect erosion rates. If all erosion between 1967 and 2003 occurred during the last 20 years, the rates based on 1967 to 2003 photos would be increased by a factor of 1.8. It is unlikely that erosion ceased between 1967 and 1983, so multiplying the rates by this factor is not justified. We will add the RMS value to each mean rate as a way of adding the appropriate level of conservatism while still honoring the observational data. An appropriate mean rate will therefore be 0.54 ft/yr plus the RMS of 0.36 ft/yr or 0.9 ft/yr (Table 7). An appropriate high rate is 0.84 ft/yr plus the RMS of 0.42 ft/yr or ~1.3 ft/yr (Table 7).

Nesika Beach to Euchre Creek (Segments 2 and 3): Nesika Beach has a bluff composed of highly sheared, incompetent mudstone and sandstone overlain by poorly consolidated Quaternary marine terrace sand with extensive groundwater seepage at the formation contact and at clay-rich layers within the terrace sand. Where waves have regular access to this material, erosion can be rapid. It is apparent from inspection of the historical photos and modern field data that little bluff erosion has occurred adjacent to Euchre Creek owing to dunes that shield the bluff from waves. Fronting dunes disappear 4000 feet south of the creek, resulting in substantial erosion of the bluff. Where Highway 101 follows the bluff edge, substantial placement of crushed rock fill has been used to stabilize the highway embankment. The efficiency of this material or highway fill in stopping or slowing erosion was not taken into account when drawing interpretive erosion hazard zones for this investigation.

Few geographic points could be found on 1939 air photos that correspond to 2003 or 1967 photos in this segment south of Euchre Creek, but numerous points were available between 1967 and 2003 photography. This allowed rubber sheeting of the 1967 to the 2003 orthophoto in one highly developed area, using houses and streets as geographic control points (Figure 16). Mean bluff toe retreat in this section is 1.3 ft/yr (Table 6). Toe erosion rate measured at six points immediately south of this segment was 1.9 ft/yr (Table 6). These are some of the highest bluff toe erosion rates measured so far on the Oregon coast (e.g. compare to Allan and Priest, 2001; Priest and Allan, 2004). The relatively low standard deviations on these measurements of 0.01 ft/yr for the 1.3 ft/yr rate and 0.04 ft/yr for the 1.9 ft/yr rate (Table 6) indicate that toe erosion at the measurement site proceeded quite uniformly. This is consistent with the observed uniformly close spacing of fractures and shears in the basal rocks.

As discussed above, the 1967-2003 interval was a time of unusually high waves and total water levels, so these high rates may not be representative of longer time intervals. However, it is also possible that we are in a prolonged period of high wave activity. The incompetence of the bluff in this segment leads us to take a conservative approach and assume that these rates are representative. We will assume that a representative rate for the most of Nesika Beach (Segment 2) is approximated by 1.3 ft/yr. At the southernmost end of Nesika Beach (Segment 3) we will assume a rate of 1.9 ft/yr where the point data for that value is clustered (Table 7). For conservative (high) rates we will add the RMS error to each, giving values of 1.6 ft/yr and 2.2 ft/yr, respectively (Table 7).

Table 7 summarizes the high and low erosion rates that will be used in each segment for hazard mapping. The rates listed as "low" are the ones to be used to define the outer boundary of the high-risk erosion hazard zone. The ones listed as "high" will be used in mapping the outer boundary of the low-risk zone (worst-case or most conservative scenario).

3.3.3.2.3 Subaerial Erosion

While the above data are useful for wave erosion estimates, rates of gradual subaerial erosion from wind, slope wash, and soil creep are also important. For example, at the Jumpoff Joe landslide, a large translational block slide in Newport, about 160 feet of slide debris was removed by waves between 1939 and 1993, giving an erosion rate of about -3 feet per year (Priest and Allan, 2004). Until this slide debris is removed by waves, retreat of the headwall behind the landslide will be by subaerial processes such as wind, sheet wash, and soil creep. At Euchre Creek and the North Jetty at the Rogue River dunes effectively prevent wave erosion of bluffs, so subaerial erosion is the dominant factor there. Priest and Allan (2004) concluded that subaerial erosion on Quaternary marine terrace sand slopes at angles higher than the angle of repose (1.5:1) could be as high as -0.5 ft/yr, but slopes at the angle of repose erode very slowly by subaerial processes; probably no higher than ~-0.1 ft/yr.

For mapping erosion hazard zones we will assume that an area could become vulnerable to bluff top retreat from subaerial processes if it has a sedimentary rock, metasedimentary rock, highly sheared metamorphic rock, or Pleistocene sediment bluff guarded by slide debris or dunes that could protect the bluff from wave erosion during some part of the planning horizon (e.g., 60-100 years). If the bluff is at the angle of repose, the assumed rate of bluff top retreat will be –0.1 ft/yr for that portion of the planning horizon. Since the mapping scheme used here always starts with finding the point behind the bluff top where the angle of repose projects, only the –0.1 ft/yr rate will be used where subaerial erosion applies. Where slide debris blocks wave erosion, it will be assumed that it erodes away at ~-3 ft/yr over the 60-100 year planning horizon. If it is projected that slide debris is totally removed during that time, an appropriate wave erosion rate from Table 7 will be applied to the remaining time.

3.3.3.3 Block Failure Data

Erosion rate is only one part of the puzzle in predicting how a bluff will respond to erosion. The size of episodic block failures must also be taken into account, if the objective is to understand not only how much erosion will happen over hundreds of years but also what could happen in a single or many block failure events. Block failures could be translational slides, slumps, or even large topples in the case of

Table 8. Recommended maximum block failure widths for coastal bluffs of the study area. All data are from empirical observations of local landslides.

Bluff Height and Material Causing Block Failure	*Maximum Block Failure Width (ft)*
Headlands of hard Mesozoic rock (maximum topple width)	20
Bluffs 0-163 feet high of Cretaceous and Jurassic sedimentary and metamorphic rocks not at headlands	Bluff height//1.006
Bluffs >163 feet; ≤ 440 feet high of Cretaceous and Jurassic sedimentary and metamorphic rocks not at headlands.	(bluff height-127.33)/0.2249
Bluffs >440 feet; ≤ 790 feet high of Cretaceous and Jurassic sedimentary and metamorphic rocks not at headlands.	(bluff height+23885)/17.5
Bluffs 0-49 feet high of Jurassic metamorphic and sedimentary rocks overlain by Pleistocene marine terrace and colluvial deposits	bluff height/1.4286
Bluffs >49 feet high; ≤ 72 feet high of highly sheared Jurassic metamorphic and sedimentary rocks overlain by Pleistocene marine terrace and colluvial deposits (Nesika Beach)	35
Bluffs >72 feet high; ≤ 108 feet high of highly sheared Jurassic metamorphic and sedimentary rocks overlain by Pleistocene marine terrace and colluvial deposits	(bluff height -51)/0.6
Bluffs >108 feet high; ≤ 136 feet high of highly sheared Jurassic metamorphic and sedimentary rocks overlain by Pleistocene marine terrace and colluvial deposits	95

some high hard rock bluffs. The rate (and thus the probability) of block failures of various sizes, especially large ones, is unknown, since hundreds of years of detailed observations are not available. On the other hand, some maximum block failure widths can be derived from field measurements and analysis of aerial photographs. The location and degree of historic activity of the existing slides and large rock topples is an essential starting point for establishing the likelihood, extent, and rate of propagation of bluff slope failures. The basic techniques are discussed by Allan and Priest (2001; their Appendix C). Table 8 summarizes the maximum block widths that will be used for the study area.

Collection of empirical data on slide block failure width revealed that maximum block failure width in the study area increases with bluff height but at different rates in bluffs of different composition. The two main types of bluff are high bluffs of Mesozoic metamorphic and sedimentary rock (Sisters Rocks-Devils Backbone area) and much lower bluffs of similar but more fractured material that, because of its weaker condition, has been beveled off by Pleistocene marine transgressions (Nesiak Beach-Otter Point area). These lower bluffs are capped by poorly consolidated Pleistocene marine and colluvial deposits prone to continual slope failure from both wave undercutting and groundwater processes. Allan and Priest (2001) concluded that some landslide blocks might actually represent fragments of earlier larger blocks, whereas other large intact slide blocks at the toes of landslides may have undergone unknown amounts of wave erosion. Both factors tended to bias empirical data to smaller block failures. For the purpose of this report, the largest identified block failure width was used in prediction of "worst case" bluff retreat. Empirical equations (linear regressions) from locally derived maximum block failure width data are given in Table 8 and the digital file **slide_block_meas_sites_relief.xls**. Linear regressions are through the largest two block measurements for the listed bluff height intervals. In some cases only one value is listed for relatively narrow ranges of height (e.g., at Nesika Beach). All block widths were extrapolated to zero width at zero bluff height using the listed formulas, even if no data is available in the lowest bluff height intervals. This is justified from simple geometric considerations.

Little data were available from field observations of block topples on hard rock headlands, so the largest observed block at Sisters Rocks (20 feet; Figure 14) was used for all headlands. It is likely that this is somewhat conservative (high width) for lower elevation headlands to the south, but the heterogeneity of the Mesozoic rocks combined with the sparse field data leave us little choice.

3.4 Landslide Mapping (Mass Movements)

3.4.1 Introduction

Mass movement is the natural down slope displacement of the land surface. It occurs by a process called mass wasting, which refers to the down slope transport of soil or rock by gravity. Rock falls, landslides, flows of soil or rock, and displacement of large blocks (translational slide blocks or rotational slumps) are all forms of mass wasting.

Potentially hazardous areas of large-scale mass movement were mapped. Note that shallow mass movement of soil occurs on all slopes, increasing in rate and severity with increasing slope, decreasing material strength, and increasing degrees of water saturation. These shallow zones of soil creep are not depicted on the maps but should be considered before building on sloping ground, especially slopes in excess of ~25 % (4 horizontal:1 vertical). Only deeply penetrating landslides are mapped. Landslides are labeled and classified using the system of geologic symbols of Priest and others (1994; Table 9) supplemented by geologic symbols and formation names taken from previous investigations (Beaulieu and Hughes, 1976; Walker and MacLeod, 1991). A summary of geologic map symbols is given in Appendix B. Coastal landslide polygons and other geologic units are compiled in the GIS file, **geology_nesika_beach3**.

3.4.2 Prehistoric Mass Movements (PHls, PHb, PHf)

Many of the largest landslides and slide blocks could have prehistoric movement (older than about 150 years for historical observations on the Oregon coast). If no movement has happened since, then these slides appear deeply eroded with no evidence of recent activity. All slides mapped here appear to have evidence of some fairly recent movement.

3.4.3 Potentially Active Mass Movements (PAls, PAb, PAf)

A number of areas have mass movements that are currently stable (no bowed trees or cracked soil and pavement) but with evidence of recurrent movement in the last 150 years. Unlike the prehistoric slides, these features are generally not extensively eroded and have well preserved topography indicative of recent movement. Many show no evidence of movement since 1939 or 1967 aerial photography but are probably more likely to have movements than the prehistoric slide areas.

3.4.4 Active Mass Movements (Als, Ab, Af)

These areas have evidence such as bowed trees and cracked soil or pavement that indicate ongoing down slope movement of large masses of soil or rock. Only active or potentially active landslides were identified in the study area. Slide activity varied greatly from negligible rates of movement to rates that cause considerable damage to local roads and highways.

3.4.5 Extent and Quality of Geologic and Landslide Mapping

Landslides mapped in this investigation are compiled only for areas covered by the 2003 color orthophoto base maps[3] (Figure 19) about 2000 feet east of the coastline; all have labels with prefixes of A, or PA, as indicated in Table 9.

Field-mapped landslide boundaries were transferred

[3]April 19 and June 1, 2003 aerial photography by 3Di of Eugene, Oregon was used by 3Di to produce, orthophotos and topographic contours for the study area. Nine inch by nine inch color air photos from this flight are at a scale of 1” = 600’.

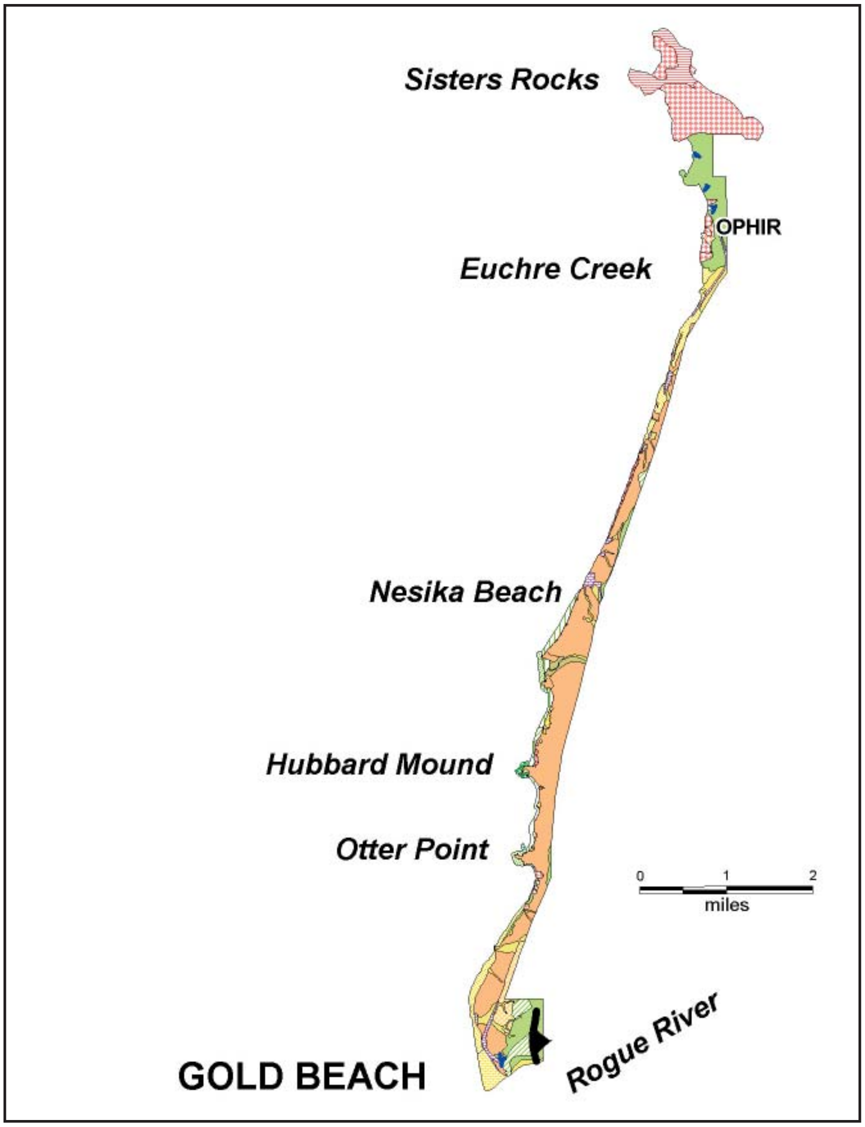

Figure 19. Geologic mapping for the study area covers the full extent of 2003 orthophoto coverage plus a small additional area on the north end of the area. Coverage is generally within about 2000 feet of the coastline, except at the north end where it was expanded to cover the large landslides there. Reddish colored dotted and lined areas at the north end of the study are examples of mapped areas of active landside. Similar but smaller landslides occur to the south. Green area north of Euchre Creek is a high bluff of Mesozoic metamorphic and sedimentary rocks. Orange area areas to the south are much lower bluffs capped by Quaternary marine terrace deposits. See Appendix B for detailed views of the mapping plus a complete map legend explaining geologic map units.

by inspection from stereographic photos to the 2003 orthophotos or, in a few areas not covered by 2003 photos, to 1994 USGS digital orthophoto quadrangles (DOQ's) using MAPINFO software. Field-mapped boundaries are located no better than the inherent error of the 2003 digital orthophotos, ± 10 feet horizontal, or 1994 DOQ's, ± 33 feet horizontal, although somewhat improved spatial resolution was achieved in a few areas with USGS 2002 LIDAR topography that was distinctive enough to allow location of geologic features. LIDAR has a data density ~ 4 feet horizontal, so features larger than about 2-5 data points (± 8-20 feet) could be distinguished. Where tonal contrast on the orthophotos was the only guideline for location of features and where contrast was low, the difficulty of information transferal increased, so that the error in these locations exceeded error inherent in the orthophotos. In some cases topographic contours and other features from 1980/1982 USGS DRG's (digital raster graphic quadrangles) were utilized to aid the transferal of the landslide data.

3.5 Explanation of Geologic Data

Geologic data are derived from original mapping along the shoreline supplemented by previous work by USGS (Beaulieu and Hughes, 1976; Walker and

Table 9 Landslide map units; "Present?" refers to presence in the study area.

Map Symbol and Label	*Description*	*Present?*
Als (Active Complex Landslide)	Complex landslide (small slide blocks with variable types of translational and rotational movement plus highly disaggregated slide debris) showing evidence of recent movement.	Yes
Ab (Active Slide Block or Slump)	Block of rock that is actively moving down slope by translation or rotation (slumping) or both and showing evidence of recent movement.	Yes
Af (Active Soil or Rock Flow)	Flow of highly disaggregated soil and rock showing evidence of recent movement. Note that the deposits themselves are not necessarily unstable but probably lie in an area vulnerable to future inundation by debris flows from upslope areas.	No
PAls (Potentially Active Complex Landslide)	Complex landslide that is currently stable but probably had recurrent movement in the last 150 years.	Yes
Pab (Potentially Active Slide Block)	Block of rock that is currently stable but probably had recurrent down slope movement in the last ~150 years.	No
PAf (Potentially Active Soil or Rock Flow)	Flow of soil and rock that probably had recurrent debris flow inundation in the last ~150 years.	No
PHls (Prehistoric Complex Landslide)	Complex landslide that is currently stable but probably formed in prehistoric times (>~150 years ago).	No
PHb (Prehistoric Slide Block or Slump)	Block of rock that has moved down slope in prehistoric times but is currently stable.	No
PHf (Prehistoric Rock or Soil Flow)	Flow of soil and rock that occurred in prehistoric times. Upland areas above these deposits need to be examined to determine if they could be sources of debris flows in the modern climate regime.	No

MacLeod, 1991). Detailed geology of the study area within about 2000 feet of the coastline is given in polygon file **geology_nesika_beach3** and vector line file **Faults**. Strike and dip of strata is given in GIS files **Labels_Strike_Dips and Strike_Dips_Nesika** (see Appendix C for summary of all digital files). All geology is illustrated in a series of map views in Appendix B. Appendix B also lists formation names, geologic symbols, and formation descriptions.

The area is composed of Mesozoic sedimentary and metavolcanic rocks all of which have been heavily deformed by tectonic forces. For further explanation of these tectonic forces and related geologic history of the area, see Orr and others (2000). This deformation has greatly weakened most Mesozoic rock units by creating numerous joints, fractures, and sheared surfaces in such profusion that mapping of every individual shear as a fault would make the map quite illegible, even at large scale. These discontinuities provide numerous opportunities for bedrock landslides on steep slopes in all directions.

South of Sisters Rocks the area has been locally cut by wave erosion during Pleistocene high sea stands, leaving behind a series of marine terraces cut in the Mesozoic rocks and surmounted by a variable thickness of slightly consolidated beach and dune sand. On the southeast end of the study area these deposits are mantled by aprons of moderately consolidated colluvial material (unit Qoc) that is a mixture of rock fragments and soil from surrounding hills commingled with the underlying sand. This material is most likely formed by mass wasting of the surrounding hills during wet climate intervals of the Pleistocene, probably during low sea stands (ice advances) when the area was much colder and wetter. At these times debris flows and floods probably poured down local drainages from highland areas, spreading out onto the relatively flat topography of the marine terraces. The resulting alluvial fans once formed a continuous apron of deposits (a bajada) at the base of the foothills but are now dissected by subaerial erosion processes.

3.6 Shoreline Protection Structures

Shoreline protection structures in the form of large quarry rock (rip rap) or smaller crushed rock and earth fills at highway embankments can slow or stop erosion, if maintained. While these structures are present in a few places where Highway 101 is adjacent to the shoreline in the Nesika Beach-Euchre Creek area, it is beyond the scope of this investigation to estimate how effective these structures are in reducing erosion; hence erosion rate data and parameters derived from adjacent unprotected bluffs and dunes are used to draw erosion risk zones in these areas. The erosion risk zones probably overestimate actual erosion risk to areas east of these features, since fill and shoreline protection, once installed will probably be maintained, unless not economically feasible.

3.7 Mapping Technique for Bluff Erosion Hazard Zones

3.7.1 Description of the zones

Four bluff erosion hazard zones will be specified in the study area:

1. Active Erosion Hazard Zone: Currently active erosion area (rapid soil creep on steep bluff or landslide headwall slopes plus active or potentially active landslides). If there was some question about whether the landslide was potentially active (i.e., it was shown as queried), then it was not placed in the active hazard zone.

2. High-Risk Hazard Zone: High probability that the area could be affected by active erosion in the next ~60-100 years. This zone boundary will, in effect, be the minimum distance that the bluff top (or landslide headwall) might retreat in the next 60-100 years.

3. Moderate-Risk Hazard Zone: Moderate probability that the area could be affected by active erosion in the next ~60-100 years. This zone boundary will, in effect, be the mean distance that the bluff top (or landslide headwall) is likely to retreat in the next 60-100 years. In general, this distance was approximately halfway between the high- and low-risk hazard zones.

4. Low-Risk Hazard Zone: Low but significant probability that the area could be affected by active erosion in the next ~60-100 years. This includes bluff tops that may retreat by a maximum block failure at the end of an interval of gradual erosion, including some subaerial erosion. Maximum block failures might be caused by Cascadia subduction zone earthquakes or unusually high groundwater conditions. This zone boundary will, in effect, be the maximum distance that the bluff top (or landslide headwall) is likely to retreat in the next 60-100 years.

The 60 to 100 years planning horizon was chosen because this is the typical time that a house might be expected to last. Sixty years is also the time frame utilized by the Federal Emergency Management Agency

(FEMA) for coastal erosion loss estimates (Heinz, 2000), the impetus for previous erosion hazard estimates in the study area (i.e., Priest and others, 1994; Priest, 1999).

3.7.2 Uncertainty in spatial location of the zones

Owing to limitations of available topographic data, none of the mapped bluff hazard zones are located closer than plus or minus 8 feet, the horizontal distance covered by 2 LIDAR data points. This distance was the minimum needed to specify breaks in slope that were the reference points for mapping the zones. The minimum bluff hazard zone width that could be depicted with this geospatial data is therefore ~20 feet, which is the minimum default width assumed for all bluff hazard zones. Breaks in slope at bluff tops were particularly hard to locate in areas of heavy vegetation where tree cover made LIDAR misleading and aerial photographic interpretation difficult. The error in these areas is probably high but was not quantitatively measured.

3.7.3 General procedure for drawing bluff hazard zones

The procedure below is essentially the same as that of Priest and Allan (2004). The north-south extent of shoreline segments mapped with specific methods is given in the geographic information database (files **BLUFF_EROSION_HAZ_ZONES** and **Active_Hazard_ZoneFINAL**) that accompanies this report (see Appendix C for summary of digital files). Hazard zones are drawn in transitions between segments utilizing professional judgment. Professional judgment is really the basis for drawing any geological hazard zone, but the procedure enumerated below has been uniformly applied to make the hazard zones reasonably reproducible by other workers. Where deviations from the procedure occur, these are explained in the description fields of the geographic information database; in particular see the database of guidelines, file **Bluff_Haz_guidelines**, used to define zone boundaries.

1. Determine bluff composition, structure, and extent of all landslides, including ancient (prehistoric) slides.

2. Map the bluff top or top edge of the active or potentially active landslide headwall. Exclude all mass movement hazard areas that are prehistoric (e.g., unit PHls) or potentially active but queried (e.g., PAls?)[6]. Everything seaward of this reference line is the active hazard zone.

3. Determine the projected bluff top (or projected landslide headwall position) at the slope of repose for the bluff material, making sure that each soil or rock unit in the bluff has the appropriate slope of repose (Table 5). On active or potentially active landslides, project the slope of repose from the toe of the headwall at its subsurface intersection with the slide plane. Use local geotechnical data to find this intersection; if no data are available, use Equation 2 or graphically project as in Figure 15. Assume a 60° seaward dip of headwall in subsurface and 12° seaward dip of slide plane to locate the toe of the headwall in the subsurface. If this dip is not geometrically possible, use professional judgment, assuming that overall slope of the slide surface approximates the slide plane dip at depth.

4. Decide how long the bluff top is likely to recede primarily by wave or subaerial erosion. If guarded by slide debris, assume that subaerial erosion prevails until the slide debris is removed; at the rate of -3 ft/yr. If the bluff is fronted by dunes, assume that subaerial erosion prevails, if the high-risk erosion hazard zone calculated for dunes does not intersect the toe of the bluff.

[6] These two units are not present in the study area, but are listed to make the procedure consistent with previous work in Tillamook and Lincoln Counties by the authors.

5. For bluffs subject to wave erosion (not guarded by large slide masses and high-risk erosion hazard zone for dunes intersects the bluff toe), using Table 6, determine an estimated minimum expansion of the active hazard zone (or projected position at the slope of repose from Table 5, whichever is the most landward) by multiplying the mean erosion rate of the basal soil or rock unit (Table 7) by 60 years. This is the landward boundary of the high-risk hazard zone.

6. For bluffs of Step 5 (those subject to wave erosion), using Tables 7 and 8, determine the maximum expansion of the active hazard zone (or projected position at the slope of repose from Table 5, whichever is most landward) by multiplying the maximum (conservative) erosion rate by 100 years and adding one maximum block failure width (Table 8). This is the landward boundary of the low-risk hazard zone.

7. For bluffs not subject to wave erosion, determine an estimated minimum expansion of the active hazard zone (or projected position at the slope of repose from Table 5, whichever is the most landward) multiplying the subaerial erosion rate of –0.1 ft/yr by 60 years (6 feet behind the bluff or projected angle of repose). This is the landward boundary of the high-risk hazard zone.

8. For bluffs not subject to wave erosion, determine an estimated maximum expansion of the active hazard zone (or projected position at the slope of repose from Table 5, whichever is the most landward) by adding one maximum block failure width from Table 8 to –0.1 ft/yr times 100 years (10 feet). This is the landward boundary of the low-risk hazard zone.

9. If in Step 4 it is determined that a bluff guarded by slide debris will be erode first by subaerial and then by wave and erosion in the next 60-100 years, determine the landward boundary of the low- and high-risk hazard zones appropriate for each erosion process as in Steps 5-8.

10. For the portion of bluffs composed of Pleistocene or Holocene sediment, move the low-risk hazard zone boundary to the projected position of a 2:1 slope (from the slope toe or projected toe of a landslide headwall), if the low-risk hazard zone boundary drawn in previous steps is not already landward of a 2:1 slope.

11. Draw the moderate-risk hazard zone boundary at the mean position between the high- and low-risk hazard zone boundaries (i.e., sum the lateral distances of the high- and low-risk hazard zones and divide by 2).

12. Adjust the low- and moderate-risk hazard zone boundaries for any inland landslides that are intersected by the projected expansion of the active coastal erosion hazard zone. Use geologic judgment and endeavor to:

    a. Encompass the parts of inland landslides that may be further destabilized by future coastal erosion.

    b. Match the general risk levels implied by the hazard zone designations (i.e., inland prehistoric or queried potentially active landslides in the “low” zone; and active or potentially active landslides in the “high-risk” or “moderate-risk” zones).

    c. Predict the probable future expansion of these inland landslides should coastal erosion reach them.

4.0 RESULTS AND DISCUSSION

Maps of the erosion hazard zones are shown in Appendix A. Maps of shoreline geology and landslides are shown in Appendix B. More useful are the digital geographic information files that are on this CD ROM and summarized in Appendix C. These files contain not only the graphic information but, in many cases, explanatory descriptions for each of the graphic objects. These descriptions list such things as data sources, field descriptions, and uncertainties.

4.1 Landslide Hazards

Potentially active and active landslides were mapped along the shoreline. Active and potentially active landslides are particularly concentrated on bluffs with minimal beaches and relatively high (>70 feet) elevation. Lower elevation bluffs tended to have small (~35 feet wide or less) slump failures that were not generally mapped as separate landslide units owing to the map scale and the ephemeral nature of such small features.

Size of individual slide block failures for bluffs tends to increase more or less regularly with bluff height. The largest single block failures are in the large landslide complex at the northern margin of the study area where the highest coastal bluffs occur.
Active and potentially active slide areas are very hazardous to development unless some form of geotechnical remediation is pursued. In some cases remediation is not economically feasible. Geotechnical investigations are recommended in any mapped landslide area to check on the accuracy of this reconnaissance-level information and to evaluate remediation alternatives.

4.2 Active Hazard Zone

The active hazard zone identified for the study area varies in width from a few tens of feet on cliffy headlands to hundreds of feet on low-sloping beaches or areas with large landslides (Appendix A). On dune-backed beaches the active hazard zone is an area of shoreline variability that can be expected to experience further changes in the immediate future. There can be no doubt that building within the active hazard zone on either coastal bluffs or dune-backed shorelines can represent considerable risk to property and lives.

As noted previously, the landward extent of the active hazard zone has been delineated according to vegetation and topographic patterns that could be identified on 2003 aerial photos and derived topographic contours, with the inclusion of some local adjustments that were derived from the 2002 LIDAR dataset[7]. The westward extent is defined by the shoreline derived from the 2002 LIDAR data. Both boundaries are affected by erosion from the 1997-98 El Niño and the severe 1998-1999 La Niña winter storms. It is possible that on dune-backed shorelines both boundaries could translate westward should the area enter less severe wave conditions in the future.

Sawed logs located in situ in the contemporary foredunes in Tillamook County (Allan and Priest, 2001.) and Lincoln County (Komar and Rea, 1976) demonstrate that the Oregon shoreline has been highly variable since European settlement (Komar, 1997). One may infer from this line of evidence, that the coast has been subjected to extremely severe storms in the past that probably contributed to widespread coastal erosion. It follows that similar types of storms are equally likely to be experienced in the future, especially if climate change persists. For example, climate modeling by the Joint Institute for the Study of the Atmosphere and Ocean Climate Impacts Group (JISAO/SMA, 1999) has revealed that large-scale climate changes are predicted to occur over the Pacific Ocean during the next 50 to 100 years. In particular, their models suggest that the Aleutian Low is likely to deepen and move progressively southward, resulting in an increase in wind speeds and hence larger waves along the PNW coast. These changes are likely to

[7]See Brock and others (2002) for explanation of LIDAR topographic mapping for coastal studies.

result in a higher incidence of situations similar to the 1982-83 and 1997-98 El Niño events (JISAO/SMA, 1999). As a result, it is possible that the ensuing decades could be characterized by stormier conditions, further increases in North Pacific wave energies, and therefore an increase in coastal erosion problems. If this is the case, then the active hazard zone boundaries may never translate westward on the dune-backed shorelines unless local sand accretion is occurring. Likewise, erosion rates estimated from historical photos may not be representative of future erosion rates.

Accretion of sand has occurred north of the North Jetty at the mouth of the Rogue River and appears to have occurred locally around the mouth of Euchre Creek. These areas are most likely to see westward shifts of the active hazard zone.

Tectonic subsidence from a great subduction zone earthquake estimated at ~6.2 feet (1.9 m) will cause severe erosion some time in the future. The active hazard zone will almost certainly translate eastward in all areas at that time unless large injections of sediment occur into the beach system at the same time.

Table 10. Maximum potential erosion distances determined for the Euchre Creek area. Mean is calculated from the total area of the erosion east of the beach-dune toe junction divided by the shoreline length.

Hazard zone scenarios	*Min (ft)*	*Max (ft)*	*Average MPED (ft)*
HIGH	341	415	**343**
MODERATE	553	825	**587**
LOW	864	1542	**1036**

Table 11. Maximum potential erosion distances determined for northern Nesika Beach (Ophir Wayside).

Hazard zone scenarios	*Min (ft)*	*Max (ft)*	*Average MPED (ft)*
HIGH	82	214	**141**
MODERATE	207	332	**239**
LOW	287	497	**350**

4.3 Beach-dune Erosion Hazard Zones

Beach dune erosion hazard zones mapped in this investigation emulate the possible shoreline change in response to a variety of extreme scenarios. Estimates of maximum potential erosion distances (MPED) for the dune-backed beaches have been determined by the geometric model (Figure 4) according to the three scenarios presented previously. These data have subsequently been tabulated EXCEL spreadsheet file **Dune_Eros_Haz_transectsDATA.xls** and GIS file **Dune_Eros_Haz_transectsDATA**.

Because of the considerable variability in the morphology of the beach environment along the coastline, specifically in terms of the beach-dune toe elevations (EJ) and the slopes of the beach (tan ß), the estimated MPED data were similarly characterized by a wide range of values. To standardize the data somewhat, an average MPED was determined for coherent shoreline segments. The resulting horizontal distances measured from the beach-dune toe junction were translated into a series of digital guidelines that were used to draw the erosion hazard zones. Graphic lines for these guidelines are in GIS file **Dune_Haz_guidelines_83_ft**; digital nodes in each guideline mark the boundaries between the digital hazard zone polygons.

Table 10 presents values of the MPED identified for the dune-backed shorelines around the mouth of Euchre Creek. Figure 20 illustrates historic shoreline change. As can be seen for the high-risk hazard zone, estimated erosion distances range from 341 to 415 feet, with

[8]According to Komar (1998, p. 47), a dissipative beach is "the type having a low-sloping profile, such that waves first break well offshore and continuously lose energy when they travel as breaking bores across the wide surf zone. In contrast, on the reflective beach..., the incident waves break close to shore with little prior loss of energy."

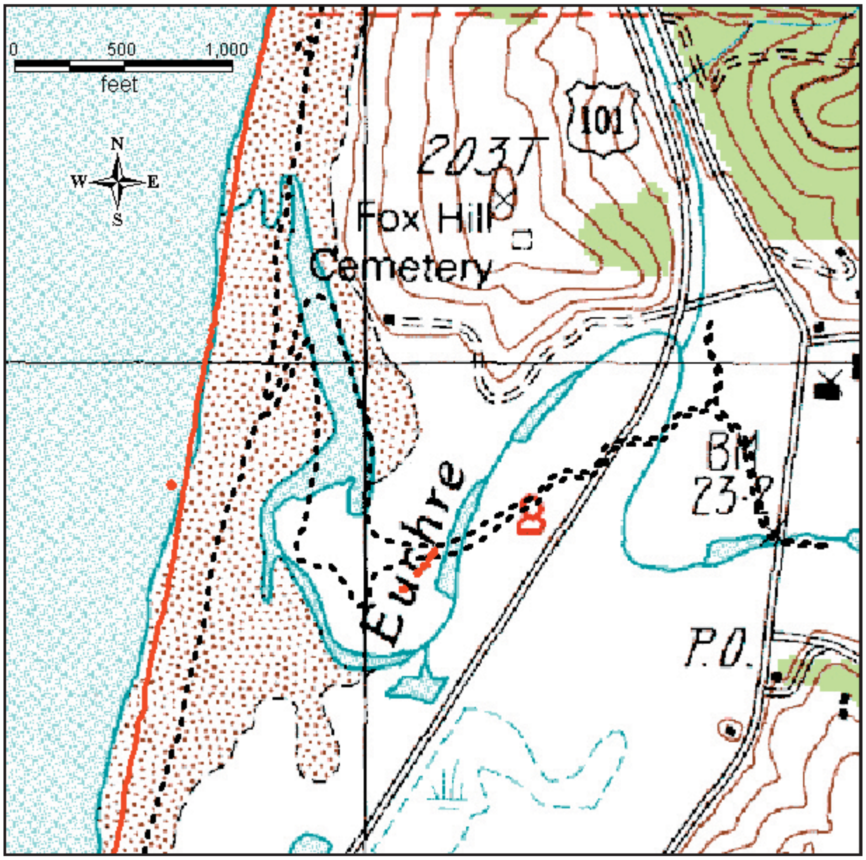

Figure 20. Historic shorelines in the Euchre Creek area. Red line is the 2002 mean higher high water shoreline defined from LIDAR data; dashed line is the same shoreline taken from a 1928 topographic map; blue shoreline is from the 1980-1982 USGS topographic base map. Note that there is overall accretion of the beach from 1928 but little change between 1982 and 2003. Also note the complex changes in position of the Euchre Creek channel.

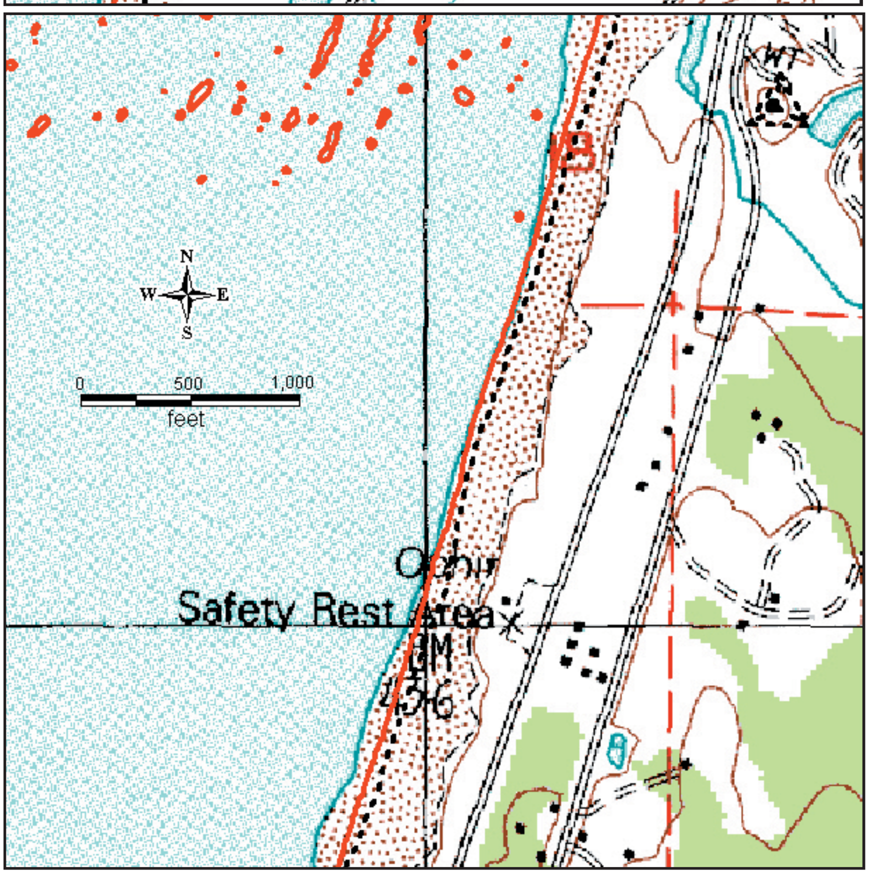

Figure 21. Historic shoreline change at northern Nesika Beach (Ophir Wayside). See Figure 20 for explanation of symbols.

Table 12. Maximum potential erosion distances determined for the beach north of the North Jetty at Gold Beach.

Hazard zone scenarios	*Min (ft)*	*Max (ft)*	*Average MPED (ft)*
HIGH	188	454	**315**
MODERATE	246	676	**441**
LOW	298	1007	**595**

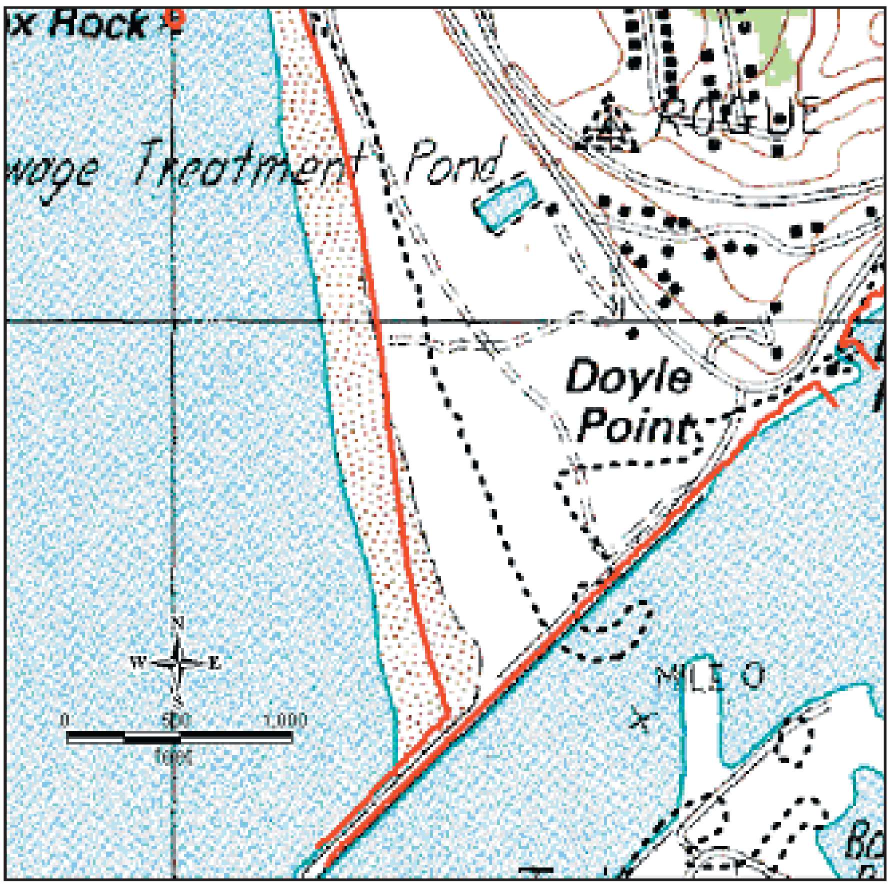

Figure 22. Beach accretion caused by construction of jetties at Gold Beach. The effect is most pronounced on the north side of the North Jetty where the pre-jetty shoreline of 1928 (dashed line) is hundreds of feet east of the 2002 shoreline (red) defined by LIDAR. The effect decreases north. The base map is a 1980/1982 USGS DRG (digital raster graphic quadrangle). Note the eastward translation of the shoreline from 1980-1982 to 2002 probably resulting from the extreme storms that occurred during the 1997-98 El Niño and 1998-99 La Niña winters.

an average MPED of 343 feet. This is roughly equivalent to the historic shoreline change of about 300 feet (Figure 20). As expected, an even larger range of values characterizes the moderate- and low-risk scenarios, with some potential erosion distances that extend up to 1542 feet in areas where beach slope has been lowered by intrusion of fluvial erosion processes. Average maximum MPED estimates for the moderate- and low-risk risk hazard zones were determined to be ~587 ft and 1036 ft respectively. These zones are shown graphically in Appendix A.

Maximum potential erosion distances are presented in Table 11 for the northern Nesika Beach area. The derived hazard zones are shown graphically in Appendix A. Figure 21 illustrates historic shoreline change. Under the high-risk scenario, estimated erosion distances are much smaller than at the mouth of Euchre Creek, ranging from 82 to 214 feet, with a mean MPED of 141 ft. This is similar to the historic shoreline change of about 120 feet (Figure 21). The smaller MPED relative to the mouth of Euchre Creek reflects the generally higher elevation of the beach-dune junction and steeper beach slope, both of which are lowered by fluvial processes at Euchre Creek. The geometric method used here for estimation of erosion hazard distances causes the steeper beach slopes to produce narrower erosion distances. The average MPED for the worst-case erosion scenario is 350 feet (Table 11), about three times the historic change.

Maximum potential erosion distances for the beach north of the North Jetty at Gold Beach are presented in Table 12. Beach slope is lower than at northern Nesika Beach, so erosion distances are larger. The lower slope is probably caused by the smaller beach sand size north of the North Jetty relative to Nesika Beach-Euchre Creek littoral cell. According to size measurements by Peterson and others (1994), sand size north of the North Jetty varies from 0.204 ± 0.053 mm near the jetty to 0.177 ± 0.039 mm at the north end of the

Table 13. Minimum, mean, and maximum lateral distances of bluff top retreat should erosion continue for 60-100 years[9]. These distances define the landward boundaries of the high-, moderate-, and low-risk hazard zones, respectively, when added to the lateral distance of the projected angle of repose for talus of each bluff. Table illustrates the uncertainty of predicting future bluff retreat from erosion rate and maximum block failure width. Values in parentheses are actual mapped widths, taking into account the limitations of the digital base maps, topographic data, and drawing accuracy. "Fine-grained interbeds" in the table refers to interbeds of siltstone, mudstone, or silty fine-grained sandstone with low resistance to shearing forces and consequent slope failure.

Bluff Type and Locality	*Minimum Retreat*	*Mean Retreat*	*Maximum Retreat*
	High-Risk Hazard Zone Feet	*Moderate-Risk Hazard Zone Feet*	*Low-Risk Hazard Zone Feet*
Mesozoic rock headlands subject mostly to rock falls and topples.	6 (20)	16 (40)	26 (60)
Bluffs 0-163 feet high of Cretaceous and Jurassic sedimentary and metamorphic rocks not at headlands (Segment 1, pocket beach south of Sisters Rocks).	6 (20)	23(40)-111	40 (60) -202
Bluffs >163 feet; < 440 feet high of Cretaceous and Jurassic sedimentary and metamorphic rocks not at headlands (Segment 1, pocket beach south of Sisters Rocks).	6 (20)	112-725	203-1430
Bluffs >440 feet; < 790 feet high of Cretaceous and Jurassic sedimentary and metamorphic rocks not at headlands (Segment 1 pocket beach south of Sisters Rocks).	6 (20)	725-735	1430-1450
Bluffs 0-49 feet high of Jurassic metamorphic and sedimentary rocks overlain by Pleistocene marine terrace and colluvial deposits (Segment 2, north central Nesika Beach)	78	119-136	160-194
Bluffs >49 feet high; < 72 feet high of highly sheared Jurassic metamorphic and sedimentary rocks overlain by Pleistocene marine terrace and colluvial deposits (Segment 2, central Nesika Beach)	78	136	195
Bluffs >49 feet high; < 72 feet high of highly sheared Jurassic metamorphic and sedimentary rocks overlain by Pleistocene marine terrace and colluvial deposits (Segment 3, south end of Nesika Beach)	114	184	255

[9]The distances do not take into account (1) the possibility of pre-existing structures like ancient landslides (step 12 in the bluff hazard zone procedure); (2) the possibility that the bluff top might erode gradually from the top by subaerial processes of slope wash and mass wasting that might lower the slope angle below the angle of repose (e.g., the 2:1 slope mapped in step 10); or (3) any hazard zone width added because the slope is higher than the angle of repose (step 3).

Table 13. Continued.

Bluff Type and Locality	*Minimum Retreat*	*Mean Retreat*	*Maximum Retreat*
	High-Risk Hazard Zone Feet	*Moderate-Risk Hazard Zone Feet*	*Low-Risk Hazard Zone Feet*
Bluffs >72 feet high; < 108 feet high of highly sheared Jurassic metamorphic and sedimentary rocks overlain by Pleistocene marine terrace and colluvial deposits (Segment 4, pocket beaches, Nesika Beach to Otter Point)	54	110-138	167-223
Bluffs >108 feet high; < 136 feet high of highly sheared Jurassic metamorphic and sedimentary rocks overlain by Pleistocene marine terrace and colluvial deposits (Segment 4, pocket beaches, Nesika Beach to Otter Point)	54	140	225
Bluffs >49 feet high; < 72 feet high of highly sheared Jurassic metamorphic and sedimentary rocks overlain by Pleistocene marine terrace and colluvial deposits (Segment 5; south of Otter Point)	6 (20)	48	75
Bluffs >72 feet high; < 108 feet high of highly sheared Jurassic metamorphic and sedimentary rocks overlain by Pleistocene marine terrace and colluvial deposits (Segment 5; south of Otter Point)	6 (20)	48-153	76-133
Bluffs >108 feet high; < 136 feet high of highly sheared Jurassic metamorphic and sedimentary rocks overlain by Pleistocene marine terrace and colluvial deposits (Segment 5; south of Otter Point)	6 (20)	78	135

beach near Otter Point; whereas samples from the Nesika Beach-Euchre Creek littoral cell varied from 0.344 ± 0.083 mm on the south to 0.426 ± 0.101 mm at the north end of the cell. These relatively coarse sand sizes cause most beaches in the study area to be steep enough to be classified as reflective beaches that do not effectively dissipate wave energy[8].

Jetty construction at Gold Beach caused shoreline change independent of the variables considered in the geometric model. The beach north of the North Jetty is an accretionary beach caused by jetty construction (Figure 22). Komar and others (1976) documented accretion of this sort on jetties throughout the Oregon coast. They show that, in general, a jetty, by projecting out into the ocean, creates an artificial embayment that is rapidly filled in until the shoreline becomes approximately parallel to the wave crests. The most rapid changes occur immediately after jetty construction. For example, a 1961 US Army Corps of Engineers survey of the beach north of the North Jetty showed that the high tide shoreline advanced ~500 feet from its pre-jetty, 1958 position (Lizarraga-Arciniega and Komar, 1975). Figure 22 illustrates that the shoreline reached ~900 feet west of its 1928 position by 1980-1982 but has not accreted greatly since that time. The shoreline near the North Jetty has, in fact, experienced about 250 feet of erosion since the 1980s, probably in

5.0 SUMMARY AND CONCLUSIONS

This report describes and documents erosion hazard zones distinguished for the 12.6 miles of the Curry County shoreline from the North Jetty at Gold Beach to the north side of Sisters Rocks. In particular, the report focuses on identifying coastal landslides and maximum potential erosion distances for bluffs and for dune-backed shorelines. Erosion distances were estimated using two quite different but complementary approaches, one for bluffs and one for dune-backed shorelines.

Hazard zones on dune-backed beaches were determined from a geometric model, whereby erosion occurs when the total water level produced by the combined effect of extreme wave runup (R) plus the tidal elevation (E_T), exceeds some critical elevation of the fronting beach, typically the elevation of the beach-dune junction (E_J). Three scenarios were used to model erosion hazard zones on dune-backed beaches:

- *Scenario 1* (HIGH-risk) is analogous to the 2-3 March 1999 La Niña winter storm. This scenario is based on the storm waves occurring over the cycle of an above average high tide, coincident with a 3.3 ft storm surge. Under this scenario maximum potential erosion distances (MPED) ranged on average from **141 to 343 ft**, depending on beach slope of the particular dune-backed beach, lower slopes giving wider zones. These values approximately equal maximum shoreline variability observed between shorelines mapped in 1928, 1980-1982, and 2003.

- *Scenario 2* (MODERATE-risk) is based on an extremely severe storm event (waves ~52.5 ft high) coupled with a long-term rise in sea level of 0.3 feet. Under this scenario average MPED ranged from **239 to 587 ft**.

- *Scenario 3* (LOW-risk) is the second "worst case" scenario, and is the same as scenario 2, but incorporating a 6.2 feet (1.9 m) subsidence from a Cascadia subduction zone earthquake. MPED estimated for scenario 3 ranged on average from **350 to 1036 ft**.

The range of shoreline retreat predicted for dune-backed beaches is clearly quite large and reflects the uncertainty in predicting future shoreline behavior based purely on extreme wave erosion events. Despite the low probabilities of some of the extreme water level scenarios adopted, the width of the resulting average hazard zones is still justified since it can accommodate in a gross sense such changes as migrating rip current embayments, the wholesale transport of sand by longshore drift, the on-offshore (cross-shore) transport of sand, and relatively quick response of reflective beaches to wave erosion events.

Coastal change at the mouth of the Rogue River is strongly affected by construction of jetties. The north jetty has caused hundreds of feet of beach accretion in the beach to the north. As a result, bluffs within about one mile north of the jetty are guarded from erosion by a wide beach and dune system. A narrower but still significant dune system greatly decreases wave erosion for an additional 1.4 miles north of the north jetty. The shoreline near the north jetty has experienced about 250 feet of erosion since the 1980s, probably in response to extreme storms that occurred during the 1997-98 El Niño and 1998-99 La Niña winters, so the dune system is vulnerable to further erosion. This lateral change is roughly equivalent to the width of the high-risk erosion hazard zone calculated from the geometric model for this area and demonstrates that the dune system is highly vulnerable to erosion events. Three complementary erosion hazard scenarios were mapped for bluffs utilizing bluff erosion rates, potential for block failures, and empirically derived angles of repose for the bluff materials. These three scenarios have similar risk levels to the dune hazard scenarios:

- *Scenario 1* (HIGH risk) portrays the zone of bluff retreat that would occur if only gradual erosion at a relatively low mean rate were to occur after the slope reaches and maintains its ideal angle of repose (for talus of the bluff material). The time interval of erosion was assumed to be 60 years. The width of the high-risk hazard zone generally ranged from **20 to 78 ft** wide, depending on the type of geology. In one small area at the south end of Nesika Beach local erosion data supported a width of **114 ft**. Where slopes were steeper than the angle of repose for talus of the bluff material, the zone width was increased by the lateral distance necessary to accommodate retreat to the angle of repose.

- *Scenario 2* (MODERATE risk) portrays an average amount of bluff retreat that would occur from the combined processes of block failures, retreat to an angle of repose, and erosion for ~60-100 years. The moderate-risk hazard zone boundary was placed halfway between the high- and low-risk boundaries, and resulted in bluff retreat that generally ranged from **40 to 735 ft**, depending on the type of geology and bluff height.

- *Scenario 3* (LOW risk) illustrates a "worst case" for bluff retreat in ~60-100 years. This zone accommodates a maximum bluff slope failure, subsequent erosion back to its ideal angle of repose, and gradual bluff retreat for ~100 years. For bluffs composed of Pleistocene marine terrace deposits and paleosols, an additional retreat of the bluff top in response to subaerial erosion is achieved by making sure that the projected bluff top retreat corresponds to at least a 50 percent factor safety for the ideal slope of repose of 1.5 horizontal to 1 vertical (i.e., a 2:1 slope). Low-risk hazard zone widths ranged from **60 to 1450 ft** wide, depending on the type of geology and bluff height. The largest zone width occurred in an area of unusually large slide blocks in the highlands east of Sisters Rocks.

In all cases, the minimum hazard zone width that could be mapped at the scale of the base maps is 20 feet, so even hard rock bluffs (generally headlands) or dune-guarded bluffs with negligible (subaerial) erosion rates on the order of –0.1 ft/yr were assigned zones with this minimum width. These bluffs have high-, moderate-, and low-risk zones of 20 feet each mapped east of the Active Hazard Zone (total of 60 feet), even though it is unlikely that erosion will actually reach 60 feet behind the bluff top in the next 100 years. This level of conservatism is appropriate given the accuracy of the base maps and uncertainties in the erosion and maximum block failure on data.

Mapped dune and bluff erosion risk zones probably overestimate actual erosion risk to areas at and east of the Highway 101 embankments in the Euchre Creek area. The highway is in places protected by large quarry rock (rip rap) or smaller crushed rock that will slow or stop erosion, and even where unprotected, it will probably be maintained against destruction by waves. It is beyond the scope of this investigation to estimate how effective shoreline protection structures and highway maintenance will be in reducing erosion; hence erosion rate data and parameters derived from adjacent unprotected bluffs and dunes are used to draw erosion risk zones at the highway embankments.

An extensive dune system at the mouth of Euchre Creek limits bluff erosion north and south of the creek. Specification of dune and bluff erosion hazard risk zones at Euchre Creek was complicated by complex interaction between wave and fluvial erosion processes. Absence of geographic points that could be used to estimate erosion rate from historical photos created large uncertainties for prediction of erosion risk. This complication added to the uncertainties associated with the Highway 101 embankments makes uncertainty of the mapped hazard zones there higher than in other parts of the study area.

An **active erosion hazard zone** has also been mapped which portrays the area of coastal bluffs and dunes that is being actively eroded by waves or undergoing active mass movement and mass wasting directly related to coastal erosion processes. This zone is by its very nature the least speculative of all the hazard zones, since it is directly observable and requires no theoretical projections into the future. On dune-backed beaches the active hazard zone is mapped at the vegetation line. On bluff-backed shorelines the active hazard zone includes all areas of active mass movement (soil creep, landslides, etc.) that are driven by coastal processes; hence it includes the bluff face and ends at the bluff top or top edge of the headscarp of an active or potentially active coastal landslide. The active hazard zone was mapped from observations of 2003 aerial photos supplemented by fieldwork and by analysis of 2002 LIDAR and 2003 topographic data. The high-, moderate-, and low-risk zones may be viewed as potential future expansion of the active hazard zone.

While this report illustrates a reasonably simple and reproducible means of establishing erosion hazard zones, it is by no means the only way. Ultimately coastal erosion is a complex process, dependent on many variables; predicting its future progress should only be done by highly experienced teams of geologists and experts in coastal processes. Ideally, these investigations should be done on a site-specific basis using extensive geotechnical and oceanographic data. The map data presented here are no substitute for this type of detailed analysis. The results of this investigation do, however, directly illustrate to the user the uncertainty that will likely accompany any mapping technique.

A major source of uncertainty in predicting gradual retreat in all of the bluffs was in the historic erosion rate data, which suffered from being:

1) Too sparse (only 1 area had continuous shoreline retreat data; all other data are spot rates),

2) Based mostly on a short (S64 years) observation period, and

3) Prone to inaccuracies from:

   a. Rubbersheeting of historical photos rather than photogrammetric orthorectification;

   b. Changes in erosion through time resulting from progressive penetration of new geologic units as bluffs retreat.

4) Possibly unrepresentative of future erosion rates: Local field observations indicate that a large but undefined proportion of the bluff retreat measured by comparison of historic photos probably occurred over the last 20 years owing to episodic wave and storm events. The episodic erosion rate is not known, but if it is considerably higher than rates documented from historical photography and characterizes future rates, then the mapped risk zones could underestimate the erosion hazard, particularly for the high-risk zone, which is most dependent on erosion rate data.

Some of the inherent uncertainty in the erosion rate data were overcome for the worst-case erosion scenario (low-risk hazard zone) by projecting all bluff tops to an empirically determined angle of repose and calculating bluff retreat at this angle for 100 years. Adding estimated error to erosion rates and adding a maximum slope failure event (slide block width) to 100 years of gradual erosion achieved additional conservatism. This conservatism was taken a step further for bluffs composed of Quaternary sediment by making sure that the worst-case erosion scenario always reached at least as far landward as the projection of 2:1 (horizontal : vertical) slope.

Another major source of uncertainty was predicting the size of single block failures that could slide or fall off of a coastal bluff. Empirical data were gathered on maximum block failure width, but it was clear that some landslide blocks might actually be fragments of earlier larger blocks, whereas other large intact landslide blocks may have undergone unknown amounts of wave erosion. Both factors tended to bias the data to smaller slide block failures. Hence, the approach of using the maximum observed block failure width to predict the "worst case" extent of bluff retreat seems justified. A series of empirical equations and locally derived maximum block failure widths guided the use of these data in drawing the bluff hazard zones. Block width increased with bluff height, which allowed estimation of maximum block width using a series of linear regression equations fit to the empirical data for each bluff type.

The two main types of bluff are high bluffs of Mesozoic metamorphic and sedimentary rock and much lower bluffs of similar but more fractured material that, because of its weaker condition, has been beveled off by Pleistocene marine transgressions. These lower bluffs are capped by poorly consolidated Pleistocene marine and colluvial deposits. The Pleistocene deposits are mostly beach and dune sand with groundwater flowing at the contact with underlying, less permeable Mesozoic rocks. Groundwater saturation and flow at this contact can weaken cementation of the Pleistocene sand, contributing to sloughing and slumping. The combination of weak, highly fractured Mesozoic rocks overlain by poorly consolidated sand leads to wave erosion rates that are some of the highest yet documented for Oregon coastal bluffs. Even though the rate of relative sea level rise is modest, only about 0.04 in/yr, areas like Nesika Beach with narrow beaches and the lowest bluffs have erosion rates of -1.6 to -1.9 ft/yr. Obviously building close to the bluff edge is particularly hazardous in these areas.

The bluffed coastline between Nesika Beach and Otter Point is characterized by somewhat higher elevations than at Nesika Beach and numerous small headland-bounded pocket beaches with narrow beaches. Pocket beach areas in this segment have gradual erosion rates intermediate between the extreme rates at Nesika Beach and the negligible rates characteristic of headlands and of the pocket beach south of Sisters Rocks. Rates are on the order of -0.5 ft/yr, which is similar to rates measured on sand-starved pocket beaches in Lincoln County (e.g., the Beverly Beach littoral cell; Priest and Allan, 2004).
No attempt was made to estimate the frequency of block failures. The historical data to accomplish this would require annual or more frequent observations over many decades. Such data were not available.

Ground cracks, broken pavement, and other recent deformation at all of the coastal landslides mapped in this study indicate that all are active, although degree of activity varies widely from a few millimeters per year of lateral movement to movements large enough to cause serious property damage. All of the mapped landslides should be considered unsuitable for development without extensive remediation, unless a site-specific investigation can demonstrate that proposed development sites are not within an active portion of the landslide feature and have a low risk of being impacted.

Large landslides with single block failures of hundreds of feet are limited to high bluffs of Mesozoic rocks in the northernmost part of the area east of Sisters Rocks. Bluffs at Nesika Beach composed of highly fractured Mesozoic rocks overlain by poorly consolidated Quaternary sedimentary deposits did not form large landslides but failed in small slumps up to ~35 feet wide. Landslides with single block failures intermediate in size between these two extremes characterized bluffs at pocket beaches between Nesika Beach and Otter Point.

6.0 RECOMMENDATIONS

Available time and support for this project was insufficient to provide an accurate assessment of erosion rates along the bluff-backed shorelines of the study area. Those few erosion rate estimates presented in this report are based on local "rates-of-opportunity" and were derived from features that could be easily relocated on historical and more recent aerial photos. To overcome this deficiency, additional work should be directed towards ortho-rectifying[10] a number of historic aerial photographs. For example, this approach would enable the bluff top, bluff toe and landslide headwall positions to be accurately mapped over periods of decades. Tracking bluff changes continuously along the length of littoral cells could reveal significant variation in erosion rates, which is a function of variations in rock strength and bluff-toe protection afforded by such things as shoreline protection structures, beach sand, and dunes. Generation of accurate erosion rates for all bluff-backed shorelines should be the highest priority for refinement of the hazard zones presented in this report.

Ortho-rectification of historical aerial photography would also enhance understanding of the temporal and morphological response of beaches and dunes. This information, when added to available historical shorelines from topographic maps, would provide additional historical perspective and improve our ability to better predict future beach and dune evolution.

Detailed geologic mapping allows depiction of boundaries where bluff composition changes or where composition will change during future coastal retreat. Landward penetration of new geologic units by eroding bluffs makes historical erosion rate data and landslide history inapplicable to predictions of future erosion and slide behavior. Coastal geologic hazard mapping must be based on a firm foundation of detailed geologic mapping and interpretation.

Monitoring shoreline and bluff changes in the future is particularly critical. Perhaps most importantly, regular monitoring can provide early warning of shoreline and slope stability changes that could threaten lives and property. Changes in beaches that might be caused by progressive installation of shoreline protection structures, removal of sand from the littoral system by dredging, or other human interventions can also be documented by a careful monitoring program.

Monitoring is also fundamental to testing the validity of the assumptions made in the geometric model for dune-backed shorelines. At this stage, the geometric model does not account for "hotspot" erosion that occurs at the southern ends of littoral cells and mouths of the bays. As a result, further efforts are required to better define maximum potential erosion distances in these regions by incorporating empirical observations into the analysis. In addition, it is evident that the geometric model predicts an instantaneous beach response to a major storm. The reality however, is that there is some lag in the response time of the beach. In other words, does the beach require several storms to produce the type of maximum erosion predicted by the geometric model, or are the erosion estimates achieved over an entire season? Further efforts directed towards examining these issues would provide greater confidence in the predictions made by the geometric model.

Mapping of previous erosion cuts resulting from coseismic subsidence from Cascadia subduction zone earthquakes would give a ground truth check on the cuts predicted by the geometric model in combination with the fault dislocation model. Ground penetrating radar coupled with radiocarbon and other dating techniques would help delineate these pre-historic erosion events. Other paleoseismic data such as buried soils in marshes would also lend credence to the fault dislocation model. Unfortunately, it appears that overall coastal uplift rates in the area have prevented development of extensive coastal marshes that have

[10]Ortho-rectification means removing distortions from the photo, so it can be used as an accurate map of the features that it depicts.

been useful in documenting coseismic subsidence on the northern Oregon and southern Washington coasts (e.g., note lack of Gold Beach data in the compilation of Peterson and others, 1997).

Analysis and monitoring of offshore bathymetry is essential for tracking large-scale sand movement. These data when combined with acquisition of measured beach and shoreline data would allow more sophisticated and accurate modeling of each littoral system. The ultimate effect of these refinements would be to decrease the amount of uncertainty and probably the width of the predictive hazard zones.

Hazard zone widths depicted in this study are necessarily conservative (wide) in order to account for relatively high uncertainty in the data. The user is further cautioned that both the geologic and hazard zone mapping in this report are no substitute for detailed, site-specific mapping, sampling, and interpretation by qualified professionals.

7.0 ACKNOWLEDGMENTS

This investigation was supported by an intergovernmental agreement with Curry County and from resources of the State of Oregon Department of Geology and Mineral Industries (DOGAMI). County funds were derived from a grant by the Oregon Department of Land Conservation and Development. We are especially grateful to Wendy Niem (retired geologist, Oregon State University) for her careful editing of the report and data tables. Thanks must also be extended to Randy Dana and Tanya Hadod, Department of Land Conservation and Development, for their help in providing historical shorelines derived from NOS T-sheets. Keith Massey of Jackson County Geographic Info provided useful information on street names as did Grant Young of Curry County. Finally, we are indebted to John Marra (now of NOAA; formerly of Shoreland Solutions), Paul Komar (Professor Emeritus, Oregon State University), and J. Douglas Gless (H. G. Schlicker & Associates, Inc.) for developing many of the basic concepts used here for coastal erosion hazard mapping.

8.0 REFERENCES CITED

Allan, J.C. and P.D. Komar, 2000a, Are ocean wave heights increasing in the eastern North Pacific?: EOS, Transaction of the American Geophysical Union, v. 81, no. 47, p. 561 and 566-567.

Allan, J.C. and P.D. Komar, 2000b, Spatial and temporal variations in the wave climate of the North Pacific: Unpublished report to the Oregon Department of Land Conservation and Development, Salem, Oregon, 46 p.

Allan, J.C. and P.D. Komar, 2001, Wave climate change and coastal erosion in the US Pacific Northwest: Proceedings of the 4th Conference on Ocean Wave Measurement and Analysis, WAVES 2001, San Francisco, California, ASCE, p. 680-690.

Allan, J.C. and P.D. Komar, 2002, Extreme storms on the Pacific Northwest Coast during the 1997-98 El Niño and 1998-99 La Niña: Journal of Coastal Research, v. 18, no. 1, p. 175-193.

Allan, J.C. and G.R. Priest, 2001, Evaluation of coastal erosion hazard zones along dune and bluff backed shorelines in Tillamook County, Oregon: Cascade Head to Cape Falcon: Open file report O-01-03, Oregon Department of Geology and Mineral Industries, Portland, Oregon: 126 p.

Atwater, B.F. and E. Hemphill-Haley, 1997, Recurrence intervals for great earthquakes of the past 3500 years at northeastern Willapa Bay, Washington: U.S. Geological Survey Professional Paper 1576, 108 p.

Atwater, B.F., A.R. Nelson, J.J. Clague, G.A. Carver, D.K. Yamaguchi, P.T. Bobrowsky, J. Bourgeois, M.E. Darienzo, W.C. Grant, E. Hemphill-Haley, H.M. Kelsey, G.C. Jacoby, S.P. Nishenko, S.P. Palmer, C.D. Peterson and M.A. Reinhart, 1995, Summary of coastal geologic evidence for past great earthquakes at the Cascadia subduction zone: Earthquake Spectra, v. 11, no.1, p. 1-18.

Beaulieu, J.D. and P.W. Hughes, 1976, Land use geology of western Curry County: Oregon Department of Geology and Mineral Industries Bulletin 90, 95 p.

Brock, J.C., C.W. Wright, A.H. Sallenger, W.B. Krabill and R.N. Swift, 2002, Basis and methods of NASA airborne topographic mapper lidar surveys for coastal studies: Journal of Coastal Research, v. 18, no. 1, p. 1-16.

Cabanes, C., A. Cazenave, and C. Le Provost, 2001. Sea level rise during the past 40 years determined from satellite and in situ observations: Science, v. 294, p. 840–842.

Darienzo, M.E. and C.D. Peterson, 1995, Magnitude and frequency of subduction zone earthquakes along the northern Oregon coast in the past 3,000 years: Oregon Geology, v. 57, no. 1, p. 3-12.

DLCD, 1995, Oregon's statewide planning goals & guidelines: Department of Land Conservation and Development, 42 p.

Gless, J.D., C.C. Humphrey, and J. Marra, 1998, Formula-based hazard assessment methodologies for coastal bluff-backed and slide-backed shorelines, Yaquina Head to Seal Rock, Lincoln County, Oregon in Burns, S., ed., Environmental, groundwater and engineering applications from Oregon: Belmont, California, Star Publishing Company, p. 451-463.

Graham, N.E. and H.F. Diaz, 2001, Evidence for intensification of North Pacific Winter Cyclones since 1948: Bulletin of the American Meteorological Society, v. 82, p. 1869-1893.

Hampton, M.A., 2002, Gravitational failure of sea cliffs in weakly lithified sediment: Environmental & Engineering Geoscience, v. 8, no. 3, p. 175-191.

Heinz, J.H., III, 2000, Evaluation of erosion hazards summary: Washington, DC, The H. John Heinz III Center for Science, Economics and the Environment, 1001 Pennsylvania Ave, NW, Suite 735 South, 23 p. (from world wide web site: http://www.heinzctr.org/publications.htm).

Huyer, A., W.E. Gilbert and H.L. Pittock, 1983, Anomalous sea levels at Newport, Oregon, during the 1982-83 El Niño: Coastal Oceanography and Climatology News, v. 5, p. 37-39.

JISAO/SMA, 1999, Impacts of climate variability and change in the Pacific Northwest: Pacific Northwest Regional Assessment Group, U.S. Global Change Research Program, 109 p.

Komar, P.D., 1986, The 1982-83 El Niño and erosion on the coast of Oregon: Shore and Beach, v. 54, no.2, p. 3-12.

Komar, P.D., 1997, The Pacific Northwest Coast: Living with the Shores of Oregon and Washington: Durham and London, Duke University Press, 195 p.

Komar, P.D., 1998, Beach processes and sedimentation, second edition: Upper Saddle River, New Jersey, Prentice Hall, 544 p.

Komar, P.D. and J. Allan, 2000, Analyses of extreme waves and water levels on the Pacific Northwest coast: Unpublished report to the Oregon Department of Land Conservation and Development, Salem, Oregon, 24 p.

Komar, P.D., J.C. Allan, G.M. Dias-Mendez, J.J Marra, and P. Ruggiero, 2000, El Niño and La Niño-erosion processes and impacts: Proceedings of the 27th International Conference on Coastal Engineering.

Komar, P.D., W.G. McDougal, J.J. Marra and P. Ruggiero, 1999, The rational analysis of setback distances: Applications to the Oregon coast: Shore & Beach, v. 67, p. 41-49.

Komar, P.D. and C.C. Rea, 1976, Erosion of Siletz Spit, Oregon: Shore and Beach, v. 44, no. 1. p. 9-15.

Komar, P.D., J. R. Lizarraga-Arciniega, and T.A. Terich, 1976, Oregon coast shoreline changes due to jetties: Journal of the Waterways Harbors and Coastal Engineering Division, ASCE, v. 102, no. WW1, Proceedings Paper 11933, p. 13-30.

Lizarraga-Arciniega, J.R. and P.D. Komar, 1975, Shoreline changes due to jetty construction on the Oregon Coast: Sea Grant Publication No. ORESU-T-75-004, Oregon State University, Corvallis, Oreg..

Merriman, T. and T.H. Wiggin, 1947, Civil engineers' handbook: New York, NY, John Wiley & Sons: 892 p.

Mitchell,C.E., P. Vincent, R.J. Weldon, II and M.A. Richards, 1994, Present-day vertical deformation of the Cascadia margin, Pacific Northwest, United States: Journal of Geophysical Research, v. 6, p. 12,257-12,277.

OCZMA, 1979, Beaches and Dunes Handbook for the Oregon Coast: Unpublished report to the Oregon Department of Land Conservation and Development, Salem, Oregon: 161 p.

Orr, E.L., W.N. Orr, and E.M. Baldwin, 2000, Geology of Oregon: Kendall/Hunt Publishing Co, Dubuque, Iowa, 254 p.

Peltier, W.R., 1986, Deglaciation-induced vertical motion of the North American continent: Journal of Geophysical Research, v. 91, p. 9,099-9,123.

Peterson, C.D., E.T. Barnett, G.G. Briggs, G.A. Carver, J.J. Clague and M.E. Darienzo, 1997, Estimates of coastal subsidence from great earthquakes in the Cascadia subduction zone, Vancouver Island, B.C., Washington, Oregon, and Northernmost California: Oregon Department of Geology and Mineral Industries Open file report O-97-05, 43 p.

Peterson, C.D., M.E. Darienzo, D. Hamilton, D.J. Pettit, R.K. Yeager, P.L. Jackson, C.L. Rosenfeld and T.A. Terich, 1994, Beach-shoreline database, Pacific Northwest Region, USA: OFR 0-94-2, Oregon Department of Geology and Mineral Industries, Portland, OR: 29 p., digital disk.

Peterson, C.D., D.L. Doyle and E.T. Barnett, 2000, Coastal flooding and beach retreat from coseismic subsidence in the Central Cascadia Margin, USA: Environmental and Engineering Geoscience, v. 6, no. 3, p. 255-269.

Peterson G.L., D.H. Scofield, L.R. Squier, and F.N. Toot, 1998, Engineering geology and drainage of the Arizona Inn Landslide, US Highway 101, southern Oregon coast, in Burns, S., ed., Environmental, groundwater and engineering geology: applications from Oregon: Star Publishing Company, 940 Emmett Ave., Belmont, CA 94002, p. 231-247.

Priest, G.R., 1999, Coastal shoreline change study, northern and central Lincoln County, Oregon: Journal of Coastal Research, Special Issue No. 28, p.140-157.

Priest, G.R. and J.C. Allan, 2004, Evaluation of coastal erosion hazard zones along dune and bluff backed shorelines in Lincoln County, Oregon: Cascade Head to Seal Rock: Oregon Department of Geology and Mineral Industries Open-File Report O-04-09, digital files on CD.

Priest, G.R., A. Chawla, and J.C. Allan, 2003, Tsunami hazard map of the Alsea Bay (Waldport) area, Lincoln County, Oregon: Oregon Department of Geology and Mineral Industries Interpretive Map Series, IMS-23, digital map and supporting files on CD.

Priest, G.R., I. Saul and J. Diebenow, 1994, Explanation of chronic geologic hazard maps and erosion rate database, coastal Lincoln County, Oregon: Salmon River to Seal Rocks: Oregon Department of Geology and Mineral Industries Open-File-Report O-94-11, 45 p.

Ruggiero, P., P.D. Komar, W.G. McDougal, and R.A. Beach, 1996, Extreme water levels, wave runup and coastal erosion: Proceedings of the 25th Conference on Coastal Engineering, ASCE, p. 2793-2805.

Ruggiero, P., P.D. Komar, W.G. McDougal, J.J. Marra, and R.A. Beach, 2001, Wave runup, extreme water levels and the erosion of properties backing beaches: Journal of Coastal Research, v. 17, no. 2, p. 407-419.

Schlicker H.G., R.J. Deacon, G.W. Olcott, and J.D. Beaulieu, 1973, Environmental Geology of Lincoln County, Oregon: Oregon Department of Geology and Mineral Industries Bulletin 81, 171 p.

Shih, S.M., P.D. Komar, K.J. Tillotsen, W.G. McDougal, and P. Ruggiero, 1994, Wave run-up and sea-cliff erosion: 24th International Conference on Coastal Engineering, American Society of Civil Engineers, p. 2170-2184.

Vincent, P., 1989, Geodetic Deformation of the Oregon Cascadia Margin: Master's thesis, University of Oregon, Eugene, 86 p.

United States Geological Survey, 2000, http://www.csc.noaa.gov/crs/tcm/index.html

Walker, G.W. and N.S. MacLeod, 1991, Geologic map of Oregon: US Geological Survey Special Geologic Maps, 1:500,000 scale.

APPENDIX A – Erosion Hazard Zones

Coastal erosion hazard zones for the study area are depicted on the maps below. Note that the active erosion hazard zone includes any areas along the coastline mapped as active or potentially active landslides. Most of the active hazard zone in the Sisters Rocks area is an area of active landslides. Base maps are 2003 orthophotos, except the map of the Sisters Rocks area, this area, in order to cover areas north of the 2003 orthophoto coverage, is on standard U.S. Geological Survey digital raster graphic topographic quadrangles (DRG's) produced from 1980-1982 aerial photography. The 2003 orhtophotos were produced for Oregon Department of Land Conservation and Development (DLCD) by 3Di of Eugene, Oregon. Street names and digital street lines are taken from files of the Oregon Department of Transportation (ODOT) and from files provided by Keith Massie of Columbia Cartographic, Ashland, Oregon. The maps below are raster images at a resolution of 120 dots per inch produced from MapInfo software. All but the first one are at approximately 800 feet per inch; the first map is at approximately 1 inch = 2000 feet, the original scale of the DRG base map.

Maps progress sequentially from the Sisters Rocks on the north, to the North Jetty at Gold Beach on the south. Consult the digital GIS files for detailed descriptions of each polygon.

Key to Appendix A, Erosion hazard maps

- Active erosion hazard zone
- High-risk coastal erosion hazard zone
- Moderate-risk coastal erosion hazard zone
- Low-risk coastal erosion hazard zone

EROSION HAZARD RISK ZONES - SISTERS ROCKS AREA

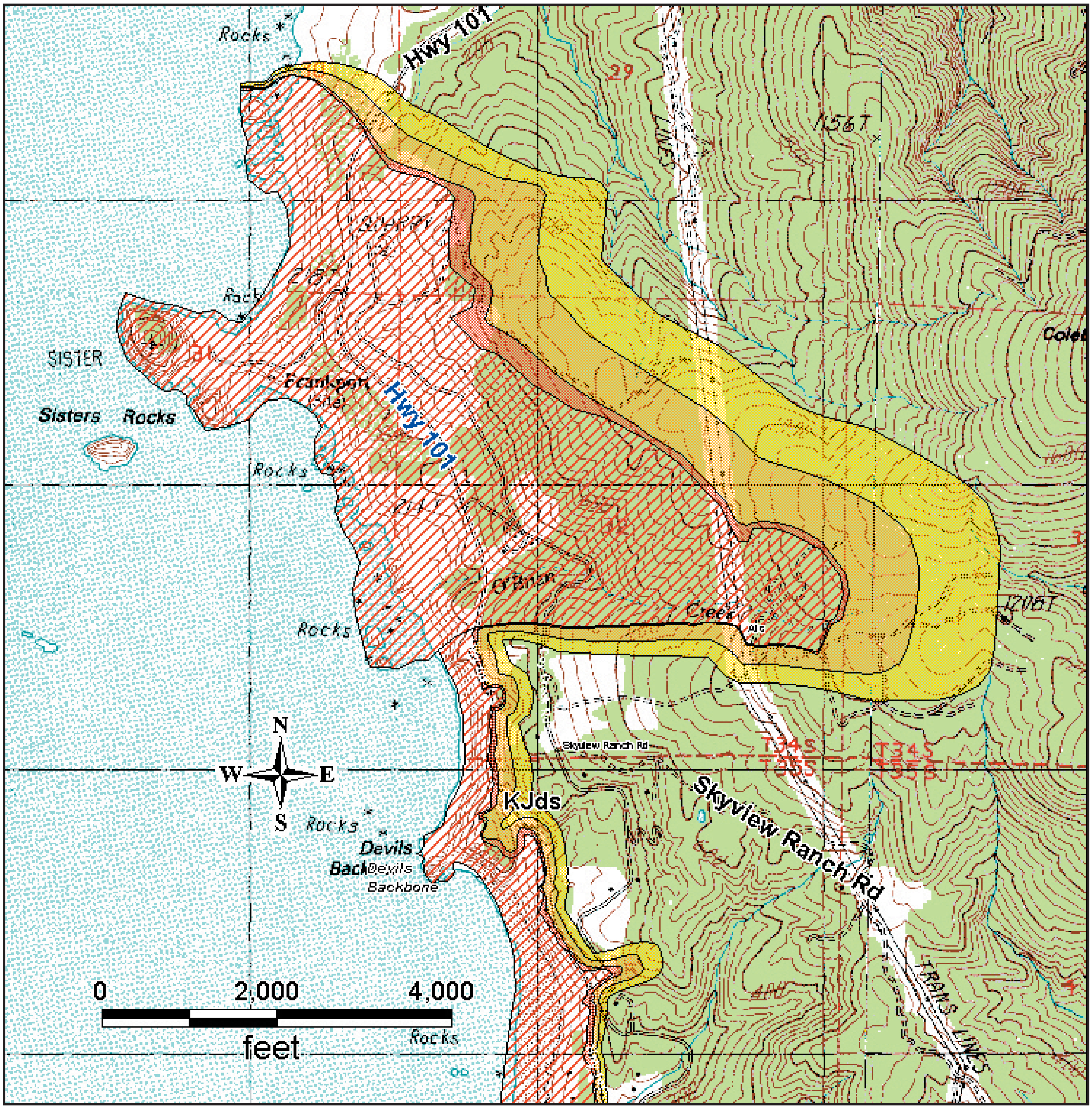

EROSION HAZARD RISK ZONES – DEVILS BACKBONE AREA

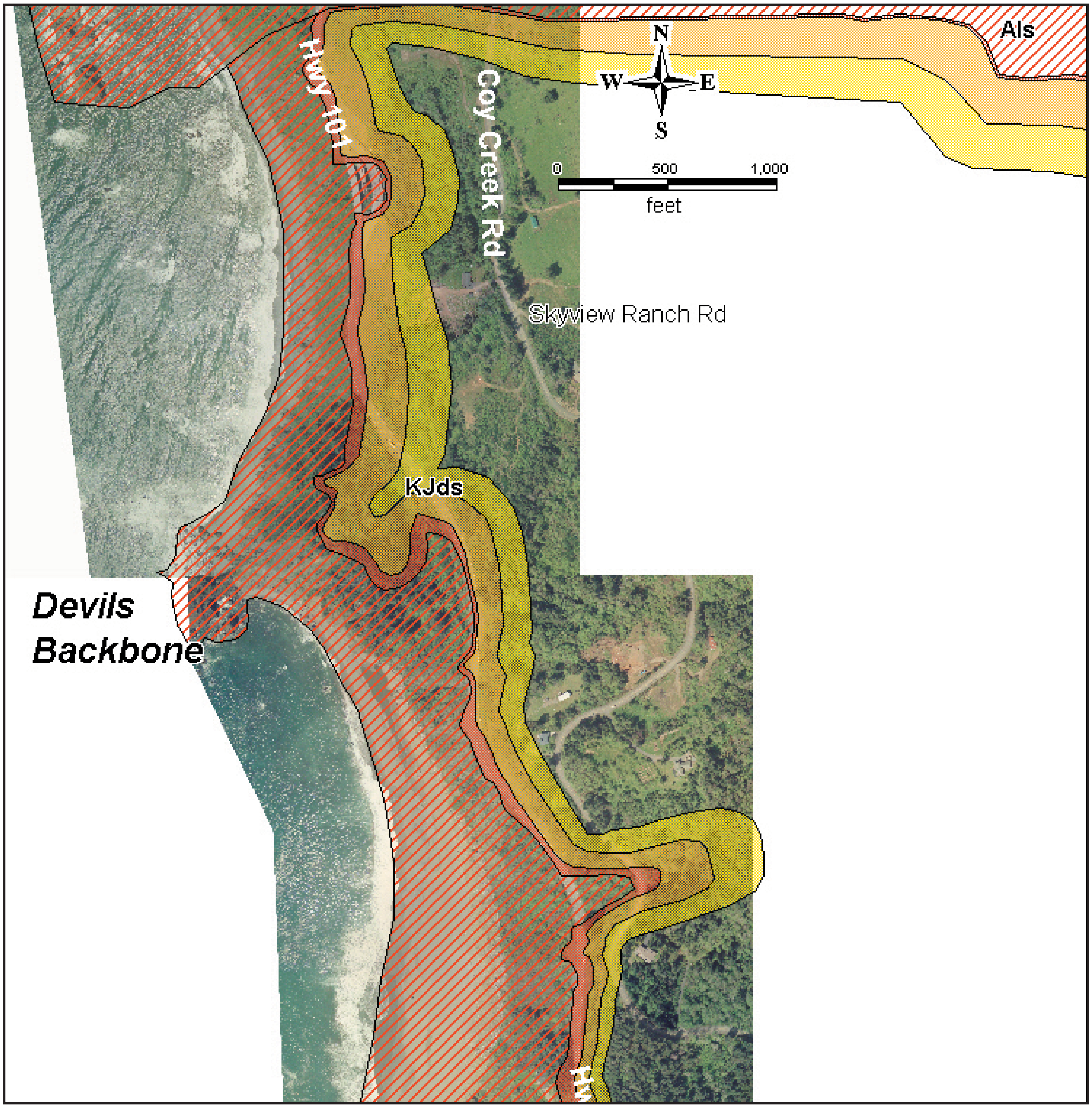

EROSION HAZARD RISK ZONES - EUCHRE CREEK-OPHIR-AREA

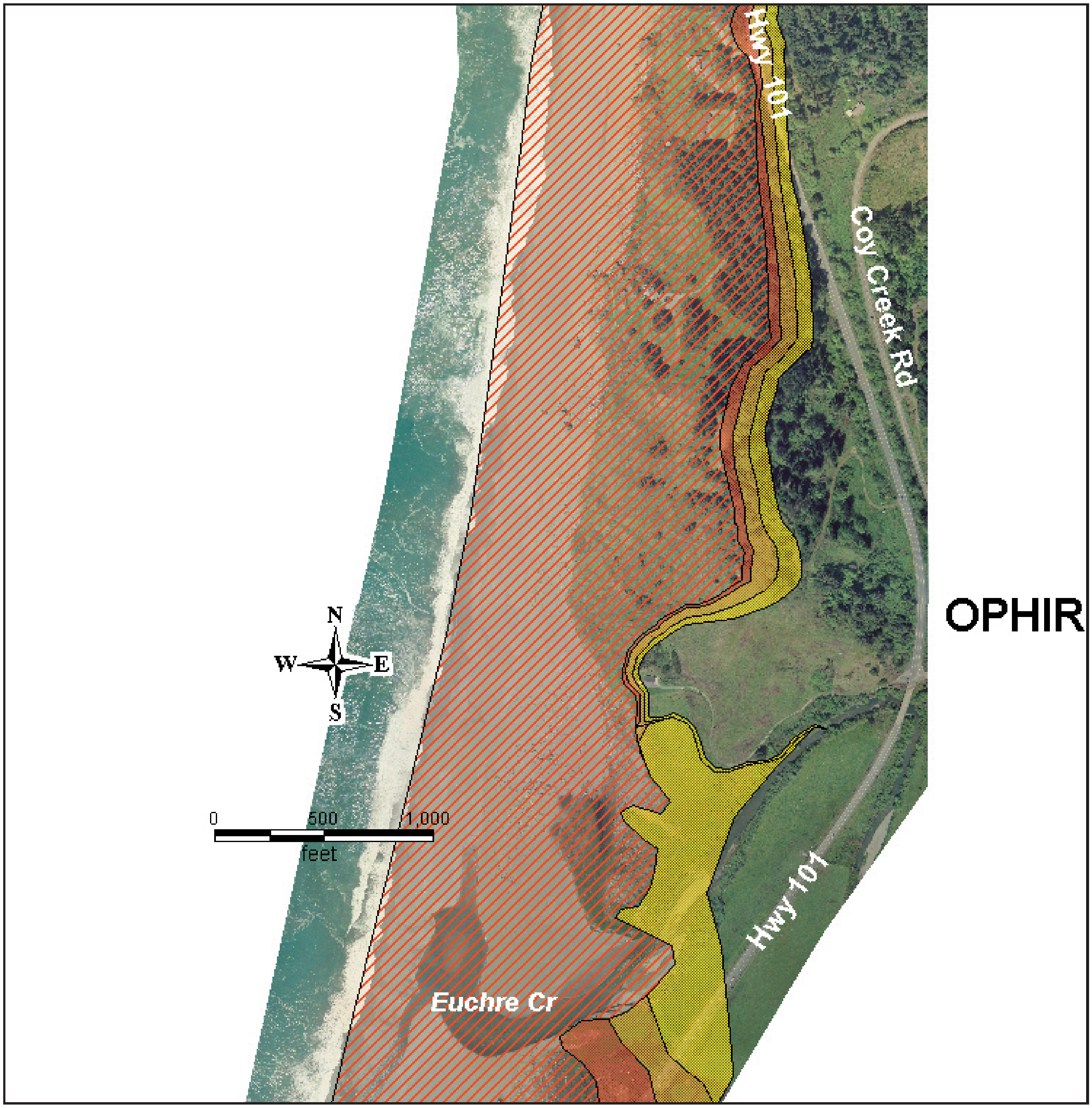

EROSION HAZARD RISK ZONES – SOUTH EUCHRE CREEK TO WELSH DRIVE

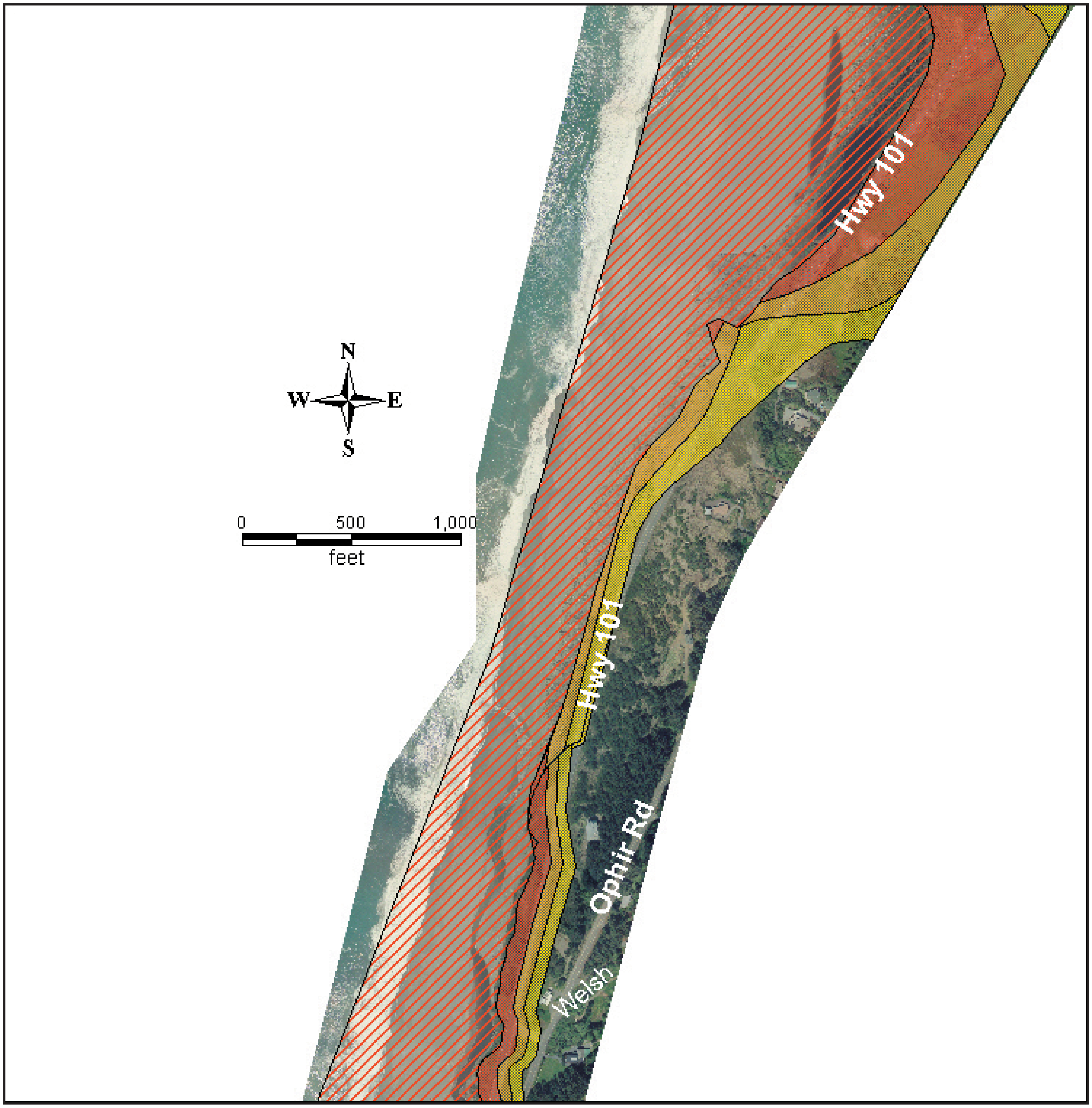

EROSION HAZARD RISK ZONES – GREGGS CREEK TO MILLER ROAD

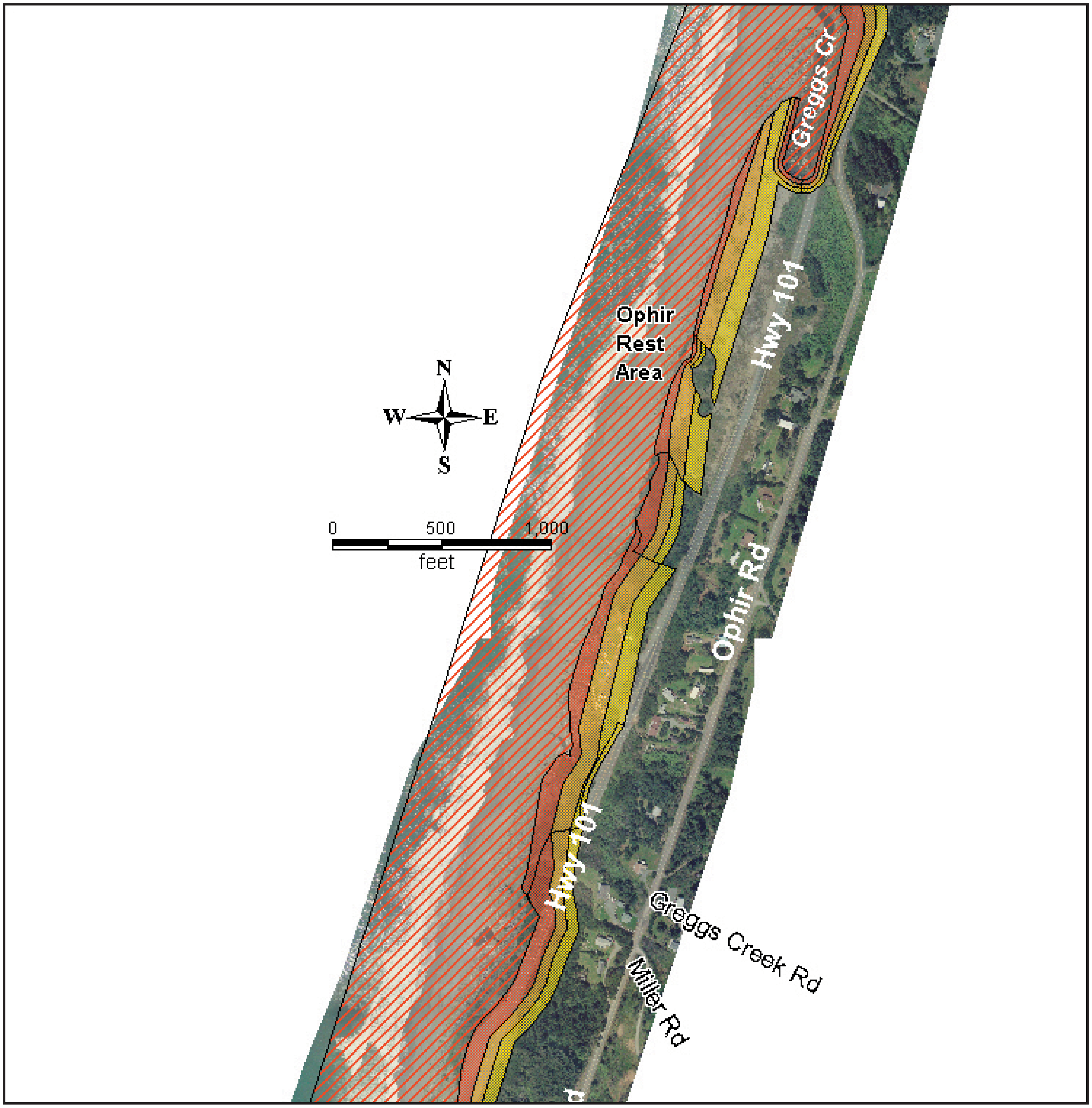

EROSION HAZARD RISK ZONES – NORTH NESIKA BEACH

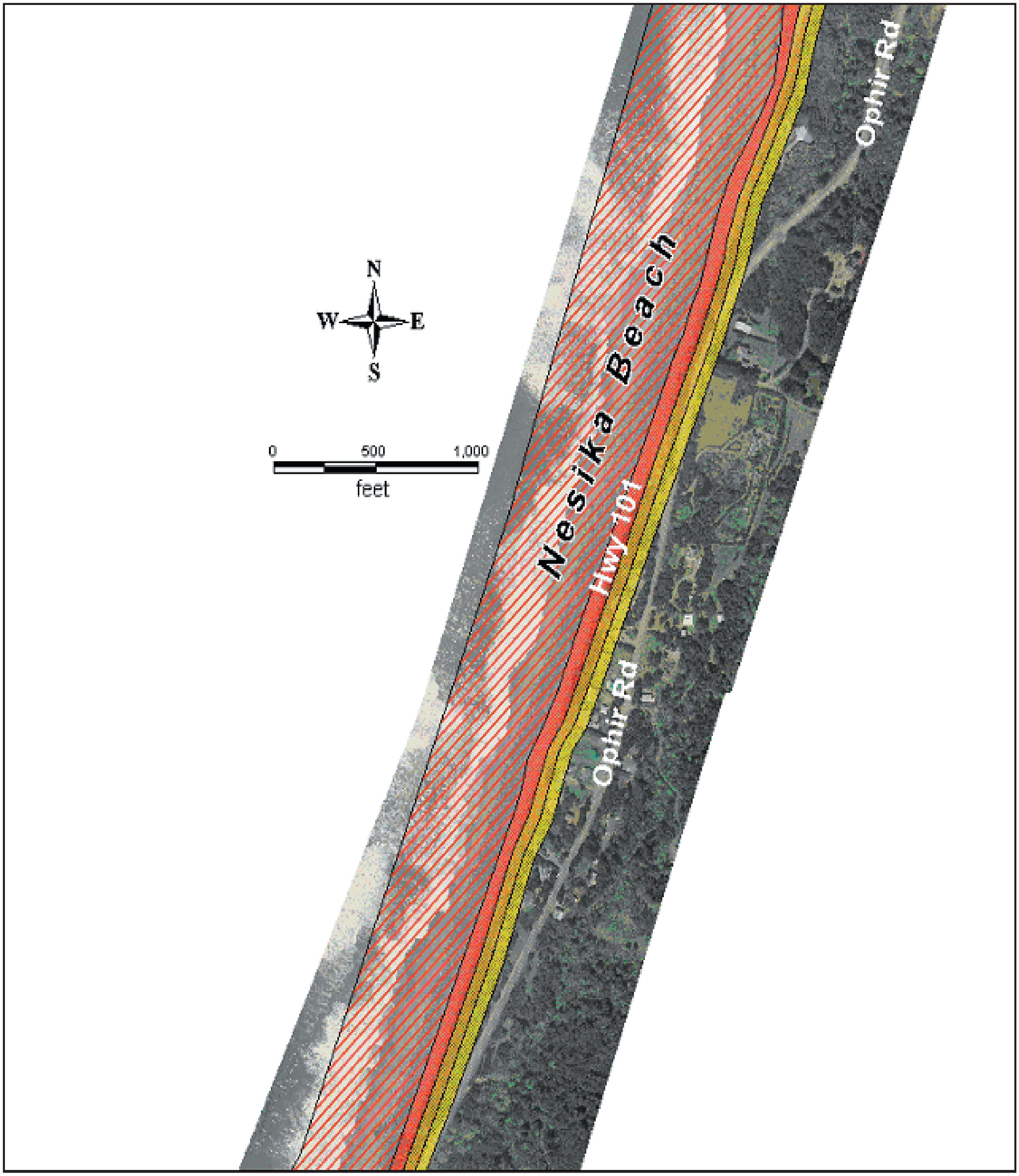

EROSION HAZARD RISK ZONES – CENTRAL NESIKA BEACH (ANDY-GRANGE ROAD)

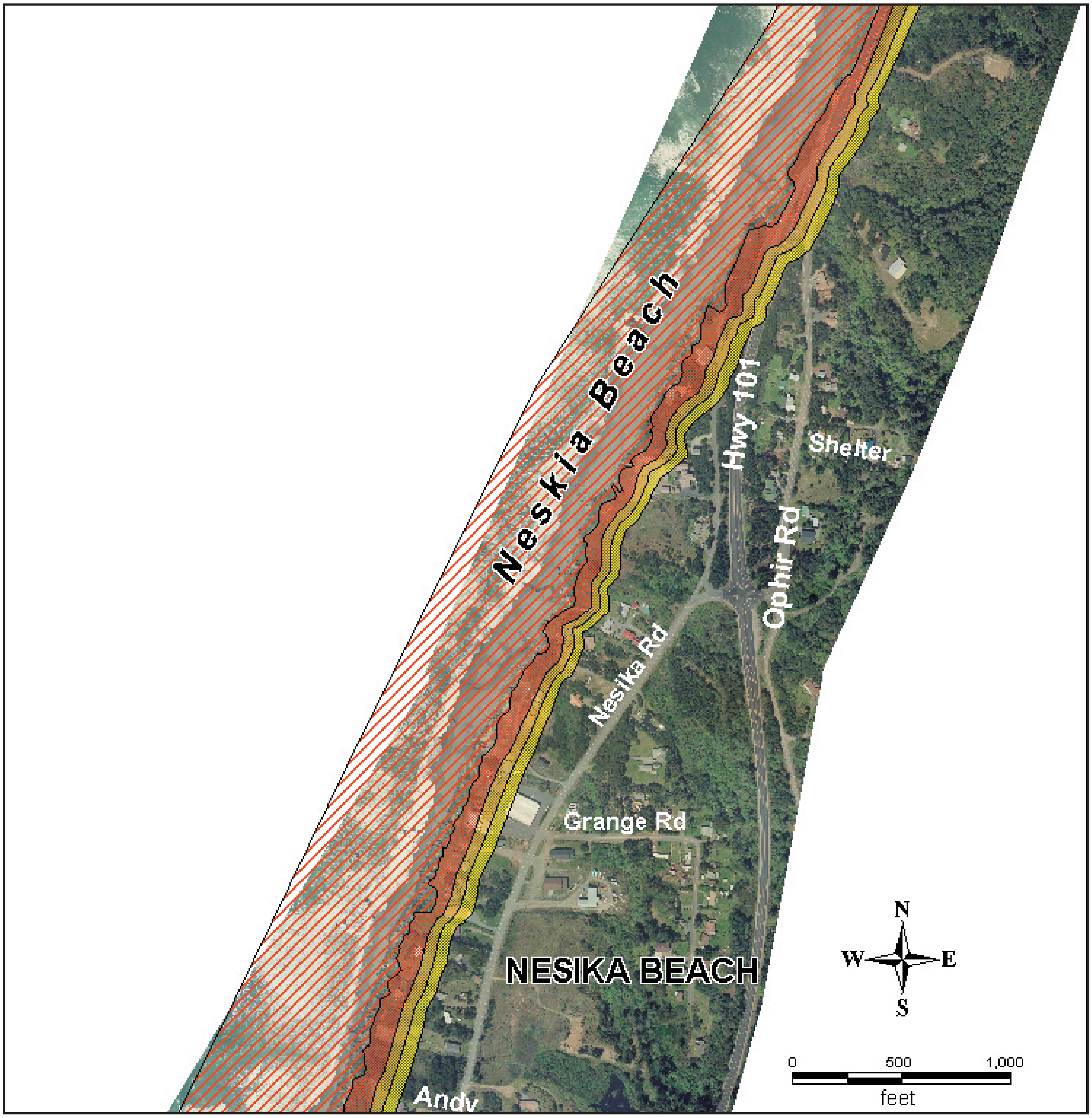

EROSION HAZARD RISK ZONES – SOUTH NESIKA BEACH (ANDY-GUN CLUB ROAD)

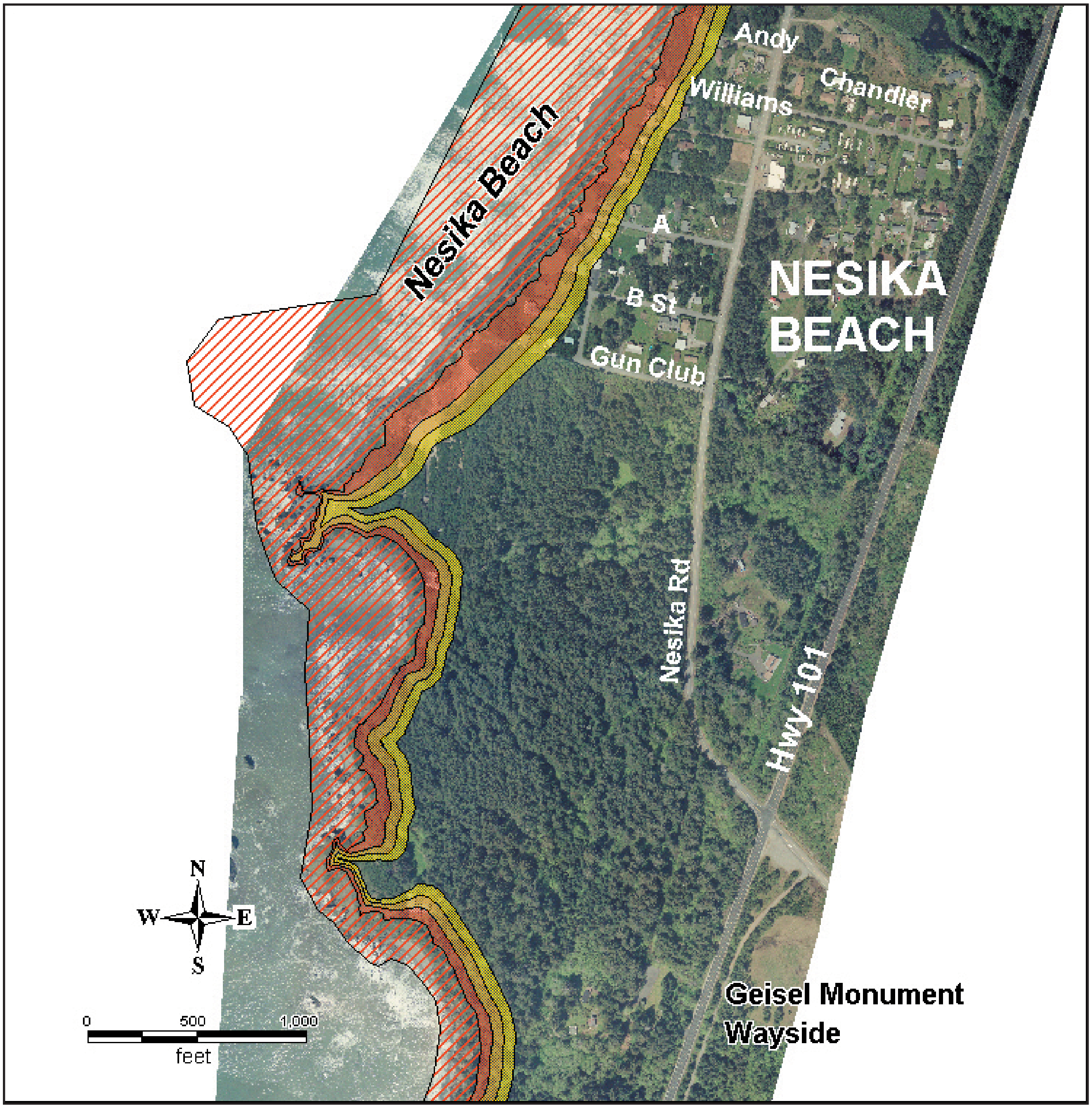

EROSION HAZARD RISK ZONES – WAKEMAN BEACH TO HUBBARD MOUND

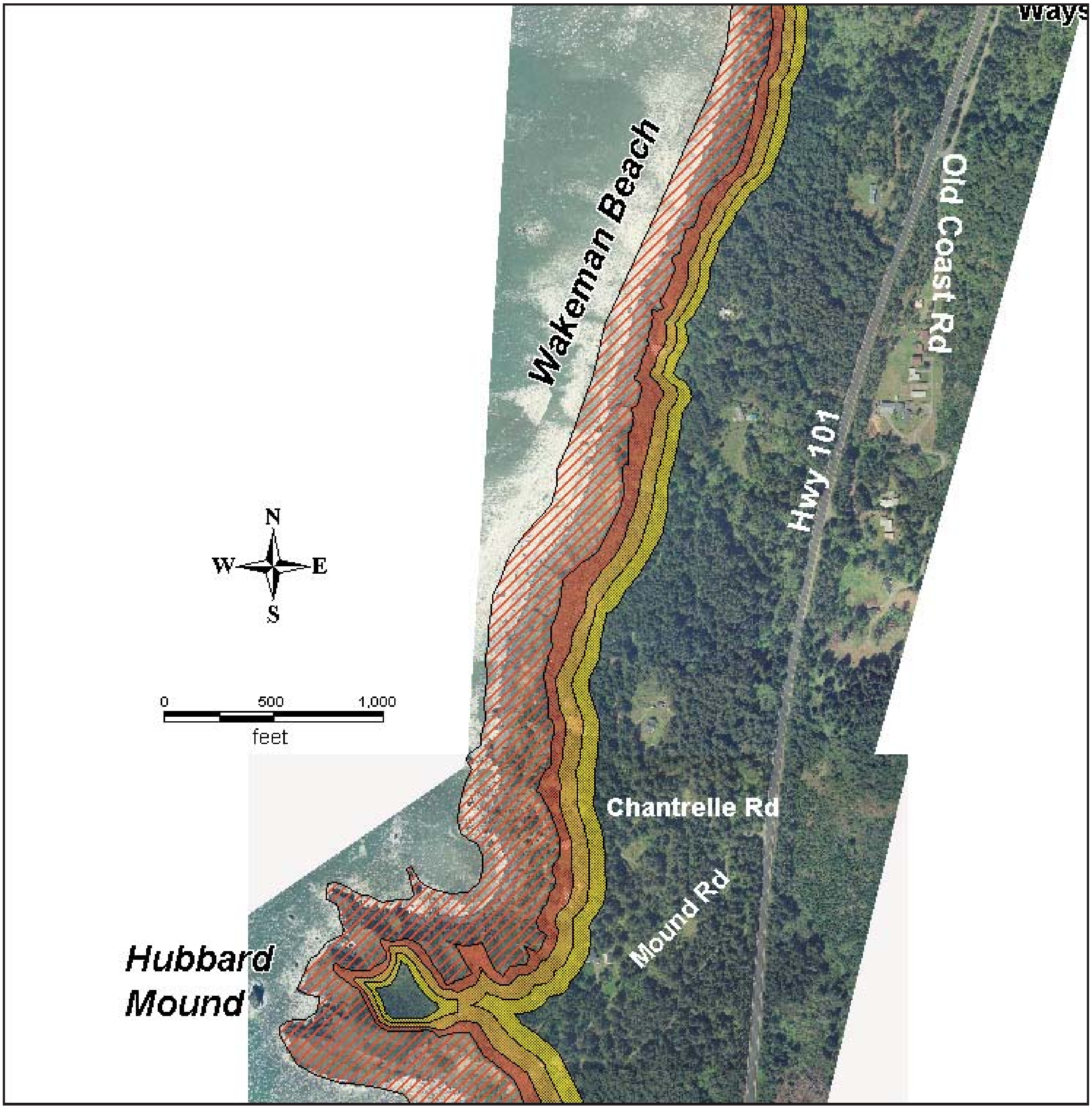

EROSION HAZARD RISK ZONES – SOUTH HUBBARD MOUND TO OTTER POINT

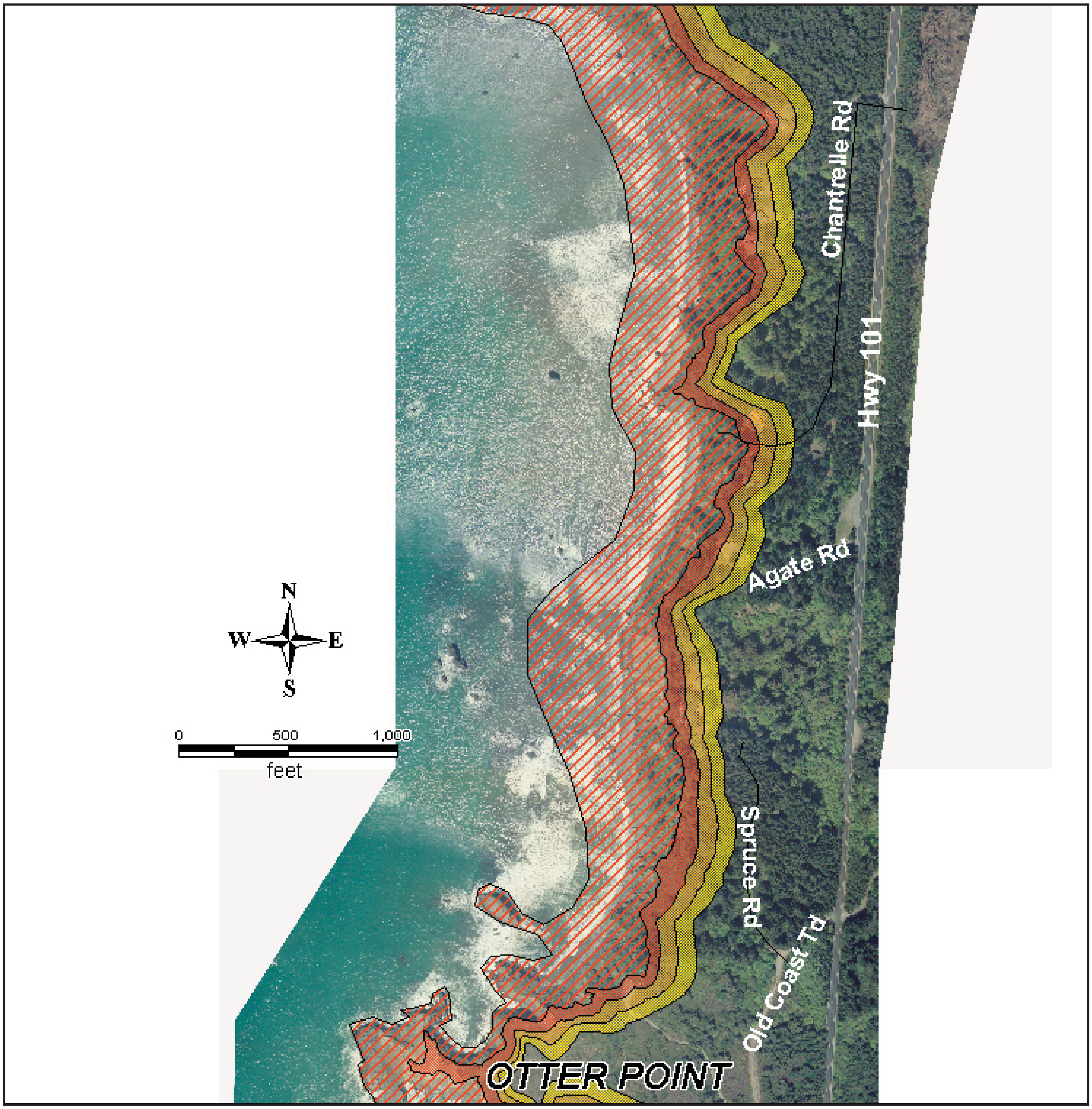

EROSION HAZARD RISK ZONES – BAILEY BEACH

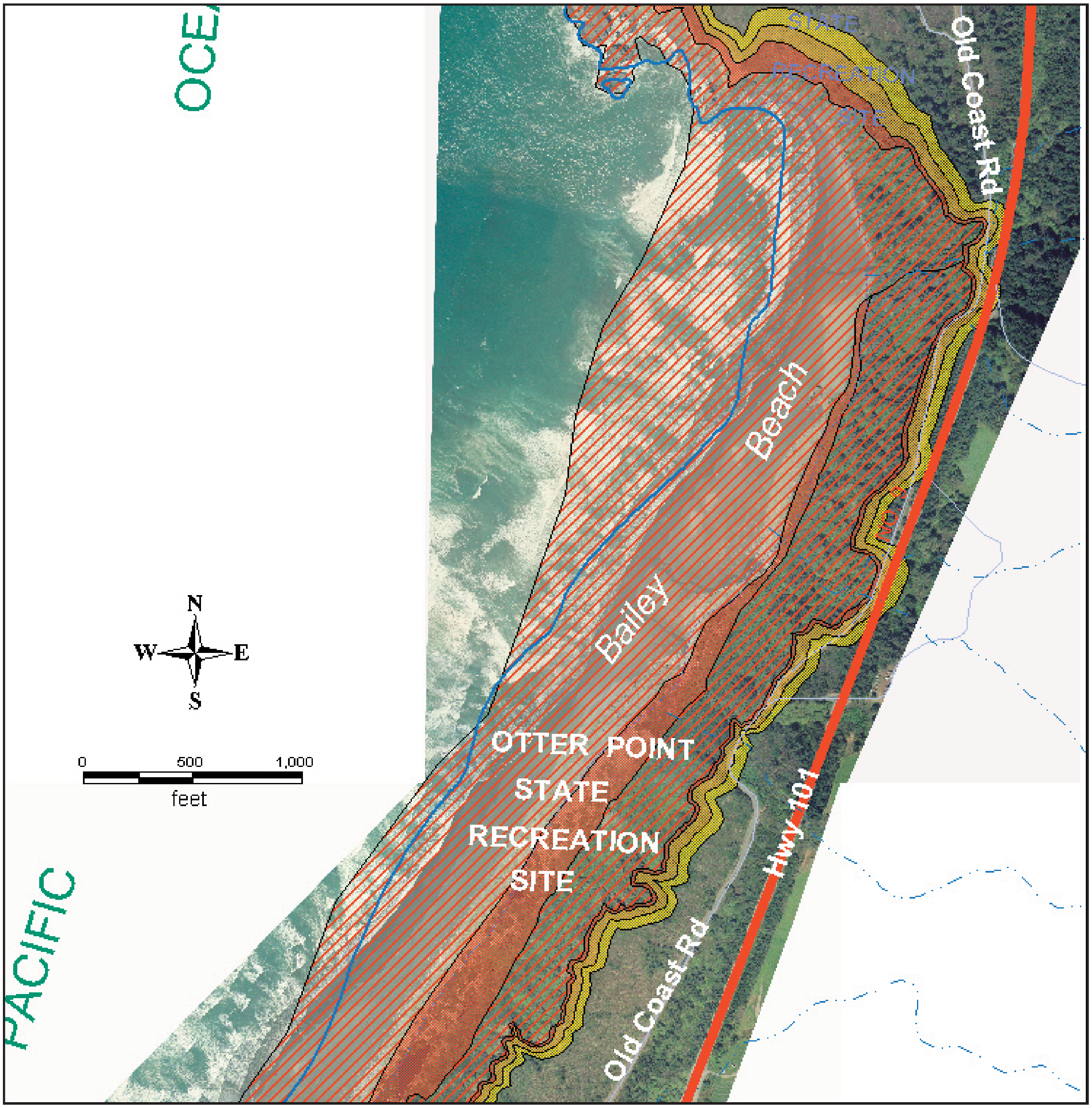

EROSION HAZARD RISK ZONES – SANDY – COBBLESTONE ROAD AREA

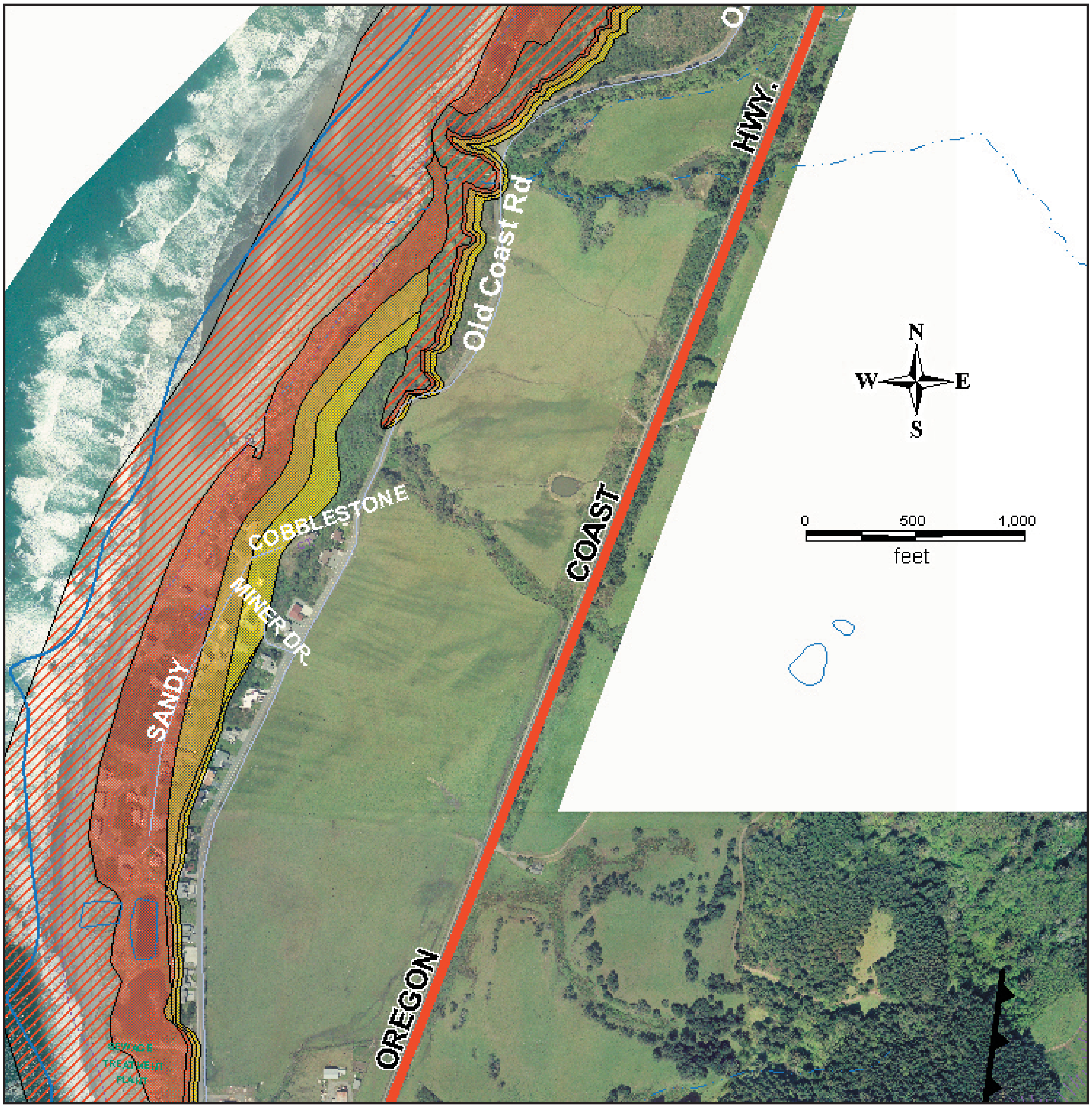

EROSION HAZARD RISK ZONES – NORTH JETTY OF ROGUE RIVER

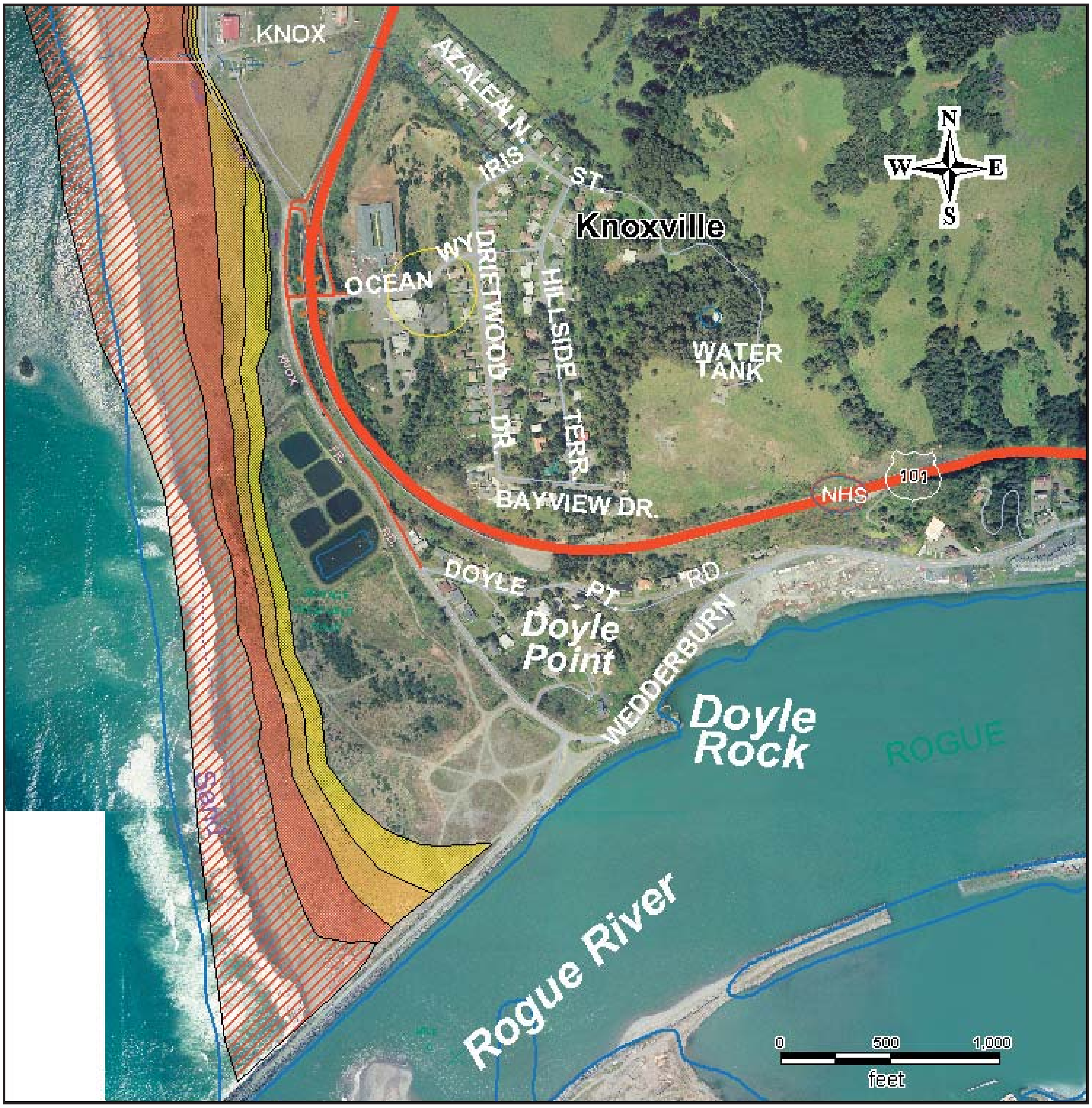

APPENDIX B - LANDSLIDE AND GEOLOGY MAPS

Shoreline geology and landslides for Sisters Rocks to the North Jetty at Gold Beach are depicted on the maps below. Base maps are 2003 orthophotos, except the map of the Sisters Rocks area, this area, in order to cover areas north of the 2003 orthophoto coverage, is on standard U.S. Geological Survey digital raster graphic topographic quadrangles (DRG's) produced from 1980-1982 aerial photography. The 2003 orhtophotos were produced for Oregon Department of Land Conservation and Development (DLCD) by 3Di of Eugene, Oregon. Street names and digital street lines are taken from files of the Oregon Department of Transportation (ODOT) and from files provided by Keith Massie of Columbia Cartographic, Ashland, Oregon. The maps below are raster images at a resolution of 120 dots per inch produced from MapInfo software. All but the first one are at approximately 800 feet per inch; the first map is at approximately 1 inch = 2000 feet, the original scale of the DRG base map.

Maps progress sequentially from the Sisters Rocks on the north, to the North Jetty at Gold Beach on the south. Consult the digital GIS files for detailed descriptions of each polygon. The accompanying report has detailed description of the landslide units.

Key to Appendix B, Geology and Landslide Maps. Descriptions of Tertiary rock units are modified slightly from Snavely and others (1976a; 1978b; 1976c; and 1996).

Polygon	Geologic Symbol	Description
	Fill	Modern fill; mostly moderately consolidated, poorly sorted mixtures of rock and soil.
	Als	Holocene active landslide.
	Ab	Holocene active landslide block.
	PAls	Holocene potentially active landslide.
	Qbs	Holocene partially vegetated dune sand.
	Qac	Holocene alluvium and colluvium, unconsolidated poorly sorted to well sorted sand and gravel.
	Qal	Holocene alluvium; unconsolidated sand and gravel

	Qc	Holocene colluvium, unconsolidated rock and soil mixtures; contains interbeds of debris flow deposits and alluvial sand.
	Qaco	Pleistocene to Holocene alluvium and colluvium, partially consolidated poorly sorted to well sorted sand and gravel. Located on sides of existing valleys.
	Qoc	Pleistocene to Holocene colluvium, partially consolidated rock and soil mixtures; high sand content from underlying marine terrace deposits; contains interbeds of debris flow deposits and alluvial sand. Heavily dissected by erosion but probably once formed a continuous bajada of alluvial fans on top of Pleistocene marine terrace deposits.
	Qmtm	Pleistocene marine terrace deposits, partially consolidated deposits of well sorted, well rounded quartzofeldspathic beach and dune sand with interbeds of beach gravel at the base..
	KJds	Lower Cretaceous and Upper Jurassic Dothan Formation and related rocks; sandstone, conglomerate, greywacke, rhythmically banded chert lenses. Includes western Dothan and Otter Point
	Jop	Jurassic Otter Point Formation sandstone, marine basalt, metamorphic blocks, conglomerate, and minor chert and mudstone (Description from Beaulieu and Hughes, 1976).
	Jopms	Jurassic Otter Point Formation highly sheared mudstone and sandstone with lesser amounts of metavolcanic rock and ultramafic rock in separate tectonic blocks
	Jops	Jurassic Otter Point Formation sandstone; medium to coarse grained sandstone, typically massive beds with pebble conglomerate with minor mudstone interbeds.
	spp	Jurassic (?) highly sheared serpentinite; matrix of sheared soft serpentine with variable sized boulder sized blocks of peridotite other ultramafic rocks and greenstone.
	Jopmvs	Jurassic Otter Point Formation metavolcanic rocks (greenstone). Generally forms headlands, sea stacks and offshore reefs.
	Jopmv	Jurassic Otter Point Formation metavolcanic rocks (greenstone). Generally forms headlands, sea stacks and offshore reefs.

GEOLOGIC MAP SYMBOLS

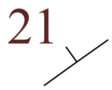

Strike and dip of bedding.

Thrust fault in melange of Otter Point Formation north side of mouth of the Rogue River separates sepentinite from graywacke-marine basalt-mudstone sequence; taken from Beaulieu and Hughes (1976).

LANDSLIDE AND GEOLOGY MAP - SISTERS ROCKS AREA

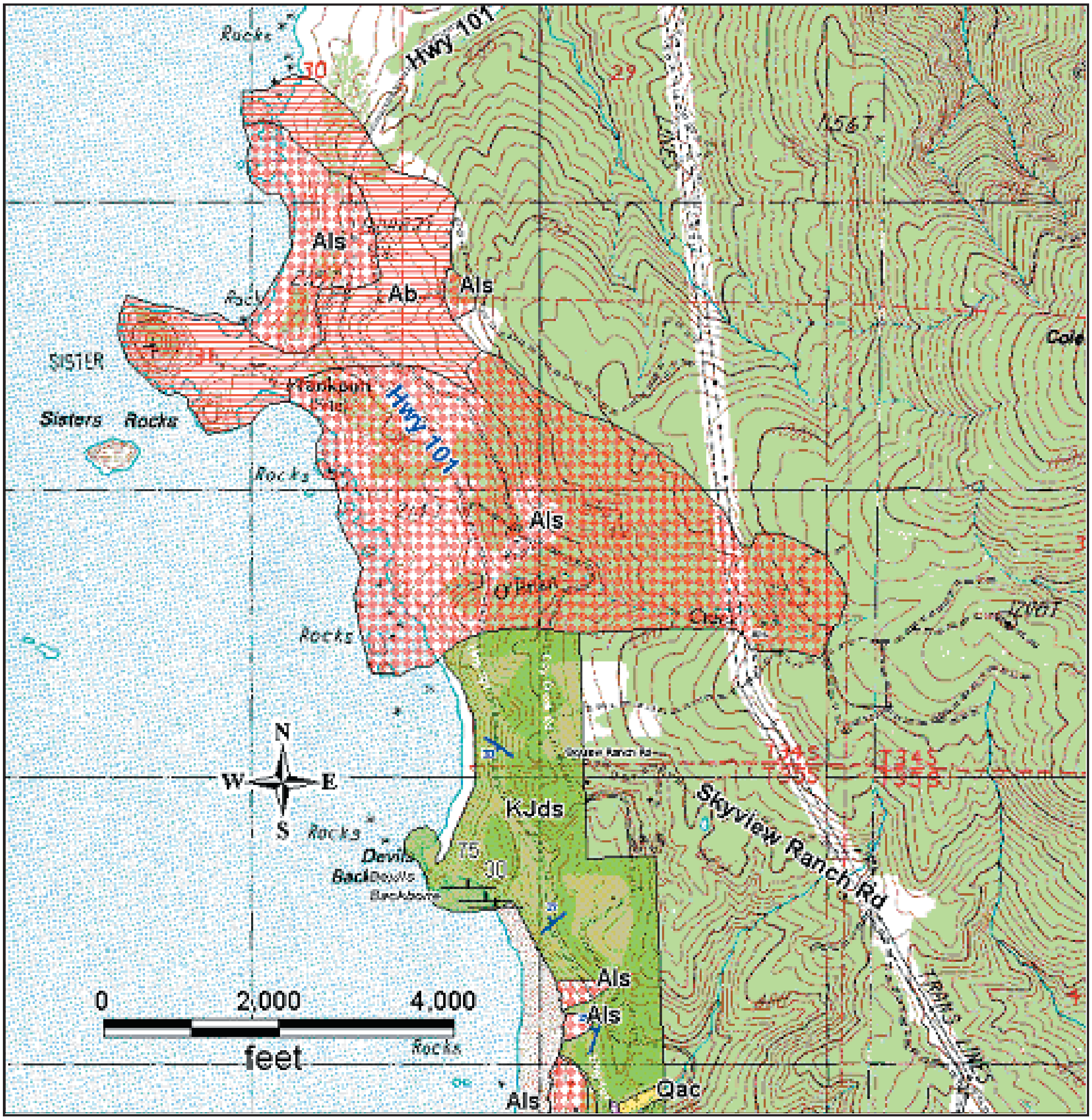

LANDSLIDE AND GEOLOGY MAP – DEVILS BACKBONE AREA

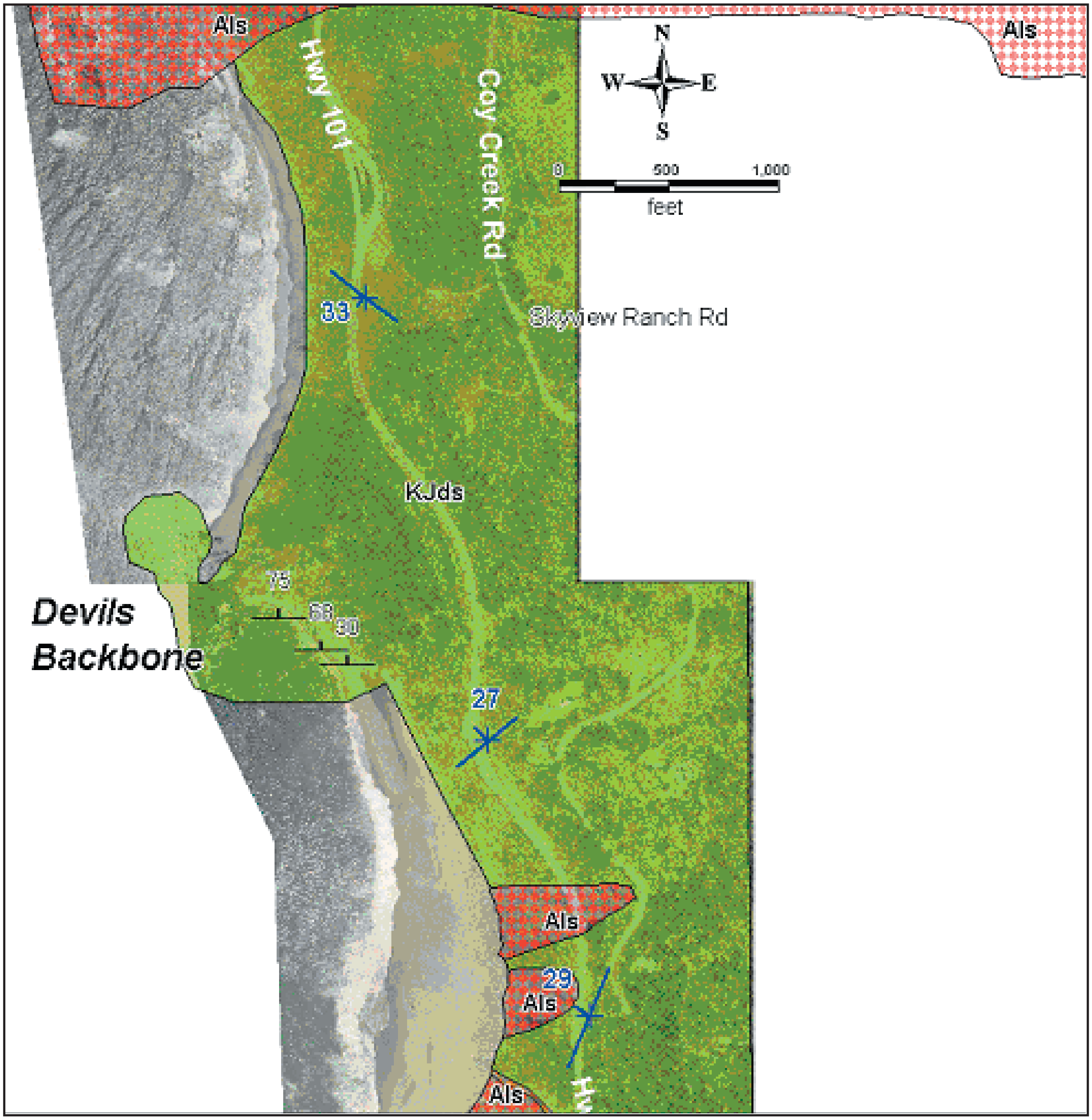

LANDSLIDE AND GEOLOGY MAP - EUCHRE CREEK-OPHIR-AREA

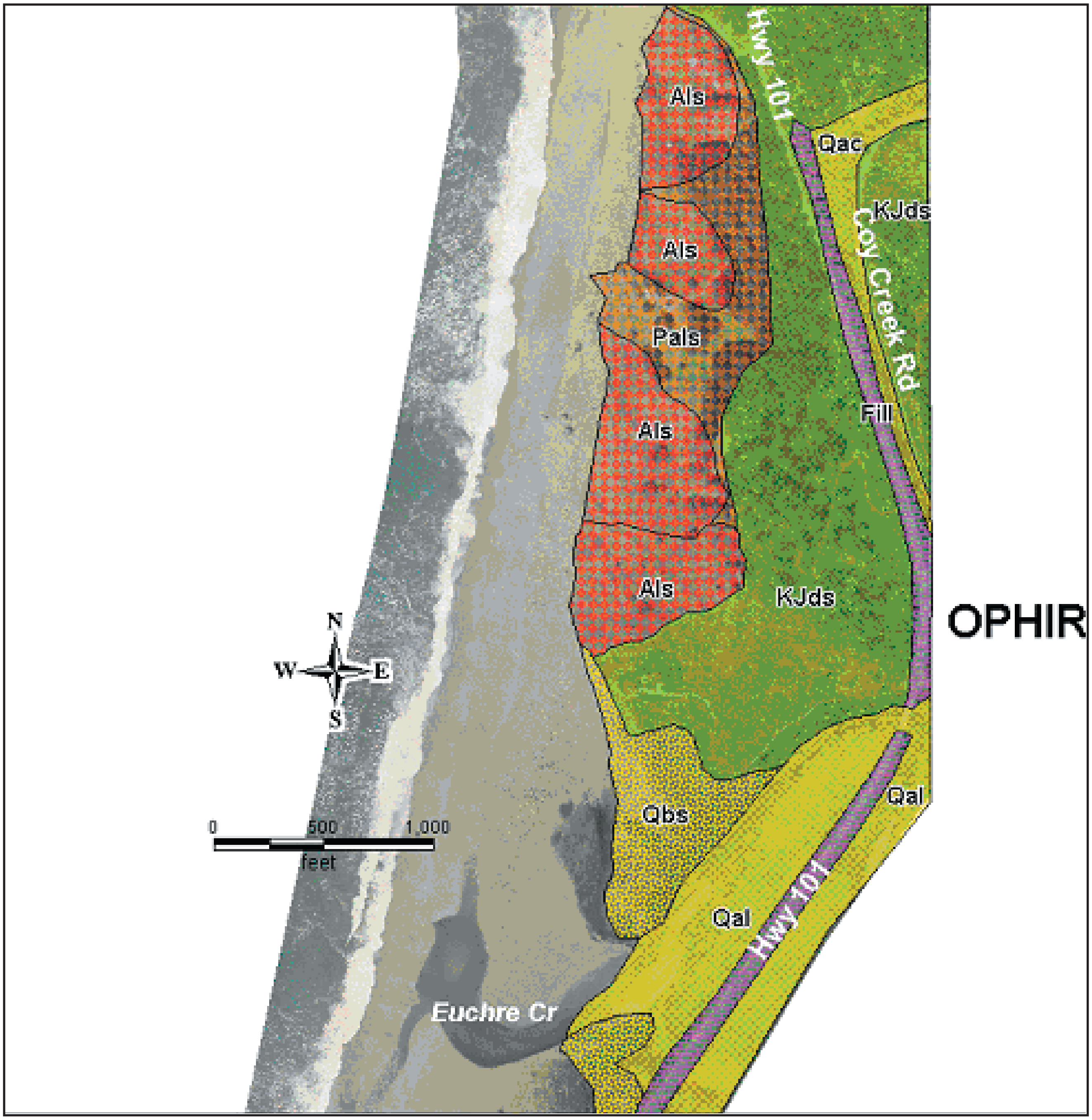

LANDSLIDE AND GEOLOGY MAP – SOUTH EUCHRE CREEK TO WELSH DRIVE

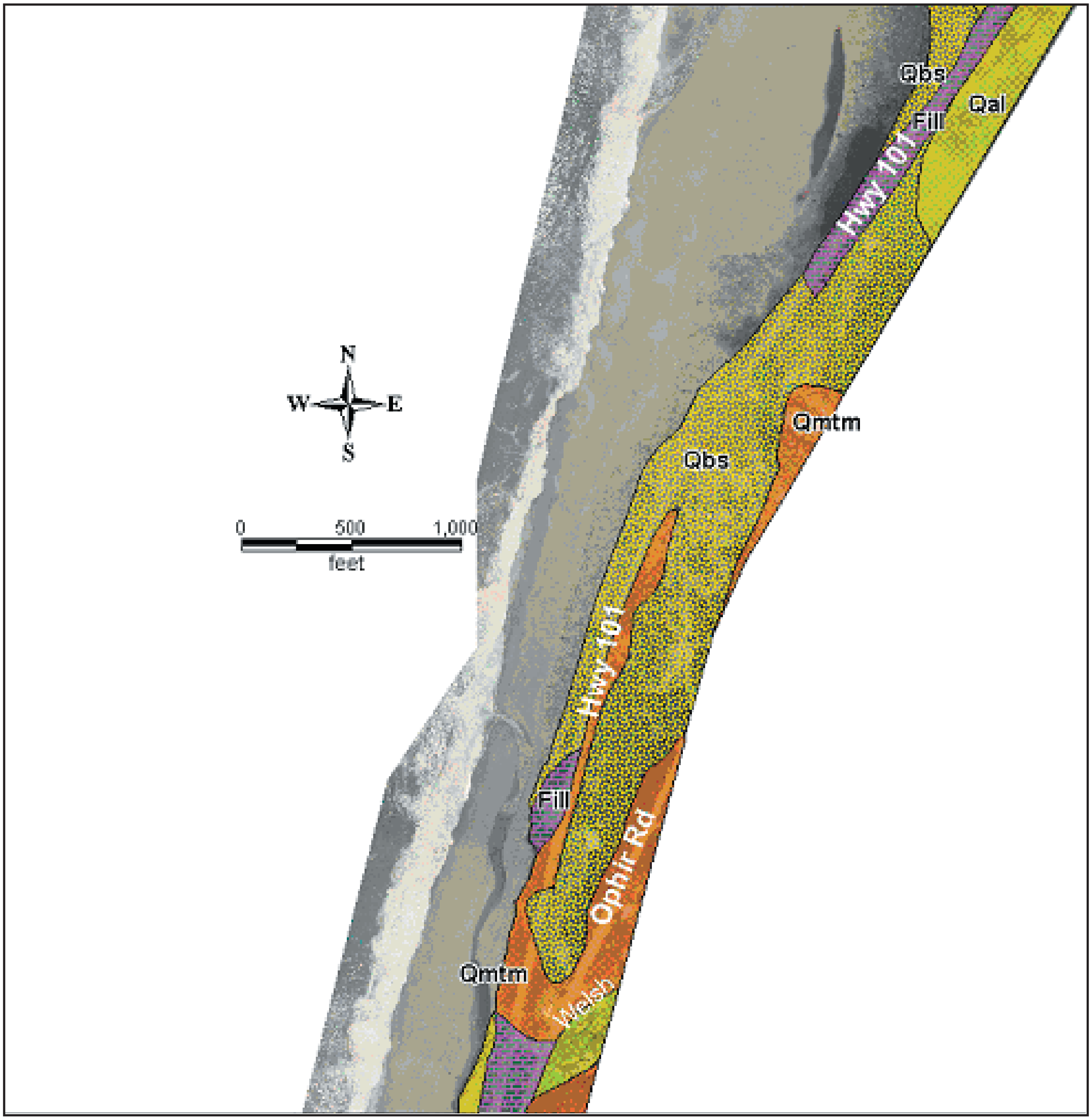

LANDSLIDE AND GEOLOGY MAP – GREGGS CREEK TO MILLER ROAD

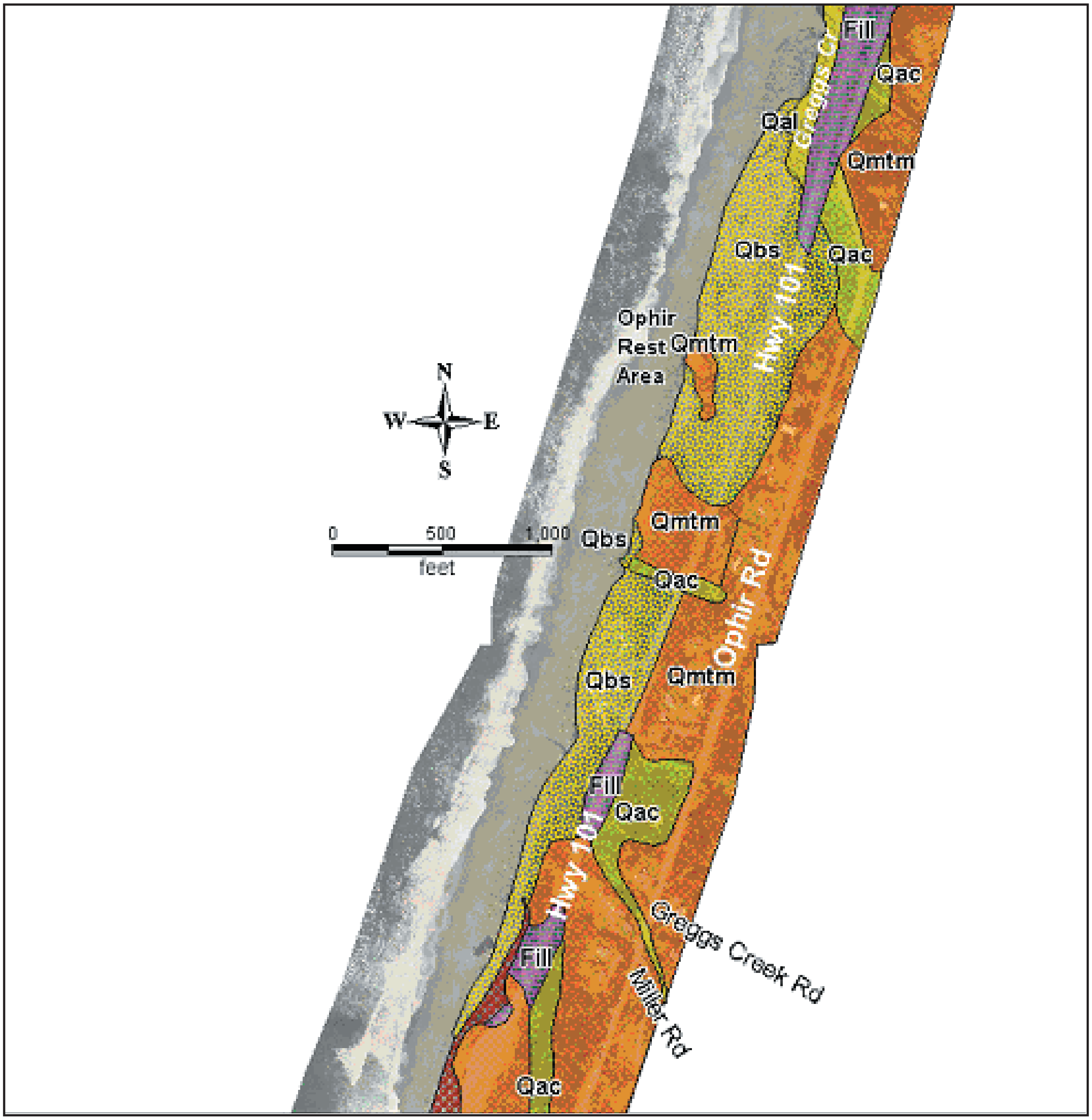

LANDSLIDE AND GEOLOGY MAP – NORTH NESIKA BEACH

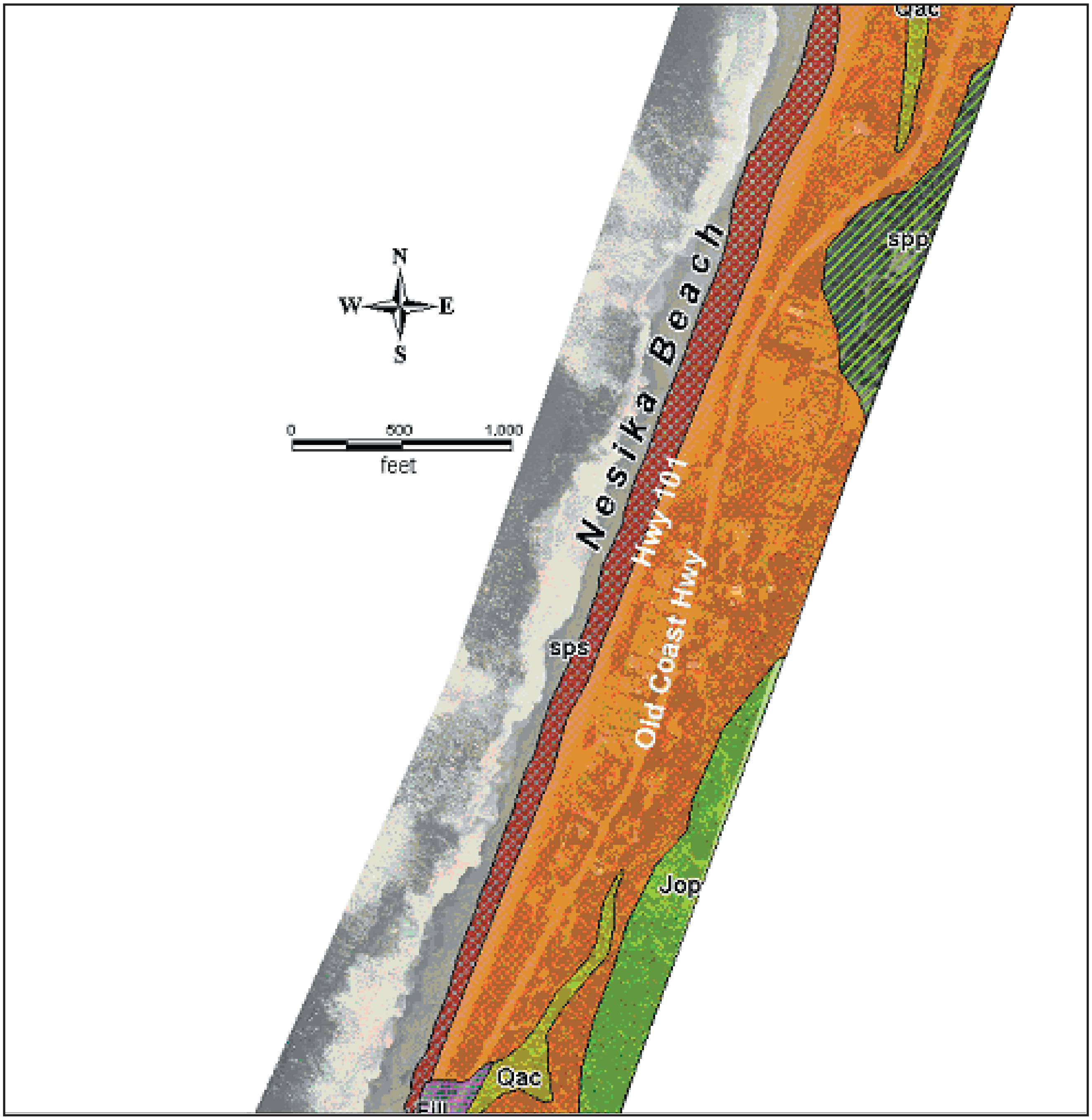

LANDSLIDE AND GEOLOGY MAP – CENTRAL NESIKA BEACH (ANDY-GRANGE ROAD)

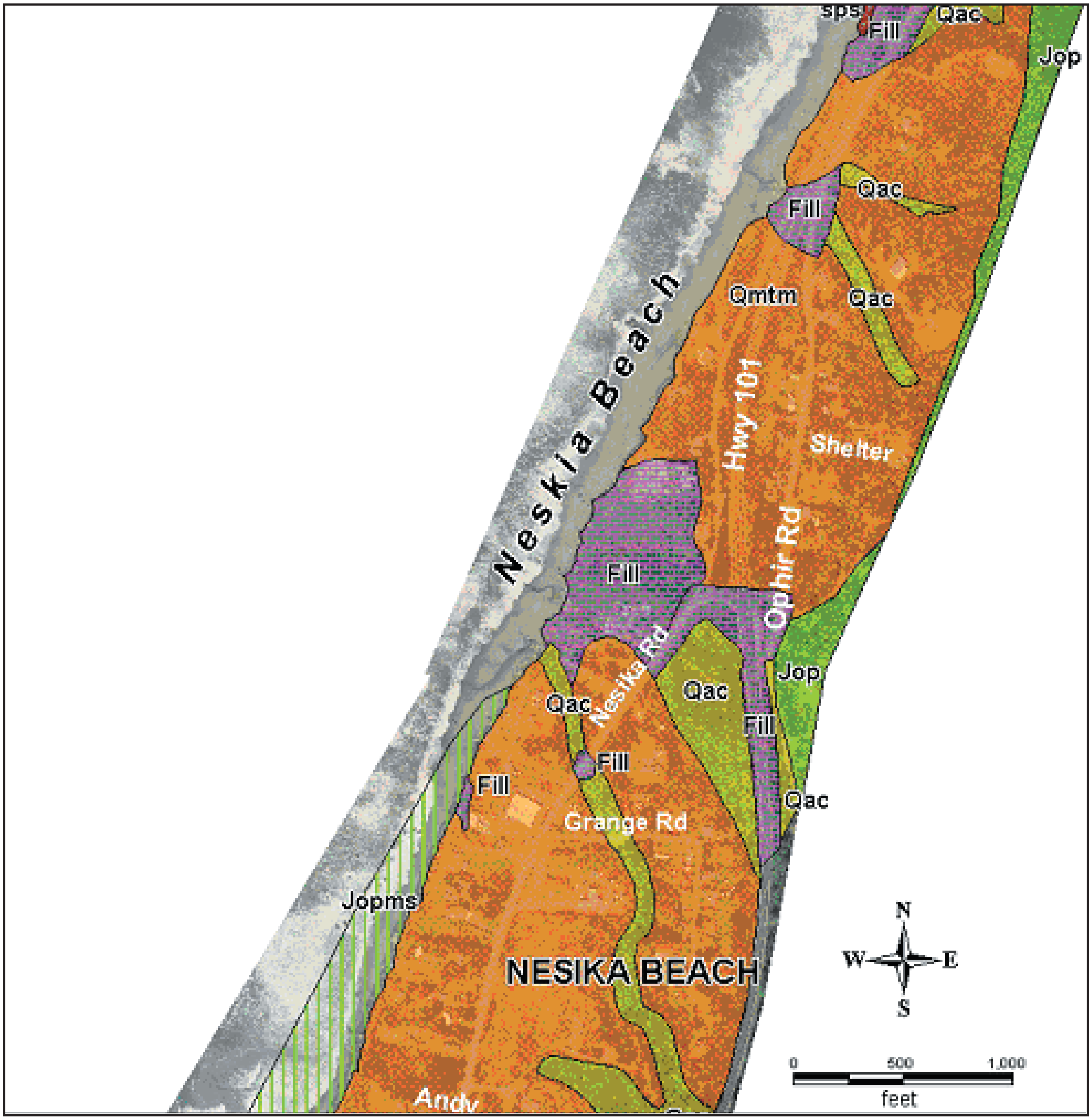

LANDSLIDE AND GEOLOGY MAP – SOUTH NESIKA BEACH (ANDY-GUN CLUB ROAD)

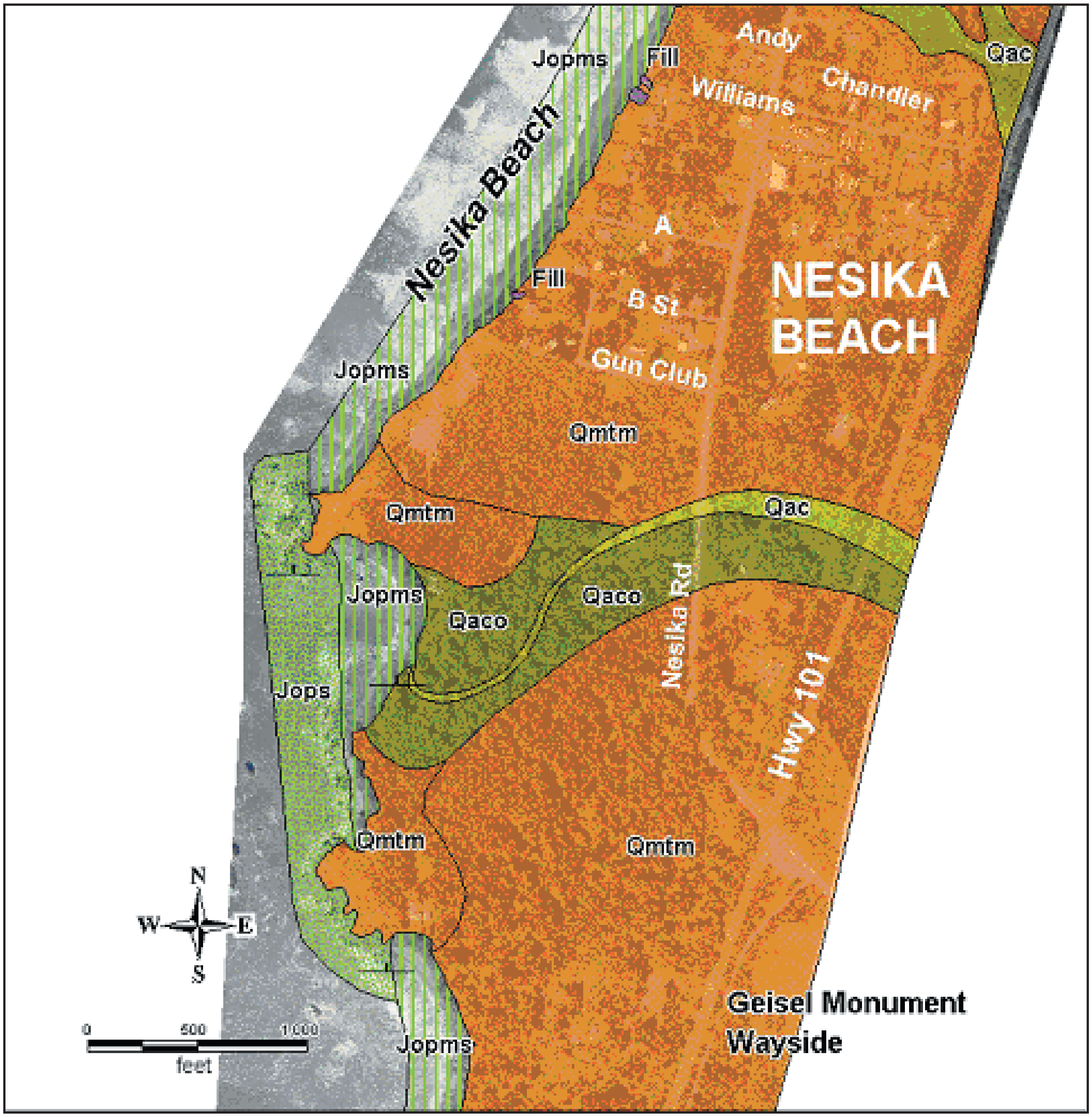

LANDSLIDE AND GEOLOGY MAP – WAKEMAN BEACH TO HUBBARD MOUND

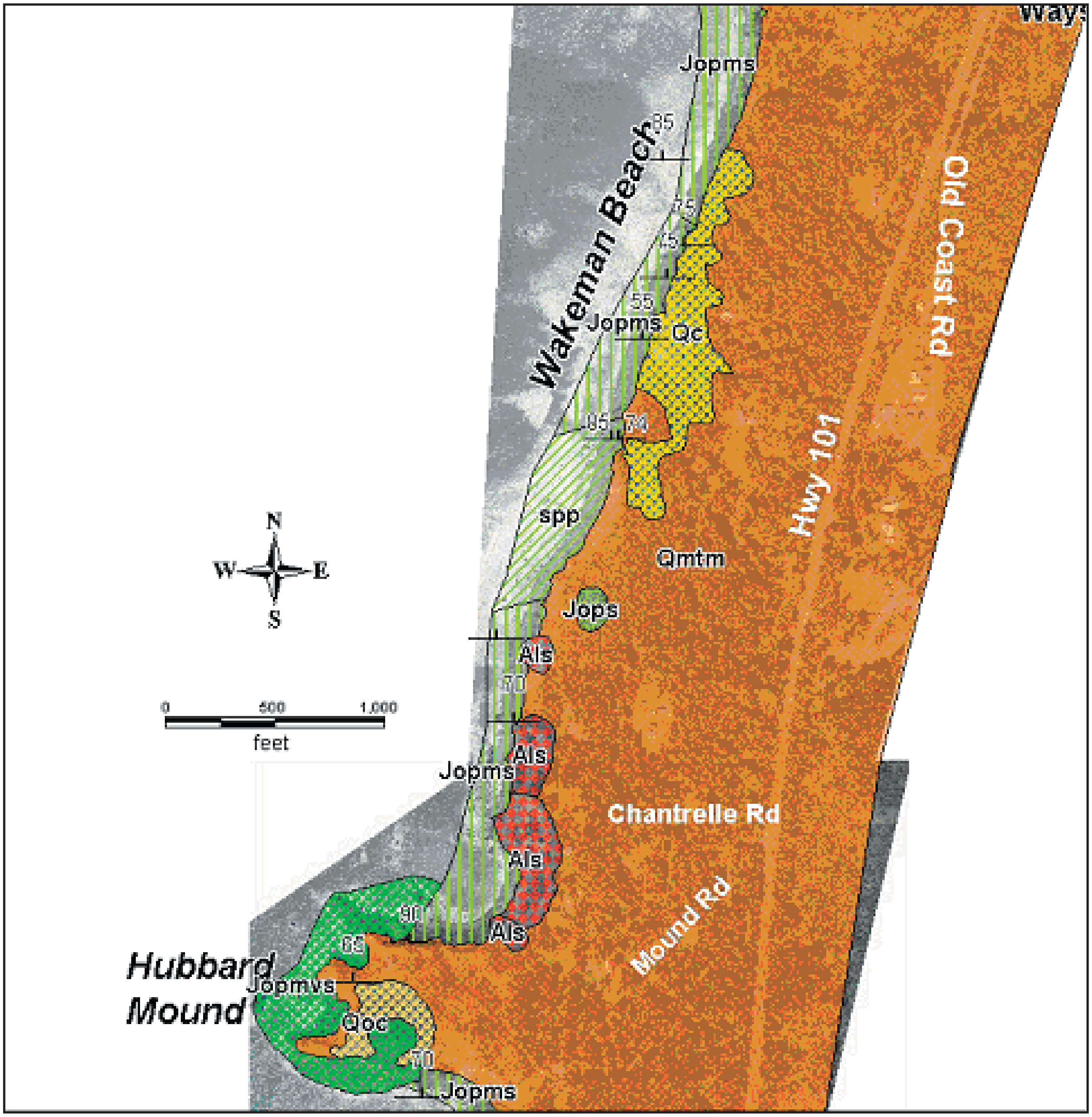

LANDSLIDE AND GEOLOGY MAP – SOUTH HUBBARD MOUND TO OTTER POINT

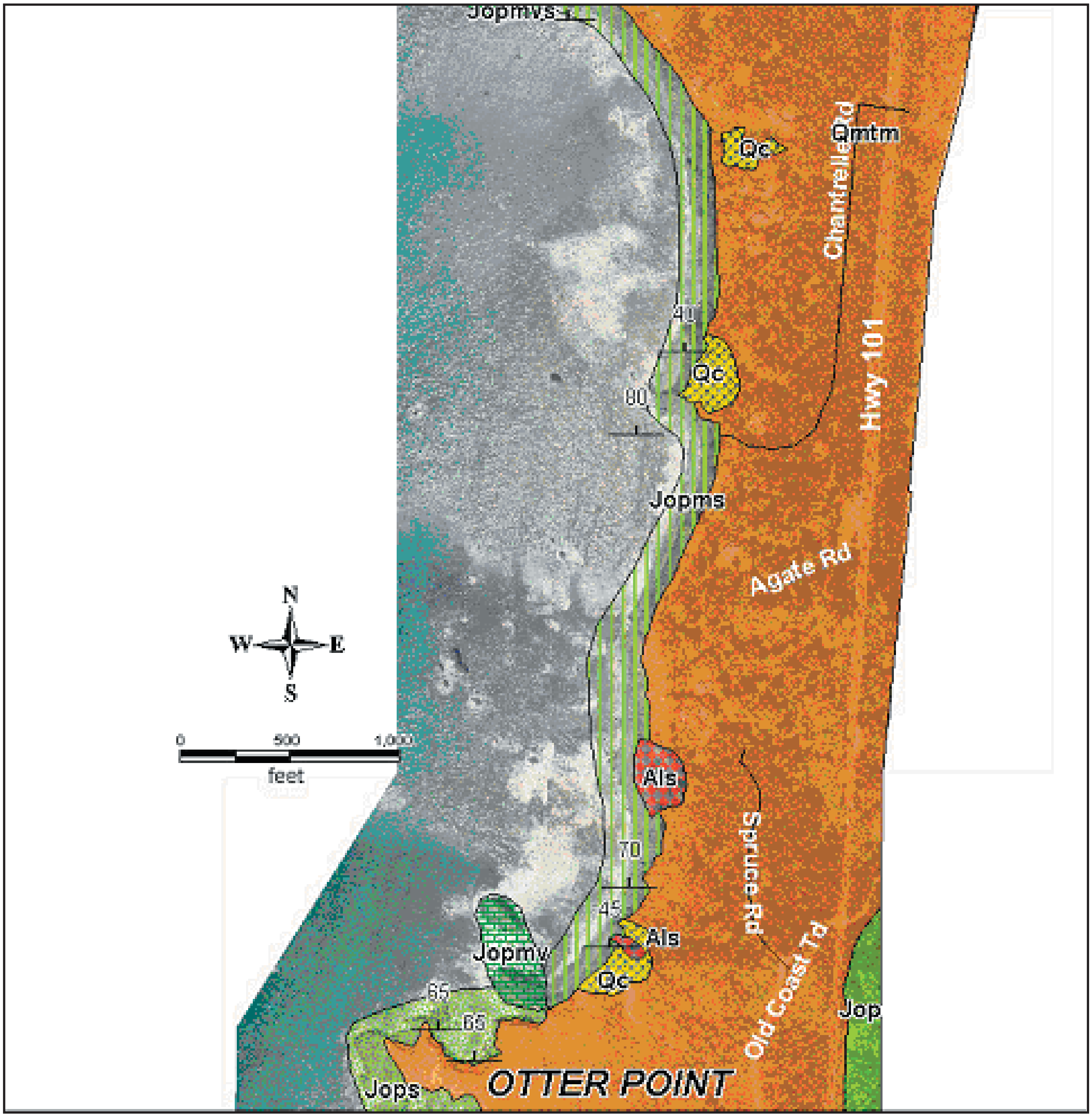

LANDSLIDE AND GEOLOGY MAP – BAILEY BEACH

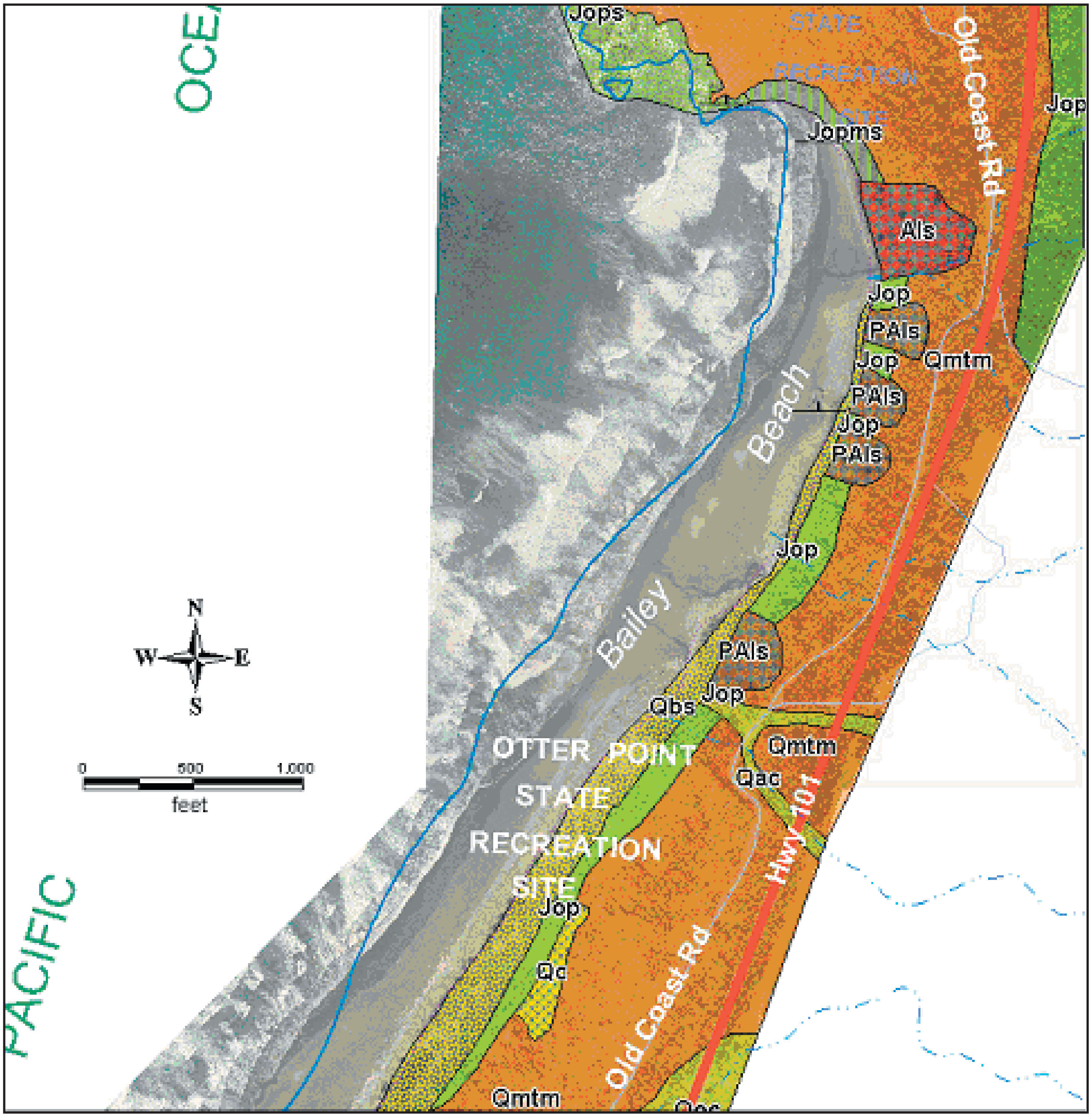

LANDSLIDE AND GEOLOGY MAP – SANDY – COBBLESTONE ROAD AREA

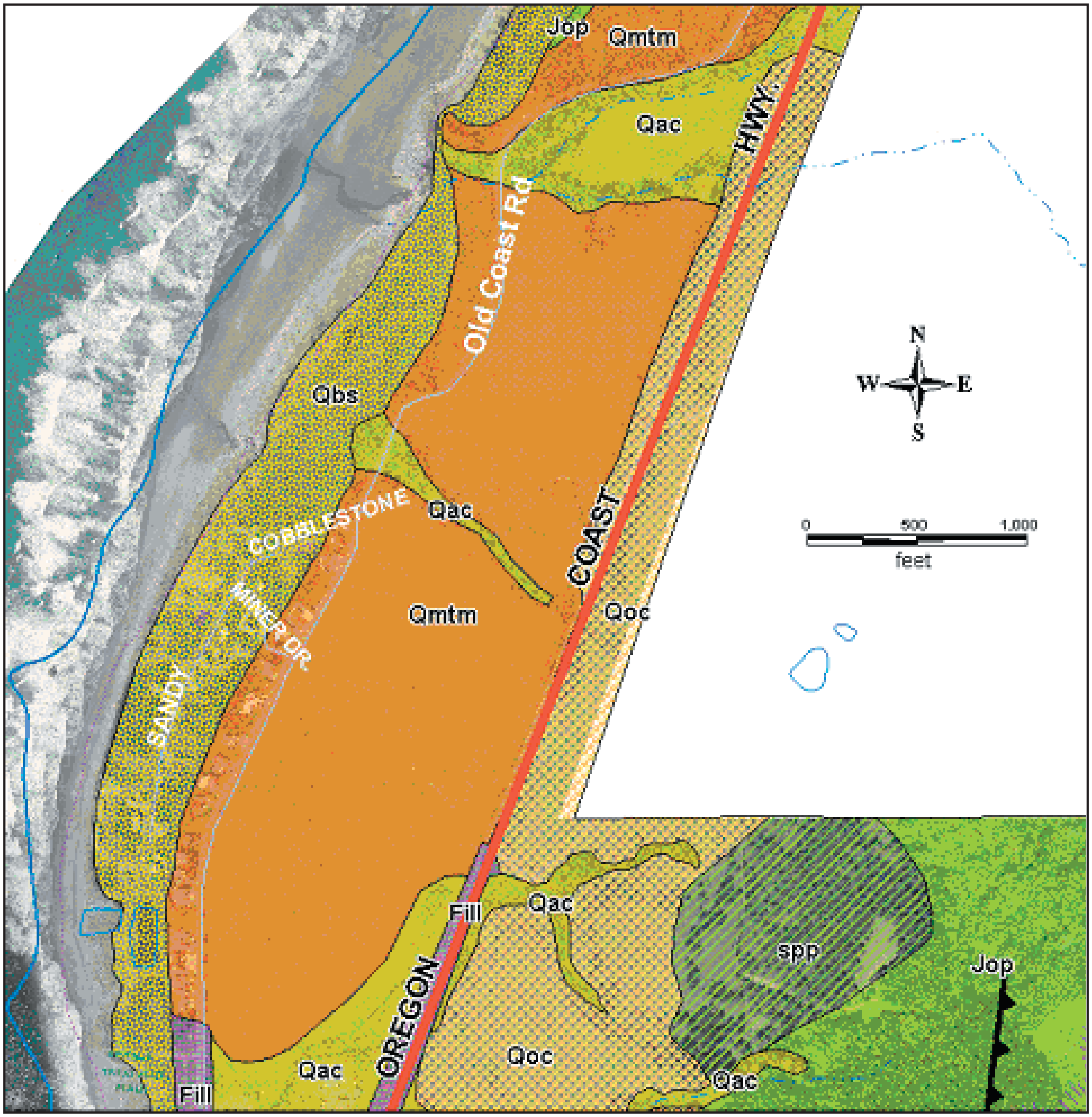

LANDSLIDE AND GEOLOGY MAP – NORTH JETTY OF ROGUE RIVER

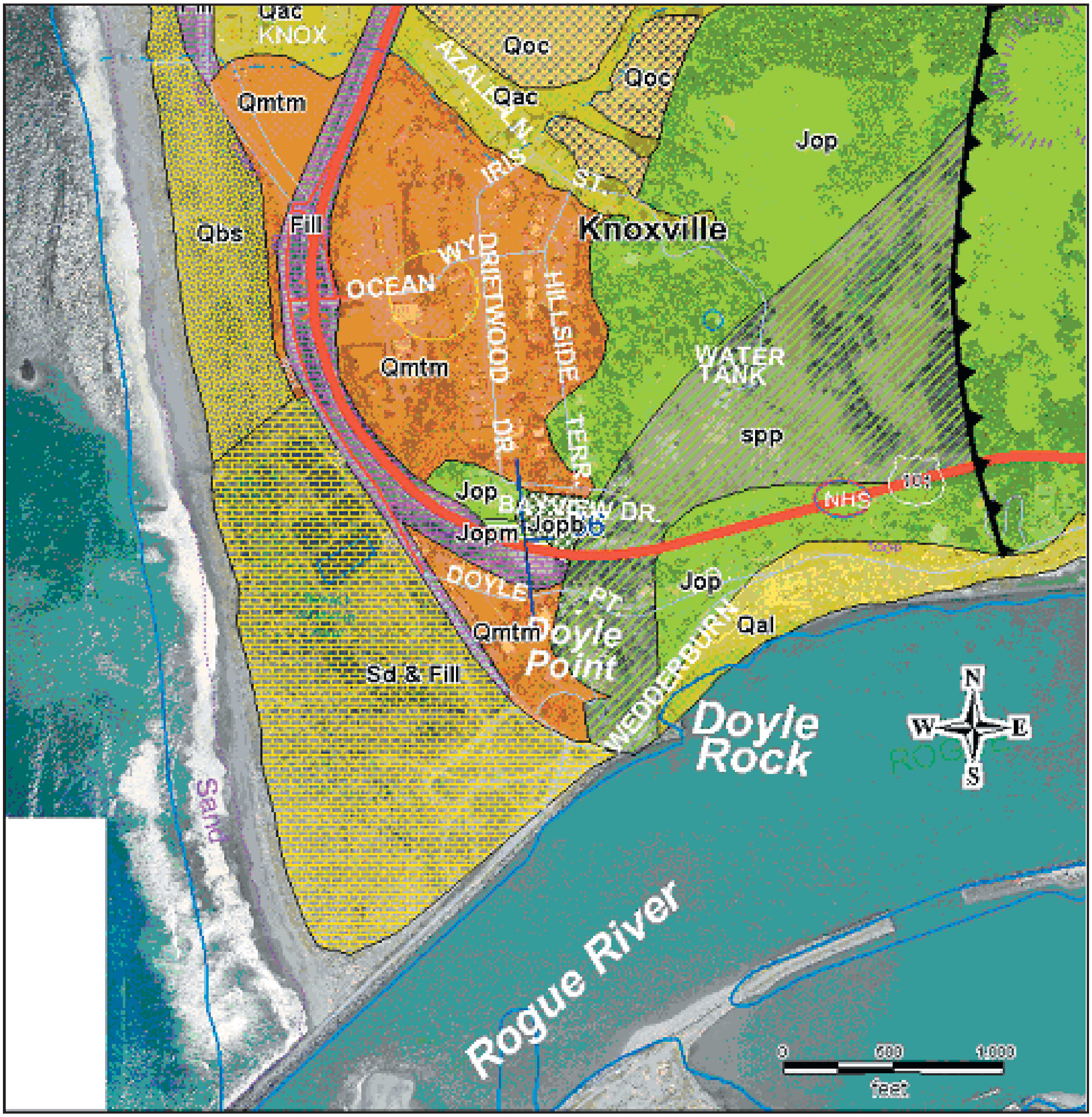

APPENDIX C: DIGITAL FILES

The following table lists digital files included on the disk. Only root file names without extensions are listed (most GIS data are specified by multiple files with a variety of extensions but the same root file name). These GIS files depict all technical information shown in map views of Appendices A and B. Original map projection for all vector GIS files is Oregon State Plan south, NAD83, feet, matching the 2003 orthophoto base maps used for most of the study area. Digital raster graphic files of orthophoto base maps and USGS digital raster graphic quadrangle maps used for base imagery are not included in this digital report. Neither are topographic contours at 2-feet intervals produced from the 2003 aerial photography. Contact USGS offices for USGS maps. Contact Curry County offices or 3Di in Eugene, Oregon for information about obtaining 2003 topography and digital orthophotos.

In addition to the native projection, all vector GIS files are also provided in the Oregon Lambert, 1997 feet. The native GIS file format is MapInfo .tab files; files are also provided in ArcView shape file format. See the appropriate subdirectories on the disk for the various combinations of file format and map projection. All GIS files have as their first attribute a data field labeled ID, which gives a number to each row of attribute data. This ID field is not listed in the table.

Table A 1. Digital vector files used to produce map views in Appendices A and B.

File Name	Description
Street_Labels	Street and other geographic labels.
Golb_textEDITED	Street and geographic labels names from ODOT archives for Gold Beach area
Active_Hazard_ZoneFINAL	Active erosion hazard zone polygons
BLUFF_EROSION_HAZ_ZONES	Erosion risk zone polygons for bluff-backed shorelines
dune_hazard_zones	Erosion risk zone polygons for dune-backed shorelines
Geology_nesika_beach3	Detailed shoreline geology and landslide polygons
Strike_Dips_ Nesika	Strike and dip symbols with attribute table listing field number, strike in quadrant system (e.g. N30W), dip amount and direction, quality of dip measurement, and geologic context. Data collected by George Priest in northern part of study area.
Labels_Strike_Dips	Dip labels for file Strike_Dips_Nesika
Nesika_Strike_and_Dips	Strike and dip symbols with attribute table listing dip azimuth, amount, dip direction and geologic context. Data collected by Ron Sonnevil.
Faults	Sawtooth line symbol for thrust fault exposed in southern part of study area.

Table A 2. GIS data files of erosion hazard map guidelines, erosion data, and slide block width measurements. All GIS files have as their first attribute a data field labeled ID, which gives a number to each row of attribute data. This ID field is not listed in the table.

File Name	Description
Bluff_Haz_guidelines	Vector lines drawn perpendicular to the shoreline at bluff and having nodes spaced at the boundaries between the HIGH, MODERATE, and LOW risk zones for coastal erosion of bluffs. Attributes attached to the graphic lines are longitude, latitude, distance in feet either east of the ACTIVE hazard zone or east of the toe of the bluff (angle of repose correction added) to east side of HIGH-risk polygon, MODERATE-risk polygon, and LOW-risk polygon; relief of the bluff; amount of lateral distance added to the HIGH-risk zone from angle of repose calculations; maximum slide block width; minimum and maximum erosion rates; and description of the calculation methods.
Dune_Haz_guidelines_83_ft	Vector lines drawn perpendicular to the shoreline at bluff and having nodes spaced at the boundaries between the HIGH, MODERATE, and LOW risk zones for coastal erosion of dunes. Attributes attached to the graphic lines are longitude, latitude.
Dune_Eros_Haz_transectsDATA	Points at centroid of each vector line from Dune_Haz_guidelines_83_ft. Attributes are Longitude, Latitude, beach slope tangent, beach slope cotangent, wave runup for high hazard zone scenario (Runup 1), moderate hazard zone scenario (Runup 2), and worst-case, low hazard zone scenario (Runup 3). The same 1-2-3 numbering system is used for other attributes, WL = water level from storm, tide and sea level factors, T_{WL} = total of Runup + storm, tide and sea level factors; Horiz = horizontal distance of erosion from beach-dune toe junction; Ej_elev = elevation of the beach-dune toe junction. Note that an Excel spreadsheet file Dune_Eros_Haz_transectsDATA.xls has the source formulas for each attribute.
Slide_block_meas_sites	Points where slide block widths were measured; attributes include: Block width, headwall elevation, geologic unit or units, notes on measurement methods, errors in measurement or other uncertainties, polygon number; measurement method, longitude and latitude. Data and linear regressions for bluff height and block width are given in Excel file Slide_block_meas_sites.xls.
Cliff_Retreat_FINAL_noREFpts2	Points where erosion rate measurements were made; attributes include Longitude, Latitude, site number, and description of

Table A 2. Continued

File Name	Description
	graphic object plotted. The site number is the identifier linking this file to a matching Excel file named Cliff_Retreat_Meas_Sites.xls with erosion data and calculations of means and errors for each geologic setting.
_1967_2003_Nesika_top_retreat	Polygon with west boundary at 1967 bluff top position and east boundary at 2003 bluff toe position from rubbersheeting of 1967 air photo to 2003 orthophoto.
_1967_2003_Nesika_toe_retreat	Polygon with west boundary at 1967 bluff top position and east boundary at 2003 bluff toe position from rubbersheeting of 1967 air photo to 2003 orthophoto plus lines along shoreline showing where segments of shoreline were lumped together to obtain a mean retreat rate weighted for shoreline length; calculations for this weighted mean are summarized in Excel file Toe Retreat at Nesika Beach (Wtd Mean).xls linked to the GIS file through the ID field. Attributes include: a label field explaining what the graphic object is and a description with further details.